

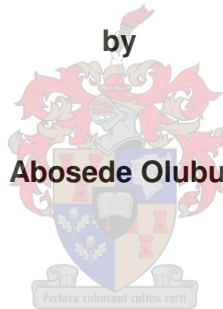


**UNIVERSITEIT  
STELLENBOSCH  
UNIVERSITY**

**BASIN-FILL OF THE PERMIAN TANQUA DEPOCENTRE, SW KAROO BASIN, SOUTH  
AFRICA.**

**by**

**ALAO Abosede Olubukunola**



Thesis presented in fulfilment of the requirements for the degree of

**Master of Science**

at the Department of Earth Sciences,

Stellenbosch University

2012

Supervisor

Dr. Daniel Mikeš

## DECLARATION

This research is submitted in fulfilment of the requirements for the degree of Masters of Science at Stellenbosch University and has not been previously accepted or concurrently submitted in candidature for any degree.

This dissertation is the result of my own independent work/research, except where otherwise stated.

Other sources acknowledged are by explicit references.

Signed.....A. O. ALAO.....

Date.....25/01/2012.....

Copyright © 2012 Stellenbosch University

All rights reserved



## ABSTRACT

Basin subsidence analysis, employing the backstripping method, indicates that fundamentally two different basin-generating mechanisms controlled Tanqua depocentre development in SW Karoo Basin. The subsidence curves display initial dominantly decelerating subsidence, suggesting an extensional and thermal control possibly in a strike-slip setting during the depocentre formation; on the other hand, subsequent accelerating subsidence with time suggests that the dominant control on the depocentre formation in SW Karoo was flexure of the lithosphere. Based on these observations on the subsidence curves, it is possible to infer that the first stage of positive inflexion (~ 290 Ma) is therefore recognised as the first stage of Tanqua depocentre formation.

Petrographic study show that most of the studied sandstones of the Tanqua depocentre at depth of ~ 7.5 Km were subjected to high pressure due to the overlying sediments. They are tightly-packed as a result of grains adjustment made under such pressure which led also to the development of sutured contacts. It is clear the high compaction i.e. grain deformation and pressure solution occurred on the sediments; leading to total intergranular porosity reduction of the quartz-rich sediments and dissolution of the mineral grains at intergranular contacts under non-hydrostatic stress and subsequent re-precipitation in pore spaces.

Furthermore, siliciclastic cover in the Tanqua depocentre expanded from minimal values in the early Triassic (Early to Late Anisian) and to a maximum in the middle Permian (Wordian -Roadian); thereby accompanying a global falling trend in eustatic sea-level and favoured by a compressional phase involving a regional shortening due to orogenic thrusting and positive inflexions (denoting foreland basin formation). The estimate of sediment volume obtained in this study for the Permian Period to a maximum in the middle Permian is therefore consistent with published eustatic sea-level and stress regime data. In addition, this new data are consistent with a diachronous cessation of marine incursion and closure of Tanqua



depocentre, related to a compressional stress regime in Gondwana interior during the late Palaeozoic.

## OPSOMMING

Die ontleding van komversakking met behulp van die terugstropingsmetode bring aan die lig dat die ontwikkeling van die Tankwa-afsettingsentrum in die Suidwes-Karoo-kom hoofsaaklik deur twee verskillende komvormende meganismes bepaal is. Die versakkingskurwes toon aanvanklike, hoofsaaklik verlangsaamde versakking, wat daarop dui dat ekstensie- en termiese beheer gedurende die vorming van die afsettingsentrum plaasgevind het, waarskynlik in 'n strekkingwaartse opset. Aan die ander kant toon daaropvolgende versnellende versakking wat mettertyd plaasgevind het dat die vorming van die afsettingsentrum in die Suidwes-Karoo eerder oorwegend deur 'n kromming van die litosfeer beheer is. Op grond van hierdie waarnemings met betrekking tot die versakkingskurwes, kan 'n mens aflei dat die eerste stadium van positiewe infleksie (~ 290 Ma) dus as die eerste stadium van die vorming van die Tankwa-afsettingsentrum beskou kan word.

Petrografiese studie toon dat die meeste van die sandsteen wat van die Tankwa-afsettingsentrum bestudeer is, op 'n diepte van ~ 7,5 Km aan hoë druk onderwerp was weens die oorliggende sedimente. Die sandsteen is dig opmekaar as gevolg van die korrelaanpassing wat onder sulke hoë druk plaasvind, wat op sy beurt ook tot die ontwikkeling van kartelnaatkontakte aanleiding gegee het. Dit is duidelik dat die sediment aan hoë verdigting, dit wil sê korrelvorming en drukoplossing, onderwerp was, wat gelei het tot 'n algehele afname in interkorreelporeusheid by die kwartsryke sedimente; die ontbinding van die mineraalkorrels in interkorrelkontaksones onder niehidrostatiese spanning, en daaropvolgende herpresipitasie in poreuse ruimtes.

Voorts het silisiklastiese dekking in die Tankwa-afsettingsentrum toegeneem van minimale waardes in die vroeë Triassiese tydperk (vroeë tot laat Anisiaanse tydperk) tot 'n hoogtepunt in die mid-Permiaanse tydperk (Wordiaans–Roadiaans). Dié ontwikkeling het gepaardgegaan met 'n algemene dalingstendens in die eustatiese seevlak, en is verder aangehelp deur 'n saamdrukkingsfase wat gekenmerk is deur 'n regionale verkorting weens

orogeniese druk en positiewe infleksies (wat met voorlandkomvorming saamhang). Die geraamde sedimentvolume wat in hierdie studie vir die Permianse tydperk bepaal is, met die hoogtepunt in die middel van dié tydperk, is dus in pas met gepubliseerde data oor die eustatiese seevlak en spanningstoestand. Daarbenewens strook hierdie nuwe data met 'n diachroniese staking van mariene instroming en die afsluiting van die Tankwa-afsettingsentrum wat met 'n spanningstoestand in die Gondwana-binneland gedurende die laat Paleosoïkum verband hou.

## **ACKNOWLEDGEMENTS**

I give thanks to Almighty God, for giving me the grace and inspiration during the course of this study. I use this opportunity to show my gratitude for His goodness and mercy in enabling me work on this dissertation.

I am also using this opportunity to show my gratitude to my supervisor Dr Daniel Mikeš, for his positive criticism, guidance, persistence and encouragement during the course and completion of my Masters dissertation.

I express my appreciation to Doug Cole, Dannie Barnado, Marinda Havenga, Amarie Smith, all at the Council for Geoscience, for providing me with data from their core library and geophysical data in the form of regional magnetic and gravity profiles.

My gratitude goes to my colleagues and friends, Ife, Candice, Byron, Malikah, my Pastor Funlola Olojede and Mr. and Mrs. Osundiran for their support in the course of this dissertation.

Finally, my heartfelt appreciation goes to my family; my loving husband, my daughter, my loving parents and siblings; particularly Biodun and Bayo for their love, prayers, moral and emotional assistance in assuring that this dream is a reality. I am most grateful for your trust and belief in me and for always being there; I love you all, for you mean the world to me.



## TABLE OF CONTENTS

<b>DECLARATION.....</b>	<b>II</b>
<b>ABSTRACT .....</b>	<b>IV</b>
<b>OPSOMMING .....</b>	<b>VI</b>
<b>ACKNOWLEDGEMENTS.....</b>	<b>VIII</b>
<b>TABLE OF CONTENTS .....</b>	<b>X</b>
<b>CHAPTER ONE: INTRODUCTION.....</b>	<b>1</b>
1.1 BACKGROUND .....	1
1.2 GEOLOGICAL SETTING .....	3
1.3 REVIEW OF PREVIOUS WORKS ON SUBSIDENCE OF THE SW KAROO .....	5
1.4 AIM AND OBJECTIVES .....	7
1.5 METHODOLOGY OF DATA COLLECTION AND PROCESSING .....	8
<b>CHAPTER TWO: REGIONAL GEOLOGY AND LITHOSTRATIGRAPHY.....</b>	<b>11</b>
2.1 TECTONIC SETTING OF THE SW KAROO BASIN.....	11
2.2 STRATIGRAPHY AND DEPOSITIONAL SYSTEMS OF THE SW KAROO BASIN.....	13
2.2.1 Cape Supergroup.....	14
2.2.2 Karoo Supergroup.....	15
Dwyka Group.....	16
Ecca Group.....	17
Beaufort Group.....	18
Stormberg Group.....	18
2.3 STRUCTURAL SETTING OF THE SW KAROO BASIN.....	22
2.3.1 Deposition within the Laingsburg and Tanqua depocentre .....	23
2.4 CORRELATION AND CHRONOSTRATIGRAPHY OF THE TANQUA AND LAINGSBURG DEPOCENTRE .....	26
2.5 LITHOSTRATIGRAPHY OF THE TANQUA DEPOCENTRE (STUDY AREA).....	31
2.5.1 Dwyka Group .....	32
2.5.2 Prince Albert Formation.....	33
2.5.3 Whitehill Formation.....	33
2.5.4 Collingham Formation .....	34
2.5.5 Tierberg Formation .....	34
2.5.6 Skoorsteenbergs Formation .....	35
2.5.7 Kookfontein Formation .....	35
2.5.8 Koedoesbergs Formation.....	36

2.5.9	<i>Abrahamskraal Formation</i> .....	36
<b>CHAPTER THREE: METHODOLOGY AND DATABASE</b> .....		<b>38</b>
3.1	CONCEPT OF THE BACKSTRIPPING TECHNIQUE .....	38
3.1.1	<i>Decompaction</i> .....	39
3.2	STUDY AREA AND DATA AVAILABILITY .....	42
3.2.1	<i>Stratigraphic relationships and lithologies</i> .....	43
3.2.2	<i>Dating estimates</i> .....	43
3.3	DECOMPACTION OF LITHOSTRATIGRAPHIC UNITS IN TANQUA DEPOCENTRE .....	48
3.4	DEPOSITIONAL WATER-DEPTH .....	49
3.5	1- D AIRY BACKSTRIPPING .....	50
3.5.1	<i>Program description and work flow</i> .....	50
3.5.2	<i>Error sources</i> .....	51
<b>CHAPTER FOUR: TECTONIC SUBSIDENCE ANALYSIS</b> .....		<b>53</b>
4.1	COMPARISON BETWEEN COMPACTED AND DECOMPACTED LITHOLOGICAL UNITS OF TANQUA DEPOCENTRE	53
4.2	RESULTS AND INTERPRETATION .....	54
4.2.1	<i>Compaction estimates</i> .....	54
4.2.2	<i>Decompaction estimates</i> .....	55
4.3	COMPACTION OF SEDIMENTS .....	58
4.3.1	<i>Petrographic descriptions</i> .....	58
4.3.2	<i>Scan Electron Microscopic (SEM) analysis</i> .....	59
4.3.3	<i>Diagenesis</i> .....	62
4.3.4	<i>Diagenetic evolution</i> .....	63
4.4	SUBSIDENCE CURVES .....	69
4.4.1	<i>Results of the 1D Airy subsidence model</i> .....	69
4.4.2	<i>The relative timing of inflections on the Tanqua depocentre subsidence curves</i> .....	77
4.4.3	<i>The implications of flexural subsidence in Karoo foreland basin</i> .....	78
4.5	SIGNIFICANCE OF PETROGRAPHIC CONSTRAINTS ON DIAGENETIC PROCESSES TO COMPACTION ESTIMATES, AND SUBSEQUENTLY ON THE SUBSIDENCE CURVES .....	79
4.6	PROPOSED BASIN-FILL MODEL FOR THE TANQUA DEPOCENTRE .....	80
<b>CHAPTER FIVE: TECTONIC LOADING AND SEDIMENTATION IN TANQUA DEPOCENTRE</b> .....		<b>84</b>
5.1	SEDIMENTATION RATES AND SEDIMENT TRENDS .....	84
5.2	RESULTS	87
5.3	RELATIONSHIP OF SUBSIDENCE AND SEDIMENTATION TRENDS IN TANQUA DEPOCENTRE .....	89
5.4	BASIN MIGRATION AND REGIONAL IMPLICATIONS .....	96

<b>CHAPTER SIX: DISCUSSIONS AND CONCLUSIONS.....</b>	<b>102</b>
6.1 SEQUENCE STRATIGRAPHY.....	102
6.2 TECTONIC SUBSIDENCE .....	103
6.3 CONCLUSIONS .....	105
6.4 RECOMMENDATIONS.....	107
<b>REFERENCES .....</b>	<b>109</b>
<b>APPENDIX A.....</b>	<b>132</b>
BOREHOLE AND SEDIMENTOLOGICAL LOGS WITH SAMPLE LOCATIONS.....	132
<b>APPENDIX B.....</b>	<b>143</b>
PETROGRAPHIC AND SEM ANALYSIS DESCRIPTION .....	143
SAMPLE MICROGRAPHS .....	144
<b>APPENDIX C.....</b>	<b>147</b>
OSXBACKSTRIPPING EQUATIONS.....	147
<b>APPENDIX D.....</b>	<b>152</b>

<b>LIST OF FIGURES AND TABLES</b>	<b>PAGES</b>
-----------------------------------	--------------

**Chapter One**

Figure 1.01: Satellite image location map of Tanqua (study area) and Laingsburg depocentre.....3

Figure 1.02: Palaeogeographic reconstruction of Gondwana during the Permian..... 3

Figure 1.03: Simplified model of the Earth's crust below the SW Karoo from near vertical reflection seismic data.....5

Figure 1.04: Flow chart of the methodology adopted in this study..... 8

**Chapter Two**

Figure 2.01: Map showing accretionary tectonics along Gondwana southern margin.....9



Figure 2.02: General tectonic setting of the Karoo Basin, indicating the SW Karoo	10
.....	
Figure 2.03: The Cape and Karoo Basin stratigraphy in the SW Karoo Basin.....	16
Figure 2.04: Simplified palaeogeographic models for the Karoo sequence	17
.....	
Figure 2.05: Schematic representation of three-stage Evolution of the southern Cape-Karoo Basin.....	18
Figure 2.06: Landsat image of SW Karoo Basin, with the Tanqua and Laingsburg depocentres .....	20
Figure 2.07: Palaeogeographic reconstruction of the SW Karoo basin.....	21
Figure 2.08: Illustration of correlation between Permian depositional sequences.....	23
Figure 2.09: Chronostratigraphic or Wheeler diagram based on the assumptions of shale depositional rates.....	23
Figure 2.10: Correlation of the Laingsburg and Tanqua depocentre deepwater successions	24
.....	
Figure 2.11: Fence diagram showing the revised correlation of the Karoo deepwater stratigraphy.....	25
Figure 2.12: Enlarged satellite image of the study area.....	26
Figure 2.13: Stratigraphy of the Cape and Karoo successions in the Western Cape.....	30

### Chapter Three

Figure 3.1: Summary of idealized porosity vs. depth curves for different lithologies.....33

Figure 3.2: Schematic diagram explaining backstripping of multiple sediment layers.....34

Figure 3.03: Photograph of the extensive and well exposed outcrops .....36

Figure 3.04: Geological map of the Tanqua depocentre .....37

Table 3.1: The lithostratigraphic units deposited in the Tanqua depocentre .....38

Table 3.2: Compaction coefficients and parameters for main lithological types .....39

#### **Chapter Four**

Table 4.1: Calculated results of parameters for lithostratigraphic units in Tanqua depocentre.....45

Figure 4.01: The thickness of compacted compared to decompact sections .....46

Figure 4.02: The percent decompaction compared to percent compaction per section ....46

Figure 4.03: Location map of the study area.....50

Plate 1: Sample Microphotographs of thin sections SWA 6.....54

Plate 2: Sample Microphotographs of thin sections SWA15-2 .....55

Plate 3: Sample Microphotographs of thin sections SWA 20 .....56

Figure 4.04: Generalized diagenetic sequence for the Tanqua depocentre sandstone.....57

Figure 4.05: Subsidence curves for Tanqua depocentre .....60

Figure 4.06: Backstripped corrected for compaction .....61

Figure 4.07: Tectonic and basement subsidence for the Western Cape province by Cloetingh *et al.*, 1992.....62

Figure 4.08: Graph illustrating subsidence rates over time and corresponding to deposition of the lithostratigraphic units in Tanqua depocentre.....62

Figure 4.09: Comparison between the tectonic subsidence curves obtained in this study and a simplified diagram .....63

Figure 4.10: Schematic illustration of a foreland basin system .....63

Figure 4.11: Hypothetical illustration of tectonic subsidence of the Tanqua depocentre.....66

Figure 4.12: Cross-section through Tanqua depocentre showing the approximation of the tectonic subsidence .....69

**Chapter Five**

Figure 5.01: Location map showing the area extent of Tanqua depocentre .....72

Table 5.1: Total sediment volumes and accumulation rates for Tanqua depocentre .....73

Figure 5.02: Graph of sediment volume and sedimentation rate against time .....74

Figure 5.03: Comparison of the subsidence and sedimentation rate .....75

Figure 5.04: Generalized chronostratigraphic nomenclature and comparison between eustatic curve and the tectonic subsidence curve .....79

Figure 5.05: Magnetic profile covering the Tanqua depocentre .....80

Figure 5.06: Gravity profile covering the Tanqua depocentre .....81

Figure 5.07: The SW - NE cross section using contour lines along the magnetic and gravity profile .....81

Figure 5.08: The W - E cross section using contour lines across the magnetic and gravity profile .....81

## **Chapter Six**

Figure 6.01: Summary data involved in estimate of Tanqua depocentre basin-fill.....88

## CHAPTER ONE: INTRODUCTION

### 1.1 BACKGROUND

Mainly the basin-forming tectonic processes control the geometry of a basin-fill. On a large scale, the general tectonic setting controls the size, shape, orientation and structural evolution of a basin, all of which exert an overall control on the sedimentary facies that can develop within that basin. Likewise, changes in the tilt of the basin floor or in the position of the depocentre due to tectonics or volcanism will influence the character of the fill at several scales, thereby changing the overall geometry of the deposits, the locations and extent of the deep and shallow water facies and the direction of clastic sediment transport (Einsele, 2000).

For foreland basins deposited onto a continental crust basement and consisting of thick sediment deposits, it is the sediment thickness rather than the subsidence which is directly observed (McKenzie, 1978). Furthermore, although the basin subsidence is maximum immediately adjacent to the mountain belt and gradually decreases onto the foreland as a result of lithospheric adjustment upon thrust loading, in order to constrain the amount of subsidence, sediment loads must be removed using either an Airy model or a flexural model for isostatic compensation.

The basin-fills of this type of foredeep or foreland basins tend to evolve from an initial phase of coarse, clastic deposition into shallow-marine environments, and then to thick, molasses-type sediments derived largely from the volcanic arc and its basement. Furthermore, palaeocurrent directions and textural trends of subareally and subaqueously deposited beds (e.g., fluvial transport, sediment gravity flows, and turbidity currents) can be used to distinguish the depositional system.

Basin-fill models are regarded as a means of quantifying the dynamic stratigraphy and exploring the effects of varying parameters like sediment supply, subsidence and sea level in a

sedimentary basin. According to Einsele (2000), basin-fill models can be subdivided into two groups:

1. Geometric models characterizing basins with constant surface geometry, i.e. a basin formed in a continental and/or intra-cratonic setting, which subsides but is filled with sediments all the time. In this case, sedimentation rate and subsidence are in balance and maintain equilibrium regardless of sea-level fluctuations and/or differential subsidence.
2. Dynamic models that take into account sediment transport and rate of deposition, which both tends to change laterally, i.e. downstream along rivers, or from the shelf-edge towards the centre of a basin. Consequently, the geometry of the sedimentary surface may undergo significant modification with time.

The first type of basin-fill model can be represented in 1D while for the second type, on the other hand, a 3D model is more applicable. The basic concept of the approach of the first type is more applicable to the purpose of this study, and is based on relevant processes controlling the accommodation space in a basin, the sediment supply, the basin dynamics and sea level fluctuations. Consequently, geometries of the sedimentary units that fill the basin and the depositional hiatus that partition them are governed by the interaction between the aforementioned factors. Therefore, to understand basin-forming tectonics and depositional environments, the basin-fill geometry and tectonic subsidence of the Tanqua depocentre SW Karoo using lithostratigraphic units is hereby studied at different scales (i.e. outcrop and drill holes). Tectonic subsidence modelling provides backstripping of lithological units deposited in the Permo-Carboniferous period.

## 1.2 GEOLOGICAL SETTING

The Tanqua depocentre is situated in the western part of the SW Karoo Basin (Fig. 1.01), and consists of strata that are almost tectonically undisturbed except for gentle folding in the extreme southern part and occasional reverse and thrust faulting with minor displacement over the central area. This structural vergence illustrates the dominance of northward compression.

A small portion of Pan-Gondwanian fold thrust belt that developed during the Late Palaeozoic due to crustal shortening associated with subduction and accretion of the paleo-Pacific plate beneath the Gondwana plate (De Wit and Ransome, 1992; Veevers *et al.*, 1994; López-Gamundí and Rossello, 1998; Milani and De Wit, 2008), along major foreland basins (Paraná, Karoo, Beacon and Bowen Basins), is now preserved in South Africa as the Cape Fold Belt (Lock, 1980). The continuous subduction resulted in northward compression with the Cape Fold Belt developing inboard of the magmatic arc (Visser, 1987; Veevers *et al.*, 1994) (Fig. 1.02).

The Cape Fold Belt (CFB) consists of a 'western' and a 'southern' branch and a syntaxial region. During the coalescence of the two branches, two major NE-trending anticlinal structures, namely the Hex River and Baviaanshoek, developed, and the syntaxial region separates the Tanqua and Laingsburg depocentres (Fig. 1.01) and displays the interference of NE- and SE-trending fold axes resulting in cross-folding (De Beer, 1990). The 'western' Cedarberg branch which borders the Tanqua depocentre is characterised by open folds. Whereas in the arcuate 'southern' Swartberg branch, which borders the Laingsburg depocentre and can be followed onto the East Falkland Island (Visser and Praekelt, 1996), isoclinal folding and thrusting dominates, with the intensity of the deformation generally decreasing craton-wards. Visser and Praekelt (1996) interpreted that the two branches of the Cape Fold Belt formed simultaneously by a NE-directed crustal shortening, concentrated in a narrow zone between the Kalahari and Rio de la Plata cratons (in South America) and the over-thickened Patagonia crustal block.

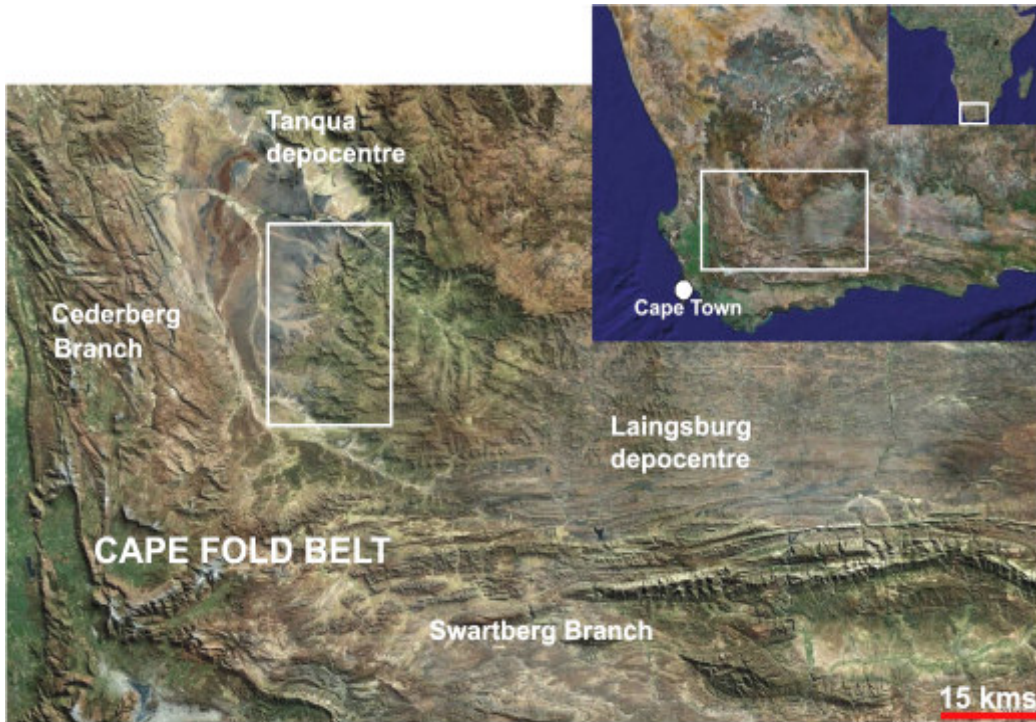


Figure 1.01: Satellite image location map of Tanqua (study area) and Laingsburg depocentres in the SW Karoo Basin, shown in relation to the two branches of the Cape Fold Belt. Outcrops of the Tanqua depocentre (focus of this study) are enveloped in the white rectangle.

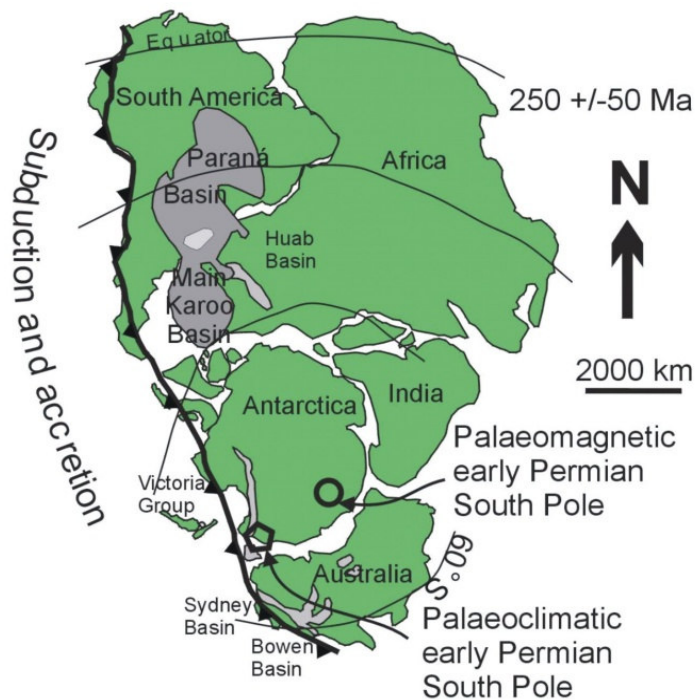


Figure 1.02: Palaeogeographic reconstruction of Gondwana during the Permian. Note the position and extent of the Paraná and Karoo basins (after Faure and Cole, 1999).



### 1.3 REVIEW OF PREVIOUS WORKS ON SUBSIDENCE OF THE SW KAROO

In an attempt at understanding subsidence of the SW Karoo Basin, Cloetingh *et al.* (1992) proposes a subsidence model of the Western and South-eastern Cape Province from published stratigraphic and sedimentological data of the SACS (South African Committee for Stratigraphy, 1980). The backstripped subsidence curve displays three episodes of subsidence, which were interpreted as follows (i) rapid subsidence expressing an extensional regime due to heating of the lithosphere (ii) slow subsidence phase expressing a thermal cooling phase following the initial heating phase and (iii) another rapid subsidence phase most likely a regional compressional event, and possibly a foreland compression. Conclusively, they propose that the origin for the Karoo Basin may be largely due to horizontal lithospheric buckling rather than vertical thrust loading.

Lindeque *et al.* (2007) describes a near vertical reflection profile that provides the first clear seismic reflection image of a ~100 km long crustal section below the Karoo Basin, the frontal section of the Cape Fold Belt, and the basement region around the Beattie Magnetic Anomaly. Although the seismic profile reveals no significant stratigraphic thickening of the Karoo Basin towards the CFB tectonic front as postulated on geological grounds (e.g. Cole, 1992; Catuneanu *et al.* 1998); it reveals three crustal layers above an undulating MOHO surface at depths between 35 and 45 km (Fig. 1.03), whereby the upper layer thickens southwards from 5 – 10 Km and is interpreted as strata of the Karoo and Cape Supergroups. This interpretation therefore suggests the need for further analysis of the presumed significant flexural component across the basin (e.g., Cloetingh *et al.* 1992; Milani and De Wit, 2007).

Tankard *et al.* (2009) studied the 3D basement architecture of Southern Africa and the stratigraphic response of the Cape and Karoo Supergroups to tectonics. They propose that large-scale subsidence during the early Permian Karoo Basin is primarily attributed to lithospheric deflection due to coupling of mantle flow to paleo-Pacific subduction controlled by crustal-scale faults. In addition, they suggest that subsidence of the Permian Karoo foredeep

pre-dates the Cape orogeny, thereby citing as evidence seismic stratigraphy, the relationship of cleavage fabrics to diagenetic mineral assemblages (De Swardt and Rowsell, 1974), and provenance studies (Johnson, 1991), all suggesting a Triassic Cape Fold Belt. Conclusively, they propose the late Karoo Basin as a Triassic-early Jurassic transtensional foreland system that was initiated by orogenic loading in the strike-slip transpressional Cape Fold Belt.

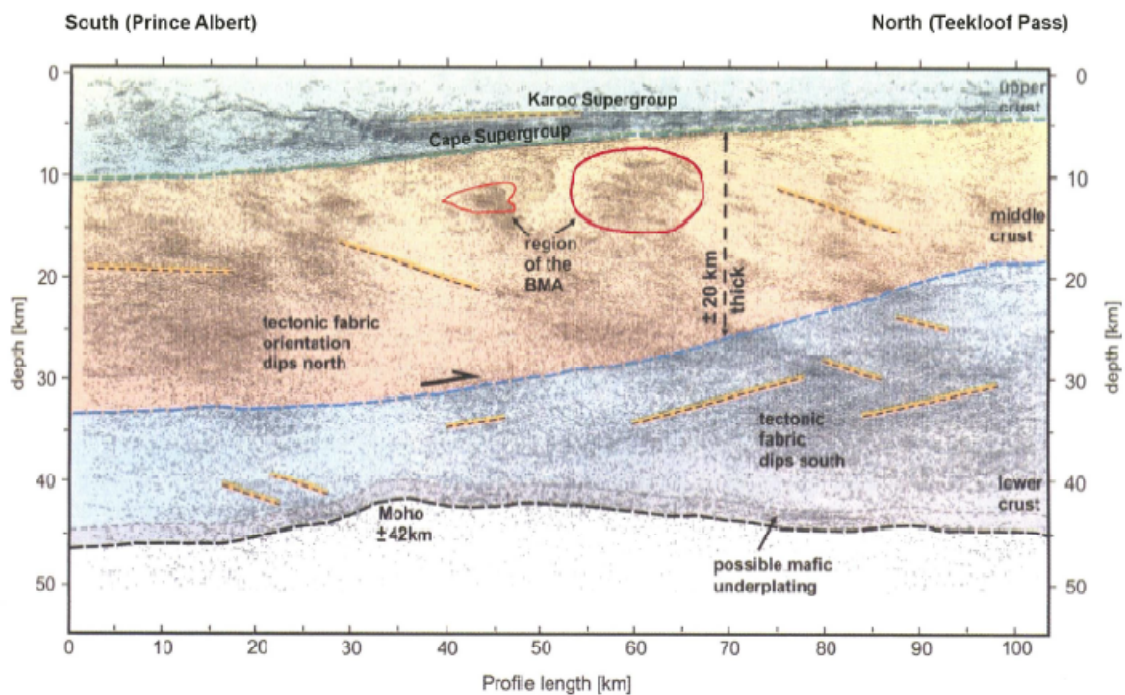


Figure 1.03: Simplified model of the Earth's crust below the SW Karoo from near vertical reflection seismic data. Figure is taken from Lindeque et al., (2007) with a southern subsidiary anomaly of the Beattie Magnetic Anomaly shown.

A depocentre refers to a local depression within a sedimentary basin, where the thickest development of the sedimentary sequence is found. In this context, the Laingsburg and Tanqua subbasins in the SW Karoo Basin are regarded as depocentres. On the other hand, whereas Cloetingh *et al.* (1992)'s forward model of the Western and South-eastern Cape Province, gives a regional-scale overview of the subsidence history of the SW Karoo Basin, this study focuses on

the investigating the subsidence history and evolution of Permian Tanqua depocentre situated within the western part of the SW Karoo Basin. In addition, the effect of subsidence in terms of compaction and diagenetic evolution of the sediments of the Tanqua depocentre is also presented, and a basin-fill model for the Permo-Carboniferous Period is proposed.

#### **1.4 AIM AND OBJECTIVES**

The focus of this research highlights the tectonic evolution, subsidence analysis and sediment-infill in the Tanqua depocentre. The main objective of the study is to investigate the basin-fill and tectonic subsidence of Tanqua depocentre using lithostratigraphic and chronostratigraphic data; thereby giving an insight into the basin dynamics and depositional systems involved.

The aim of this study entails the following:

1. Critical review and analysis of the existing tectonic models for the formation and sediment-fill of the SW Karoo so as to better understand the theoretical background of the basin evolution.
2. Tectonic subsidence analysis of the Permian Tanqua depocentre based on published stratigraphy thickness, chronostratigraphy and inferred palaeobathymetry.
3. Investigation of the interplay of accumulation rates, sediment volume and duration of sedimentation with subsidence episodes; to clarify details of basin evolution relating to major tectonic events in the adjacent orogenic belt and eustatic sea-level.
4. Compilation of all these data into one model that summarizes the evolution of the sedimentary-fill of the depocentre through the Permo-Carboniferous period.

## 1.5 METHODOLOGY OF DATA COLLECTION AND PROCESSING

The objectives of this study are best achieved through a tectonic subsidence analysis using lithostratigraphic data. Measurements of the sediment thickness of the basin-floor deposits to the base of the deltaic successions in the Tanqua depocentre are collated from previous research, rather than one profile from the basin floor to the base of the deltaic succession. A sedimentological profile is made from of the Kookfontein Formation, in locations chosen based on best outcrop positions for study of subsidence of the depocentre. A log of the Kookfontein Formation is done since the sequence is tectonically undisturbed, removed from areas of major tectonic disturbance, and has a nearly horizontal bedding plane of  $\sim 5^{\circ}$ . In addition, the absence of major unconformities in this section made it possible to assume that existing overburden stresses are essentially the maximum overburden loads experienced by the sediment grains.

Samples were taken from fresh outcrop surfaces where possible, concentrating shale sampling between the intercalated sandstone units, and sandstone samples at the start and end of major depositional facies. All samples within a specific profile were taken at vertical intervals, for the purpose of constraining compaction based on sediment load or overburden thickness.

Sedimentary outcrop logging and samples collection for petrographic analyses were carried out in Tanqua depocentre, SW Karoo Basin, South Africa. Samples were characterised through petrographic analyses, and the diagenetic evolution and possible compaction were determined. A summary diagram of the methodology is given in Figure 1.04.

Further study involving Scanning Electron Microscopy (SEM), were used to identify quartz overgrowth or cementation phenomenon. Petrographic and SEM studies and results are further discussed in Chapter Four.

Compaction and decompaction estimates were carried out for all the lithostratigraphic units in Tanqua depocentre in order to determine the effect of sediment compaction by porosity reduction. The percentage of decompaction for all the lithostratigraphic units was also

determined as the total decompacted thickness divided by the total compacted thickness of the section. The reason for this is to obtain which section decompacted more and which one less. The results of these estimates and percentages are compared and presented in chapter four.

In addition, by adopting Sclater and Christie's (1980) backstripping procedure, the tectonic subsidence of the Tanqua depocentre is obtained by removing non-tectonic subsidence attributed to sediment loading and compaction. This technique is applicable to the determining the subsidence history of the Tanqua depocentre using lithostratigraphic data, since it removes successively younger sediments and decompacts older sediments as they rise to shallower burial depths. However, despite its limitations (which is that loads are not compensated locally and not always does the porosity of the sediments decrease exponentially with depth), adoption of the 1D Airy backstripping technique is suitable to isolate tectonic subsidence and therefore reveal the subsidence history and evolution of the Tanqua depocentre.

Therefore, 1D airy-backstripping of the lithostratigraphic units of the Tanqua depocentre is hereby done via the OSXbackstripping programme, and the compacted tectonic and total subsidence curves are obtained, and subsequently critical interpretation and inferences are therefore made based on the curve profiles and related to published lithostratigraphy of the Tanqua depocentre.

Determination of sedimentation rates and pattern for Tanqua depocentre was done with a purpose of quantifying the deposition of sediments. The approach taken is by calculating sedimentation rates, whereby estimates of sediment loads (sediment volume) on the lithosphere through time were obtained. These sedimentation rates, which give the volume of sediments being accommodated in the depocentre during specific time periods, were then compared with subsidence curves, eustatic sea-level curve, deformation histories in the adjacent CFB, and sediment lithology with a view to determine the processes that control the nature of sedimentation in the Tanqua depocentre, and consequently a basin-fill model is thus proposed.

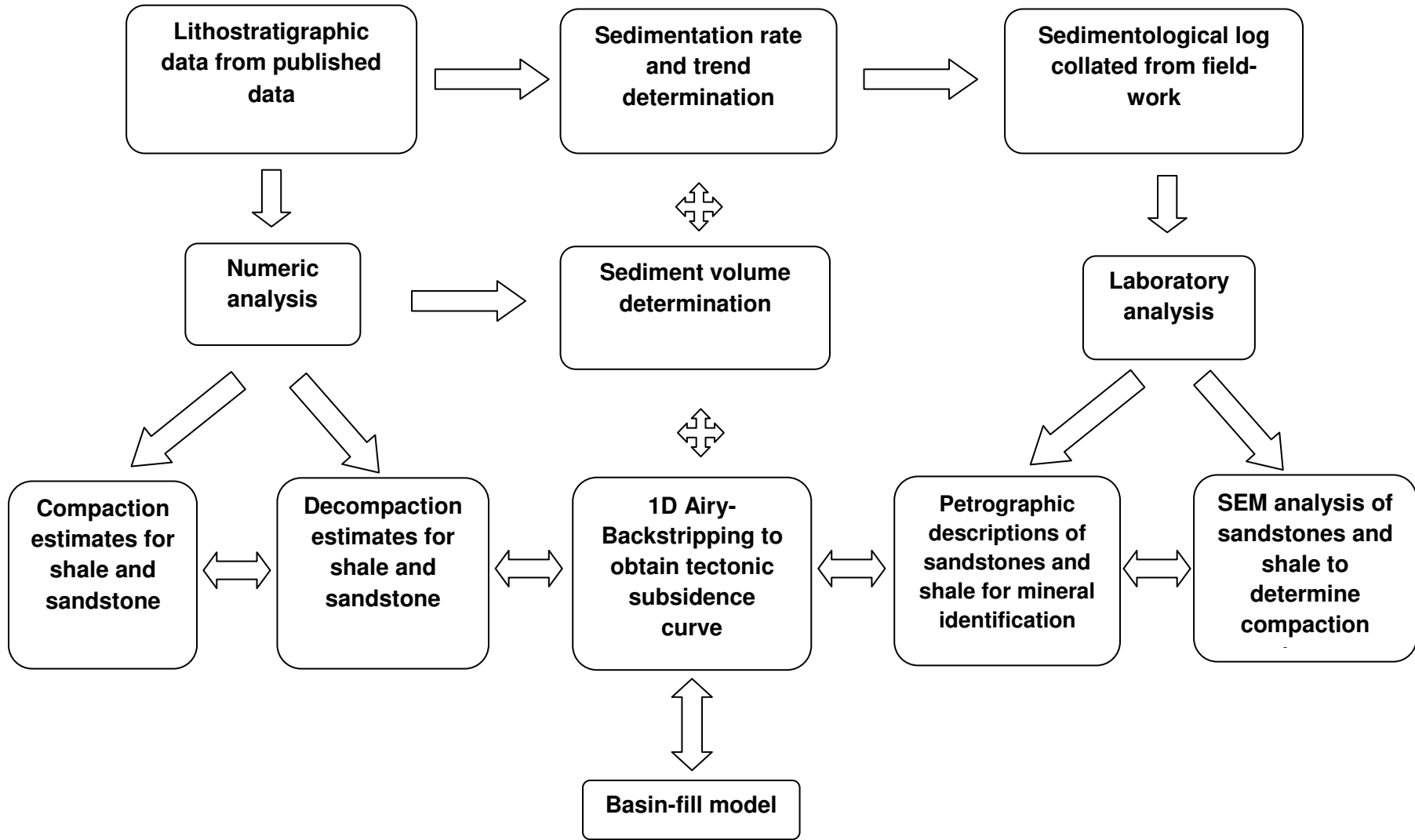


Figure 1.04: Flow chart of the methodology adopted in this study.

## CHAPTER TWO: REGIONAL GEOLOGY AND LITHOSTRATIGRAPHY

### 2.1 TECTONIC SETTING OF THE SW KAROO BASIN

The Karoo Basin is generally interpreted as a retro-arc foreland basin (Ryan and Whitfield, 1979; and Visser, 1987); and is bordered by an adjacent and prograding Cape Fold Belt (De Wit *et al.*, 1988; Johnson, 1991; and Catuneanu *et al.*, 1998). In addition, the Karoo Basin formed due to crustal shortening which was caused by subduction of the palaeo-Pacific plate beneath the Gondwana plate (Fig. 2.01: Lock, 1978, 1980; De Wit and Ransome, 1992). This interpretation of the Karoo Basin fits Ingersoll and Busby's (1995) definition of a retro-arc foreland basin, as a foreland basin on the continental sides of continental-margin arc-trench systems (which is formed by subduction generated compression and/or collision).

Furthermore, The Karoo foreland system is documented to have partitioned into foredeep and forebulge flexural provinces (Johnson *et al.* 1997), by a hinge-line which has been mapped for consecutive time-slices and documented to have migrated along-dip due to the redistribution of load in the CFB, from the end of the Carboniferous to the Triassic Period (Catuneanu *et al.*, 1998). Therefore, the intracratonic SW Karoo Basin is regarded as the foredeep region of the Karoo retroarc foreland system (Fig. 2.02).

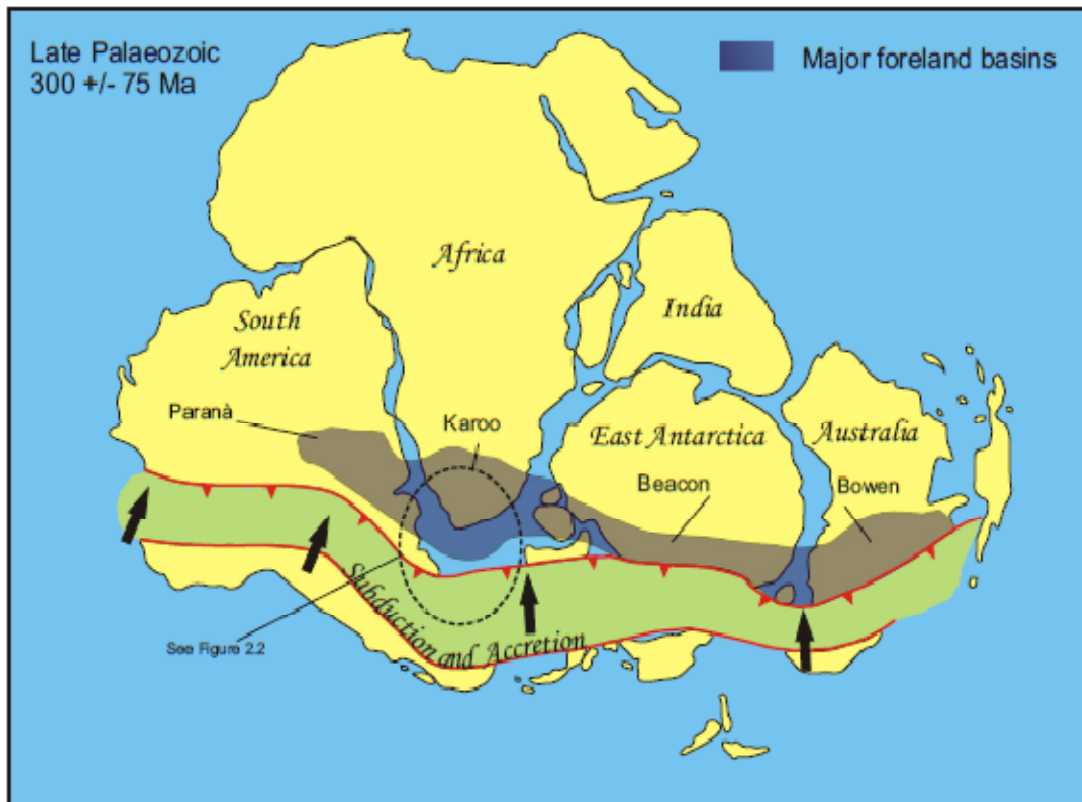


Figure 2.01: Karoo, Paraná, Beacon and Bowen Basins during accretionary tectonics along the southern margin of Gondwana (modified after De Wit and Ransome, 1992).



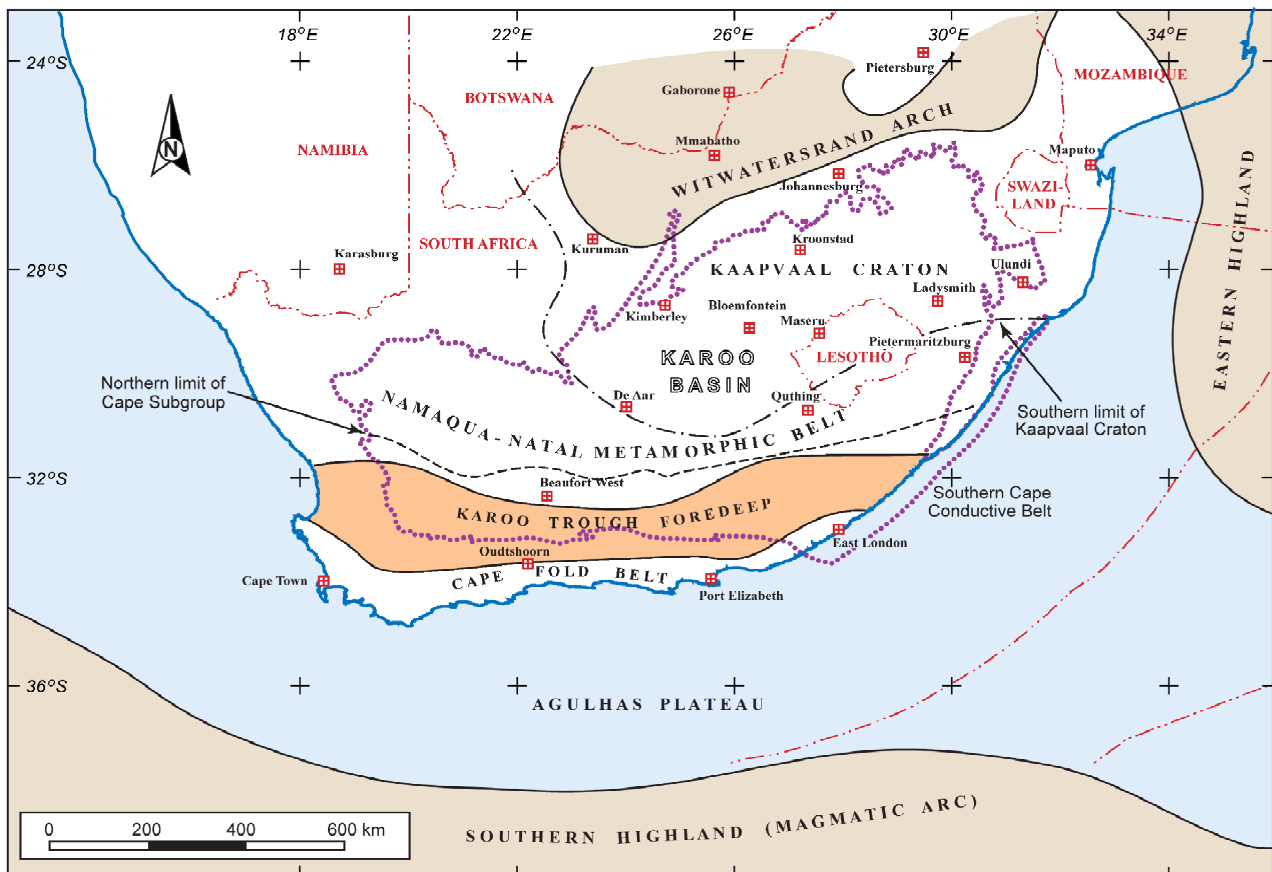


Figure 2.02: Map of the general tectonic setting of the Karoo Basin, indicating the SW Karoo as the trough foredeep (modified after Johnson et al., 1997).

## 2.2 STRATIGRAPHY AND DEPOSITIONAL SYSTEMS OF THE SW KAROO BASIN

The depositional system of the Karoo Basin evolved through a drainage-system change from endorheic to exorheic, whereby the basin was initially endorheic, with a closed drainage system that retained water and allowed no outflow outside the basin, thereby ensuring active sedimentation throughout the basin. Afterwards when the basin changed to exorheic marine incursion occurred over the foredeep region. At the southern margin of the Karoo Basin, contemporaneously with marine incursion, thrust loading of the lithosphere (CFB) caused a localized rapid deepening of the Karoo foreland basin (Cole, 1992). This led to restriction of clastic sedimentation (i.e. sequences of mudstone, siltstone, sandstone and minor conglomerate) to the Karoo foredeep.

### 2.2.1 Cape Supergroup

The Cape Supergroup succession overlies Pre-Cape rocks belonging to the late Proterozoic Gariiep, Saldania and Mozambique Provinces. The latter are composed of gneisses, schists, quartzites and metamorphosed carbonates. A deep-seated magnetic feature with low electrical resistivity, called the Southern Cape Conductive Belt (SCCB), occurs as an east-west elongated anomaly between the Namaqua-Natal Belt and the Saldania Province (De Beer *et al.*, 1982). This zone, thought to consist of serpentinitised basalt (De Beer *et al.*, 1982), has been interpreted to be 30 km wide and 7 km below the surface, dipping south and obducted against the Namaqua-Natal Belt at 0.8 Ga. The Gariiep, Saldania and Mozambique Provinces, comprising meta-sediments, were periodically deformed by the Pan-African orogeny as a result of plate convergence. The final phase of development of these provinces lasted until 0.6 and 0.5 Ga, with the intrusion of syn- and post-tectonic granitoids of the Cape Granite Suite (CGS) into the oldest rocks of the Saldania Belt (Tankard *et al.*, 1982).

The Cape Supergroup is divided into three groups, which are, from youngest to oldest: the quartzites of the Table Mountain Group; the argillaceous fine grained sandstones of the Bokkeveld Group; and the shales and subordinate sandstones of the Witteberg Group (Fig. 2.03), totalling a 8000 m thick sequence of beach, deltaic and shallow marine clastic sediments (Fig. 2.04a). The Table Mountain Group consists of shale and sandstone with thin layer of Pakhuis tillite. The Bokkeveld Group consists of shale with interbedded sandstone sheets, while the Witteberg Group consists of the Witpoort Formation which is made up of local glacial diamictites on top, and the rest is sandstone with intercalations of shale. Therefore, in details the depositional environment changed progressively from shallow-marine and terrestrial for the Table Mountain Group to deltaic and shallow-marine shelf in the Bokkeveld and Witteberg Groups respectively (Tankard *et al.*, 1982). Subsequent deformation and metamorphism of the Cape Supergroup to lower green schist facies occurred during the late Palaeozoic/early Mesozoic (Broquet, 1992). The Table Mountain and Bokkeveld groups have the greatest areal occurrence and form the majority of the surface geology of the southern coastal area. In contrast, the Witteberg Group is limited to

the northernmost extent of the Cape Supergroup exposure (Fig. 2.04a, b &c) and is overlain unconformably to the north by the Late Palaeozoic/Triassic Karoo Supergroup (Tankard et al., 1982; Turner, 1999).

### **2.2.2 Karoo Supergroup**

Sedimentation in the Cape Basin was terminated at about 335 Ma (Middle Visean). Followed by a hiatus (end Visean to Late Westphalian) of approximately 23 million years (Fig. 2.03), which signifies the transition from the presumed passive margin Cape Supergroup succession to the overlying Dwyka glacial deposits of the Karoo Supergroup (Tankard *et al.*, 2009; Isbell *et al.*, 2008). This hiatus was due to a regional uplift and shortening that matches the mid-Carboniferous assembly of Pangaea (Veevers *et al.*, 1994). This involved the episode of subduction and shortening as the Deseado terrain rejoined the North Patagonian massif at 330-314 Ma (Pankhurst *et al.*, 2006) after a period of early Palaeozoic separation, a scissor-like closure and fundamental change in regional crustal dynamics. Simultaneously, as this hiatus occurred in the Karoo Basin, the southern part of Gondwana migrated over the South Pole resulting in a major ice-sheet over the early Karoo Basin and surrounding highlands (Fig. 2.04b), and glacial sedimentation in both upland valley and shelf depositories resulted in the basal Karoo Dwyka Group (Smith, 1990).

The Karoo Supergroup in the SW Karoo Basin is divided into three Groups, namely:

- The Dwyka Group (Westphalian to early Permian in age);
- The Ecca Group (Permian shallow and deep marine successions); and
- The Beaufort Group (Permo-Triassic fluvial sediments).

The seaway transgression into the interior part of the SW Karoo Basin was during the deposition of the Dwyka and Ecca Groups, and later at the end of Ecca time complete regression occurred from the limits of the preserved basin. The bathymetric conditions of this interior seaway changed from deep marine during the Dwyka–lower Ecca interval, to shallow marine during the

upper Ecca time (Visser and Lock, 1978). Biostratigraphic correlations across the main Karoo Basin using palynomorphs in the Ecca Group (McRae, 1992) and vertebrate fossils in the Beaufort Group (Kitching, 1977; Keyser and Smith, 1979) have highlighted the diachroneity of most of the lithostratigraphic units within these strata.

### **Dwyka Group**

Gondwana glaciation is represented in South Africa by glacial Dwyka Group deposits which are the first and oldest Karoo Supergroup sediments in the Karoo Basin, and overlies the Cape Supergroup unconformably or paraconformably. The Dwyka Group deposits are Late Carboniferous to Early Permian in age i.e. 302 - 290 Ma (Bangert *et al.*, 1999) and reflect deposition associated with deglaciation that extended into the Early Permian, and presumed to continue for ~ 30 m. yr. (Visser, 1990). The Dwyka Group consists of diamictite-rich Elandsvlei Formation, and a mixed facies – diamictite, mudrock, sandstone and conglomerate – Mbizane Formation, but only the former is present as rain-out deposits in the SW Karoo (Visser *et al.*, 1990). Here, it has a maximum thickness of 750 m and rests disconformably on the Witteberg Group (Table 2.1). Some researchers infer a marine setting for the deposition of part of glacial deposits (Cole, 1992; Johnson, 1997; Visser, 1997; Catuneanu *et al.*, 1998; Rubidge *et al.*, 2000); however, there is no unequivocal evidence for this, therefore it is possible that the bulk of the Dwyka sequence of the Karoo Basin was deposited in a terrestrial setting (Du Toit, 1926).

The glacial-influenced sediments were supplied (Fig. 2.04b) from both the northern continental highlands and the southern margin (Visser 1992). Ice-flow directions indicate sources to the north (Cargonian Highlands), east (Eastern Highlands now in East Antarctica), and southwest (Southern Highlands now in West Antarctica) (Visser, 1989, 1997); however, the presence of volcanic tuffs in parts of the upper Dwyka indicates the active magmatic arc to the south as its source region (Cole, 1992). The southern ice sheet expanded, probably due to uplift of the magmatic arc associated with a large-scale compression and folding episode recorded as the initial development of the CFB south of the Karoo Basin (Hälbich *et al.*, 1983; Gresse *et al.*,

1992). This most likely records the initiation of retro-arc foreland basin tectonics (Visser 1992, see Fig. 2.05). Therefore, changes in the location of active centres probably reflect changing climatic and/or tectonic conditions during the late Palaeozoic (Isbell, *et al.*, 2008).

### **Ecca Group**

Sedimentation of Ecca Group began in the late Artiskian, and is characterized by a marine transgression across the Karoo Basin. Increased subsidence of the Karoo Basin due to deposition of the Dwyka Group resulted in partial submergence of the Cargonian highlands and marine transgression deeper into the continent (Fig. 2.04c). At its maximum extent, this transgression is estimated to have extended about 1500 – 2000 km to the north past the edge of the CFB, with the depositional setting across most of the basin primarily silt-dominated marine diamictites with dropstones derived from floating ice in a shallow marine environment (Visser, 1991a, b; Cole, 1992) due to subsidence of the major sediment source (i.e. Cargonian highlands). This sedimentation suggests deposition from suspension in a relatively low energy environment (Tankard *et al.*, 1982).

In the SW Karoo Basin, the Ecca Group comprises an approximately 1300 m thick, conformable succession of siliciclastic rocks, lying between the glaciogenic Dwyka Group and the terrestrial Beaufort Group (Fig. 2.03). Furthermore, the transition from glacial (Dwyka) to post-glacial (lower Ecca) sedimentary environments occurred much earlier in the south-western than in the northern and eastern parts of the Karoo Basin as did the transition from lower delta-plain (upper Ecca) to a fluvially dominated floodplain environment (lower Beaufort). However, it is possible that the only synchronous basin-wide sedimentary unit in the Karoo Sequence is the organic-rich Whitehill Formation of the Lower Ecca (Smith *et al.*, 1993), and Upper Ecca Group deposition began by Late Permian (Fig. 2.04d).

The lower three formations, Prince Albert, Whitehill and Collingham, are present throughout this south-western region, but the overlying formations are split into two successions, each being confined to separate depocentres i.e. Tanqua and Laingsburg; these sub-basins were

apparently formed when development of the Cape Fold Belt syntaxis (Fig. 2.06) led to the growth of a northeast-trending basin floor swell in the south-western corner of the present main Karoo Basin (De Beer, 1990; Wickens *et al.*, 1990). This may have been triggered by the second compressional paroxysm at the Cape Fold Belt dated at 278 Ma (Hälbich *et al.*, 1983).

### **Beaufort Group**

Inboard of the emerging CFB, the fining-upward continental succession of the Beaufort Group represents the final major stage of the SW Karoo Basin sedimentation in a variety of braided fluvial and subaerial systems (Fig. 2.04e) until the Early Triassic. In the SW Karoo Basin, the Beaufort Group has a maximum thickness of 3900 m (Cole and Wipplinger, 2001) and consists of a succession of reddish-maroon and greenish-grey mudstones and subordinate fine-grained, tabular and lenticular sandstones. It consists of a lower Abrahamskraal Formation up to 2500 m thick and an upper Teekloof Formation up to 1400 m thick, with its upper contact being eroded. The Abrahamskraal Formation is distinguished from the Teekloof Formation by the presence of chert beds, more abundant sandstone and a paucity of reddish-maroon mudrock (Cole and Smith, 2008). Palaeocurrent studies of the Beaufort Group indicate a centripetal drainage pattern of fluvial systems into the basin, of which a dominant northeast system and a minor east-southeast system were present in the SW Karoo Basin (Veevers *et al.*, 1994; Cole and Wipplinger, 2001). These latter systems emanated from source areas in the region of the CFB syntaxis (Fig. 2.04d and e).

### **Stormberg Group**

The Stormberg Group comprises of fluvial and aeolian-lacustrine successions of the Molteno, Elliot and Clarens Formations (Fig. 2.03 and Fig. 2.04f). Braided low-sinuosity Rivers deposited the sandstone-rich Molteno Formation, whereas high-sinuosity meandering rivers deposited the Elliot Formation. The Stormberg Group in the SW region is of Late Triassic-Early Jurassic age, and was deposited as a consequence of the final deformational phase in the CFB and subsidence of the SW Karoo Basin. Thus, the tectonic regime of the Karoo Basin region at this

time (Late Triassic-Early Jurassic Period) was still compressive and characterized by continued pulses of stress in the CFB (Hälbich *et al.*, 1983).

The Clarens Formation is overlain by the basaltic lavas of 1400 m thick Drakensberg Group (Fig. 2.04h) (Tankard *et al.*, 1982; Smith *et al.*, 1993; Johnson *et al.*, 1996; Turner, 1999); which forms the top of the Karoo sequence, and signify a halt in deposition as a consequence of regional uplift and erosion due to Gondwana breakup (Cole and Smith, 2008). Therefore, strata of the Beaufort Group and, to a far lesser extent, the Eccca Group, are intruded by Early Jurassic dolerite sills and dykes in the SW Karoo Basin. The strata are generally flat-lying north of latitude 32° 20'S, but increasingly become more intensely folded as the Southern Branch of the Cape Fold Belt is approached. In the extreme south, adjacent to the margin of the present CFB, the Eccca and Dwyka Groups have been folded into asymmetric mega folds with horizontal axes and large amplitude (Cole *et al.*, 1991). Folding took place during the Cape orogeny with deformation of the older strata beginning at about 258 Ma, the date of the third paroxysm (Hälbich *et al.*, 1983) and finishing at about 208 Ma, the date of the last phase of tectonics (Bordy *et al.*, 2004).

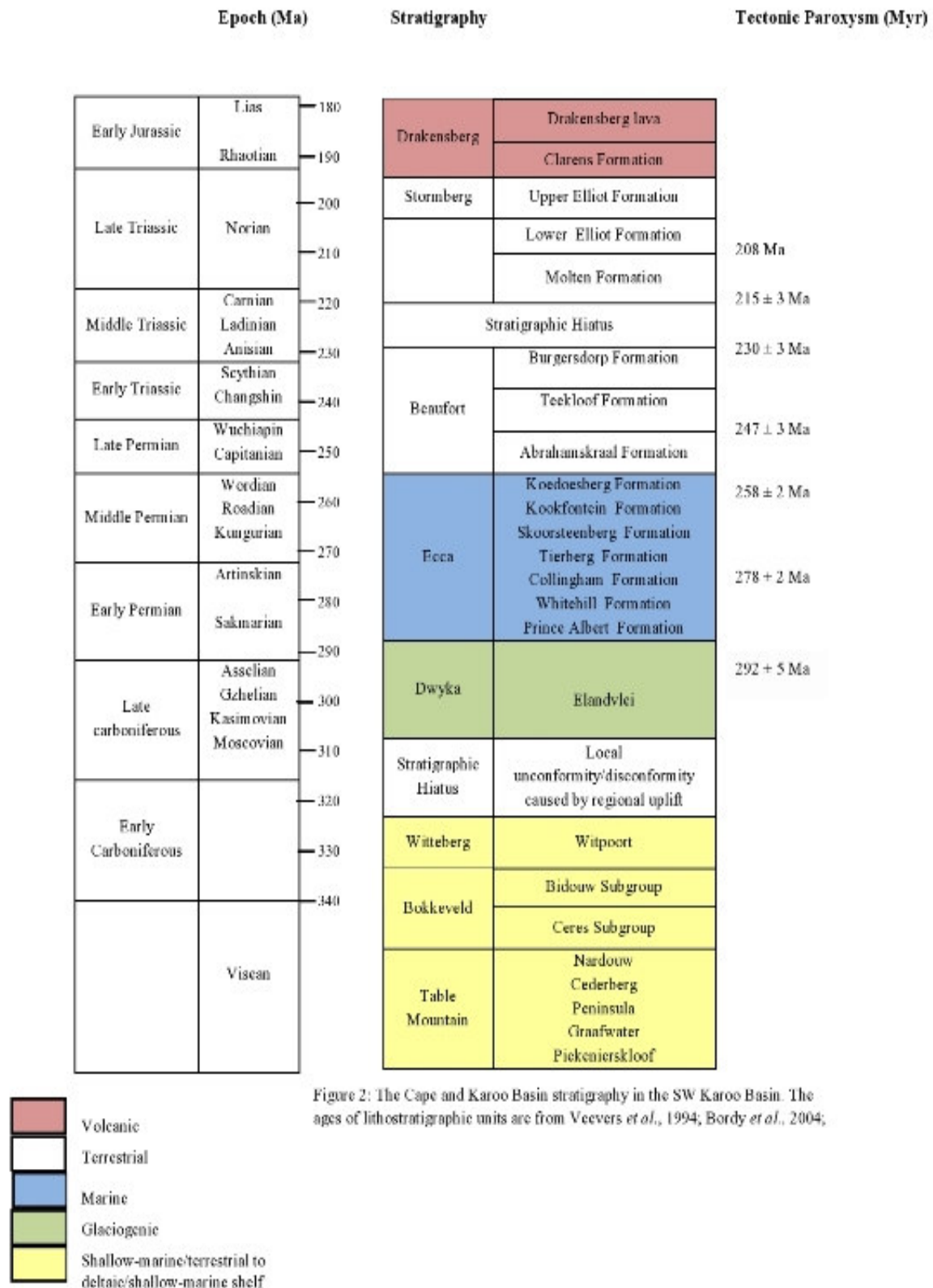


Figure 2: The Cape and Karoo Basin stratigraphy in the SW Karoo Basin. The ages of lithostratigraphic units are from Veevers *et al.*, 1994; Bordy *et al.*, 2004;

Figure 2.03: The Cape and Karoo Basin stratigraphy in the SW Karoo Basin. The ages of lithostratigraphic units are from Veevers *et al.*, 1994; Bordy *et al.*, 2004; Rubidge (2005) and Isbell *et al.*, 2008. The inserted rectangle marks the Tanqua depocentre stratigraphy and investigated time window. Ages on the far right are tectonic phases of the CFB according to Hälbig *et al.*, 1983.



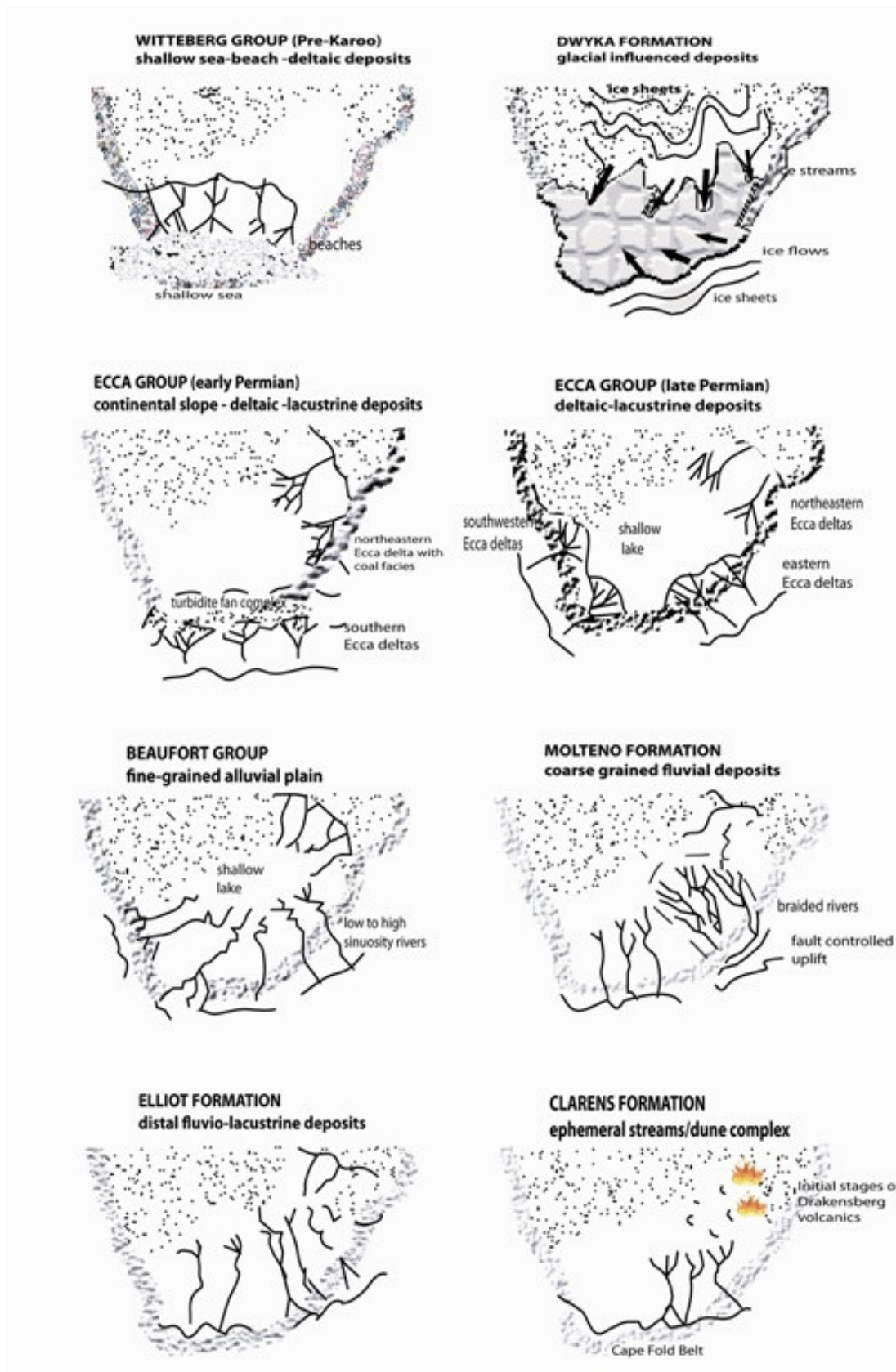


Figure 2.04: Simplified palaeogeographic models for major stratigraphic units of the Karoo sequence; modified after Turner (1980), Visser *et al.* (1980).

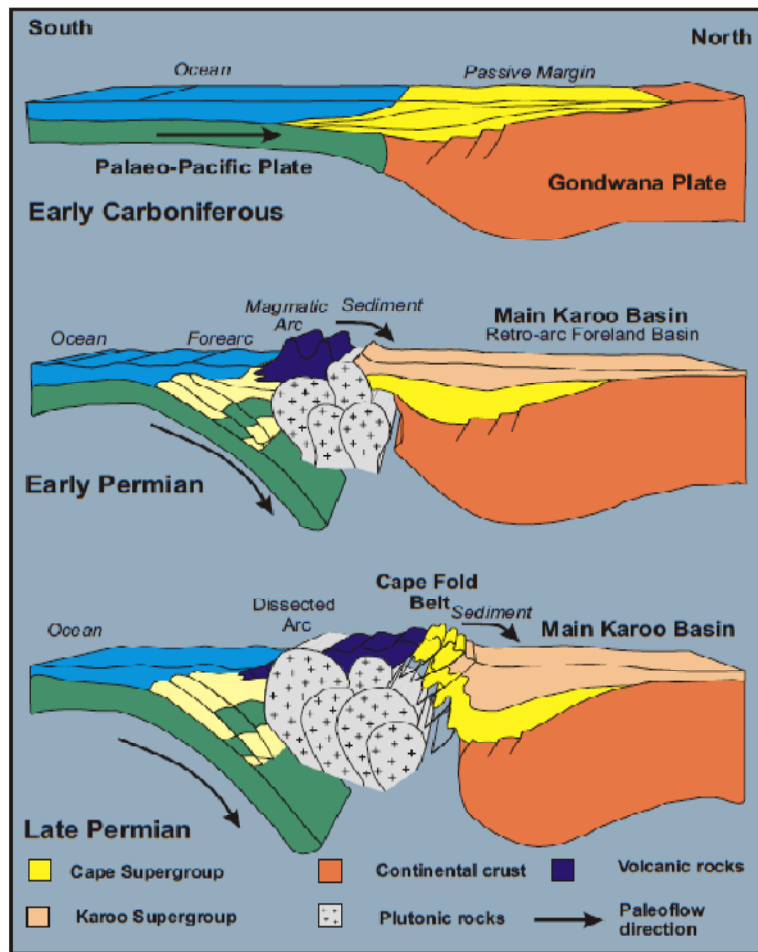


Figure 2.2 Schematic sections across southwestern Gondwana, illustrating the evolution of the main Karoo Basin and Cape Fold Belt (modified from Johnson, 1991).

Figure 2.05: Schematic representation of the three-stage Evolution of the southern part of the Cape-Karoo Basin, from the Early Carboniferous to Late Triassic (modified after Johnson et al., 1991).

### 2.3 STRUCTURAL SETTING OF THE SW KAROO BASIN

The Tanqua and Laingsburg depocentres are local subbasins which developed in the SW Karoo Basin, and are bordered by the adjacent Cape Fold Belt (CFB); a continuous and arcuate mountain chain that borders the western (N-S-trending western branch) and southern (E-W-trending southern branch) sides of the SW Karoo Basin. The northeast trending Hex River and Baviaanshoek mega anticlinorium syntaxial folds (north of Worcester Fault see Fig. 2.06)

separates these two depocentres and played a significant role in their evolution and depositional patterns (De Beer, 1990).

The arc of the CFB syntaxis proposed to have emerged as early as the 278 Ma tectonic event (Hälbich *et al.*, 1983) is reflected in the north-western to south-western paleo-coastline for Tanqua depocentre and the generally east- west coastline orientation along the southern margin of the Laingsburg depocentre (Kingsley, 1977; Theron, 1973; and Visser *et al.*, 1980). Some previous interpretation of the palaeogeography of the SW Karoo Basin describes the Tanqua and Laingsburg depocentres as contemporaneous subbasins separated by a syntectonic structural high, and that the oroclinal bend in the CFB aided the focusing of sediment into the SW Karoo Basin (Wickens, 1994; Scott and Bouma, 2003). However, structural (King, 2005) and stratigraphic (Flint *et al.*, 2004 and Wild, 2005) fieldwork has led to a new correlation for the Tanqua and Laingsburg depocentres sediments; suggesting that the Tanqua and Laingsburg depocentres represent temporally and spatially distinct depocentres within the SW Karoo basin, rather than subbasins divided by an intra-basinal high, with coeval sedimentation (Wickens, 1994).

### **2.3.1 Deposition within the Laingsburg and Tanqua depocentre**

Flint *et al.* (2004) proposed that the deposition of gravity flow sandstones initially occurred within the Laingsburg depocentre at approximately 268 Ma. In support of this, King (2005) proposed that the CFB arc aided the focusing of sediment into the bend of the fold belt so that sediment entered the SW Karoo Basin from the area close to the Hex River antiform, which is the Laingsburg, and at this time, the Tanqua depocentre was experiencing pelagic shale deposition.

In addition, King (2005) suggested that the subsequent to deposition in the Laingsburg depocentre, northward migration of the deformation front increased strains in the CFB and created larger amounts of uplift and greater structural elevation of fold structures, therefore, causing the uplift and subsequent 'blockage' of the sediment route into the Laingsburg depocentre (King, 2005) (Fig. 2.07c and d). Consequently, sediment was re-routed north-

eastwards between the hinge-line terminations of the Hex river and Bontberg antiforms into the Tanqua depocentre (Fig. 2.07c and d), and at this time, the Laingsburg depocentre became sand-starved.

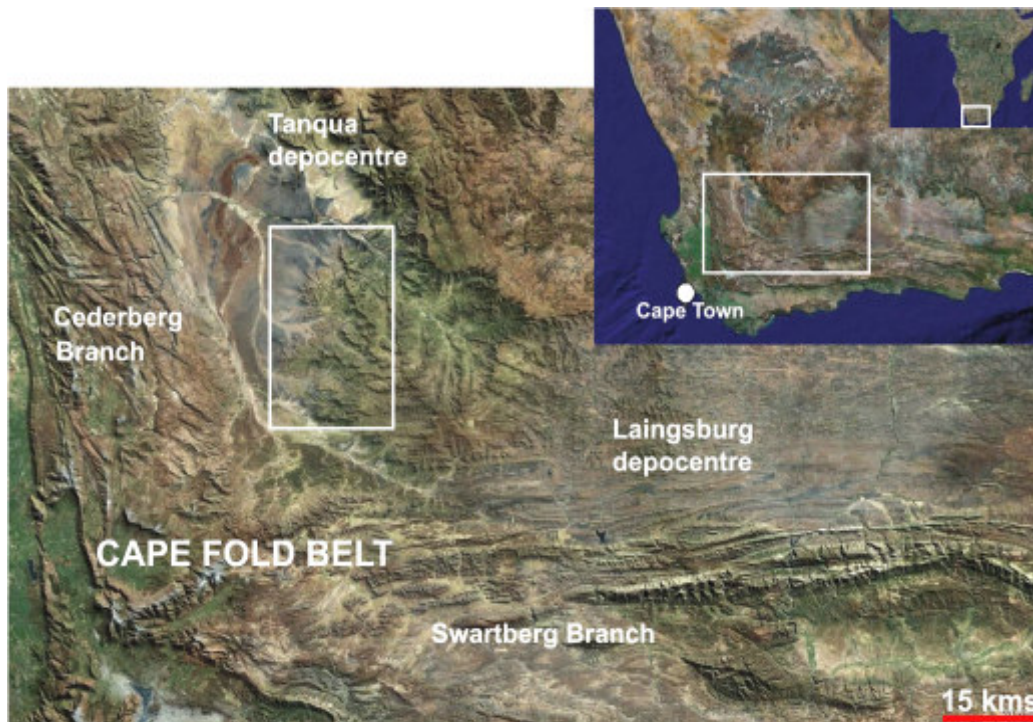


Figure 2.06: Landsat image of SW Karoo Basin, with the Tanqua and Laingsburg depocentres marked. An oroclinal bend in the Cape Fold Belt (CFB) bounds Tanqua depocentre to the west (roughly N-S trending Cederberg branch) and Laingsburg depocentre to the south (E-W trending Swartberg branch). Landsat image from: <https://zulu.ssc.nasa.gov/mrsid/>



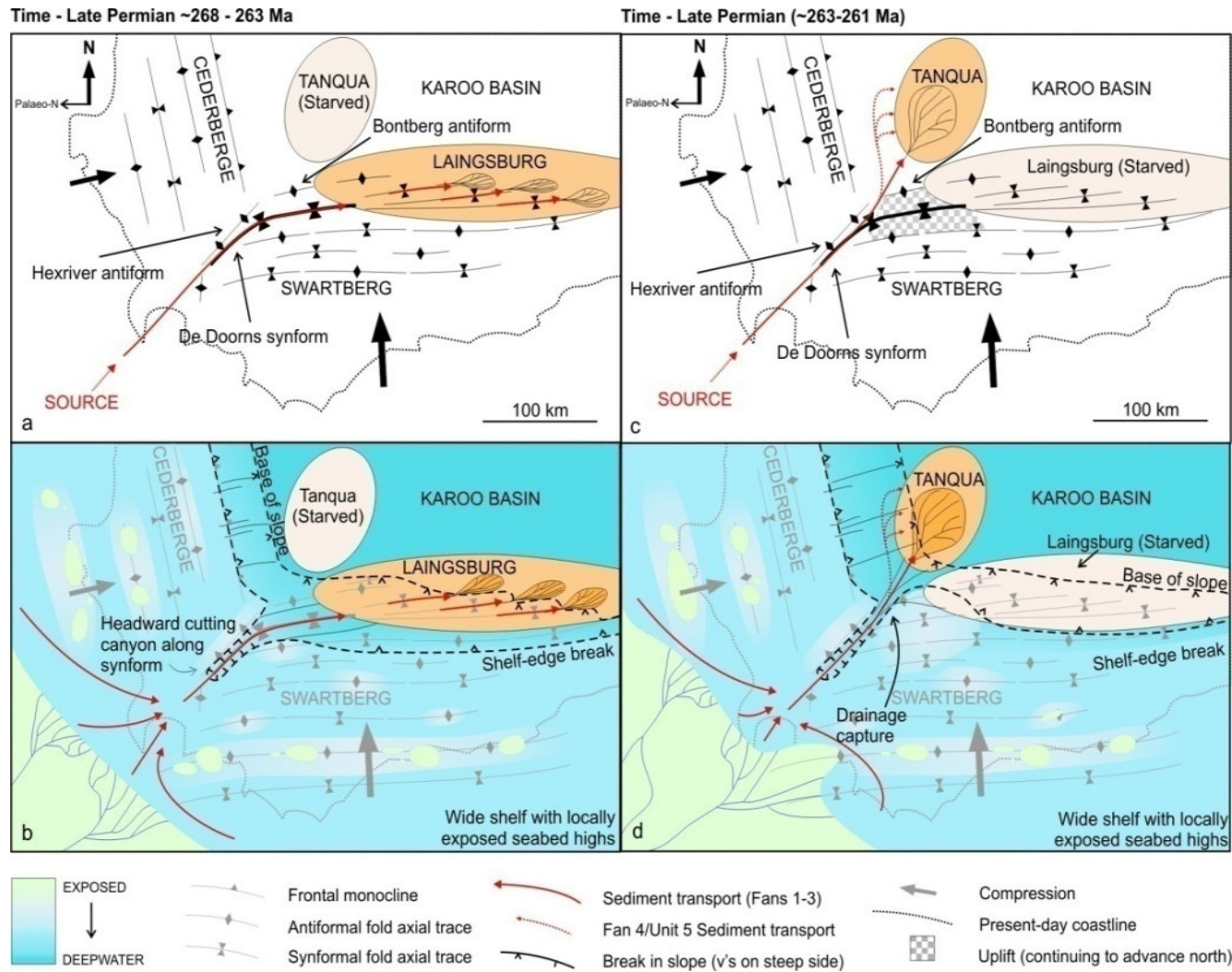


Figure 2.07: Palaeogeographic reconstruction of the SW Karoo basin during deposition in the Laingsburg (a & b) and Tanqua depocentre (c & d) (from King, 2005).

## 2.4 CORRELATION AND CHRONOSTRATIGRAPHY OF THE TANQUA AND LAINGSBURG DEPOCENTRE

Previous studies of the Tanqua and Laingsburg depocentres (Scott *et al.*, 2000; Scott and Bouma, 2003; Wickens 1994; Wickens and Bouma, 2000) suggest that shallow and deepwater deposition was broadly coeval between the two depocentres (Fig. 2.08). It was proposed that the five exposed turbidite units in the Tanqua depocentre correlate to turbidite units in the Laingsburg depocentre. For example, fan systems 1-4 and Unit 5 of the Skoorsteenberg Formation in the Tanqua depocentre have been correlated with Fan A and Units B-E of the Laingsburg Formation in the Laingsburg depocentre respectively using lithostratigraphy (Wickens, 1994; Wickens and Bouma, 2000).

However, a recent correlation consisting of stratigraphic interpretations by Flint *et al.* (2004) and structural analysis by King (2005) proposes that both depocentres represent temporally and spatially distinct depocentres within the early Karoo Basin, rather than contemporaneous submarine fan accumulations in adjacent depocentres divided by a basement high (Wickens, 1994). Furthermore, geochemical study by Flint *et al.* (2004) shows that the bulk of deepwater deposits (Vischkuil and Laingsburg Formation) in the Laingsburg depocentre are older than the deepwater deposits (Skoorsteenberg Formation) in Tanqua Depocentre (Fig. 2.09). In addition, Flint *et al.* (2004) proposes a sequence hierarchy (Fig. 2.10) that assigns the whole deepwater section and Kookfontein Formation of the Tanqua depocentre to a 3<sup>rd</sup> order highstand systems tract; which according to Miall (1990) is defined to be partly of glacio-eustatic origin or related to regional tectonics caused by global changes in spreading rates. On the other hand, a revised correlation of the Karoo deepwater stratigraphy of both depocentres by Hodgson (2004) presents a fence diagram representing deposition of the Laingsburg Formation deepwater succession as time-equivalent to condensed shale of the deepwater Tierberg Formation in the Tanqua depocentre (Fig. 2.11).

TANQUA DEPOCENTRE		LAINGSBURG DEPOCENTRE	
<b>LOWER BEAUFORT GROUP</b>			
<b>ECCA GROUP</b>	Koedoesberg Formation	Waterford Formation	<b>PERMIAN</b>
	Kookfontein Formation	Fort Brown Formation	
	Skoorsteenberg Formation	Laingsburg Formation	
	Tierberg Formation	Vischkuil Formation	
	Collingham Formation		
	Whitehill Formation		
	Prince Albert Formation		
<b>DWYKA GROUP</b>			

Figure 2.08: Illustration of the correlation between the Permian depositional sequence (i.e. deepwater to deltaic) in the Tanqua and Laingsburg depocentre SW Karoo Basin.

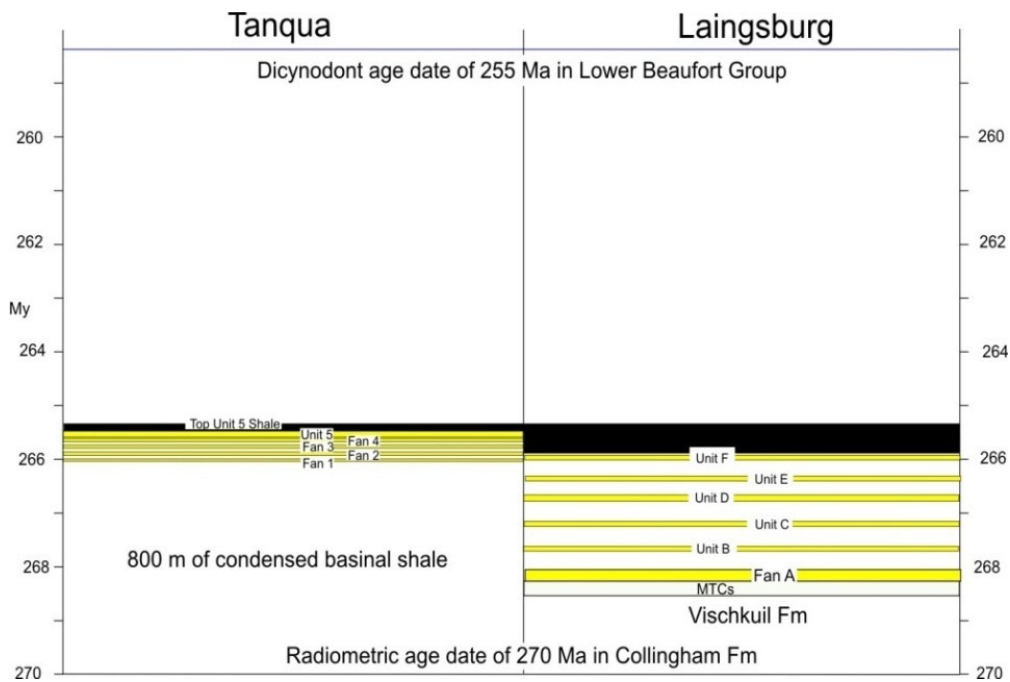


Figure 2.09: Chronostratigraphic or Wheeler diagram based on the assumptions of shale depositional rates outlined above (modified after Flint et al., 2004).

Although, the chronostratigraphic reconstruction of both depocentres by Flint *et al.*, (2004) appears to be of limited accuracy due to the absence of biostratigraphic dates within the deepwater succession, it does provide a useful relative duration control on the Tanqua and Laingsburg succession, provided that the fundamental assumption of constant sedimentation rates is true.

Furthermore, according to Flint *et al.*, (2004), the 800m condensed section indicated in figure 2.09 serves as a marine hiatus and is interpreted as an indication of rapid sea-level rise, causing sediment starvation in the basin-floor caused by temporary entrapment of the detritus in the overlying shallow-water delta complexes. However, this interpretation is erroneous, due to possible confusion between allocyclic and autocyclic causes for the event in the stratigraphic record. In addition, there is a potential for error in determining the positions of sequence boundaries from a vertical succession of lithofacies.



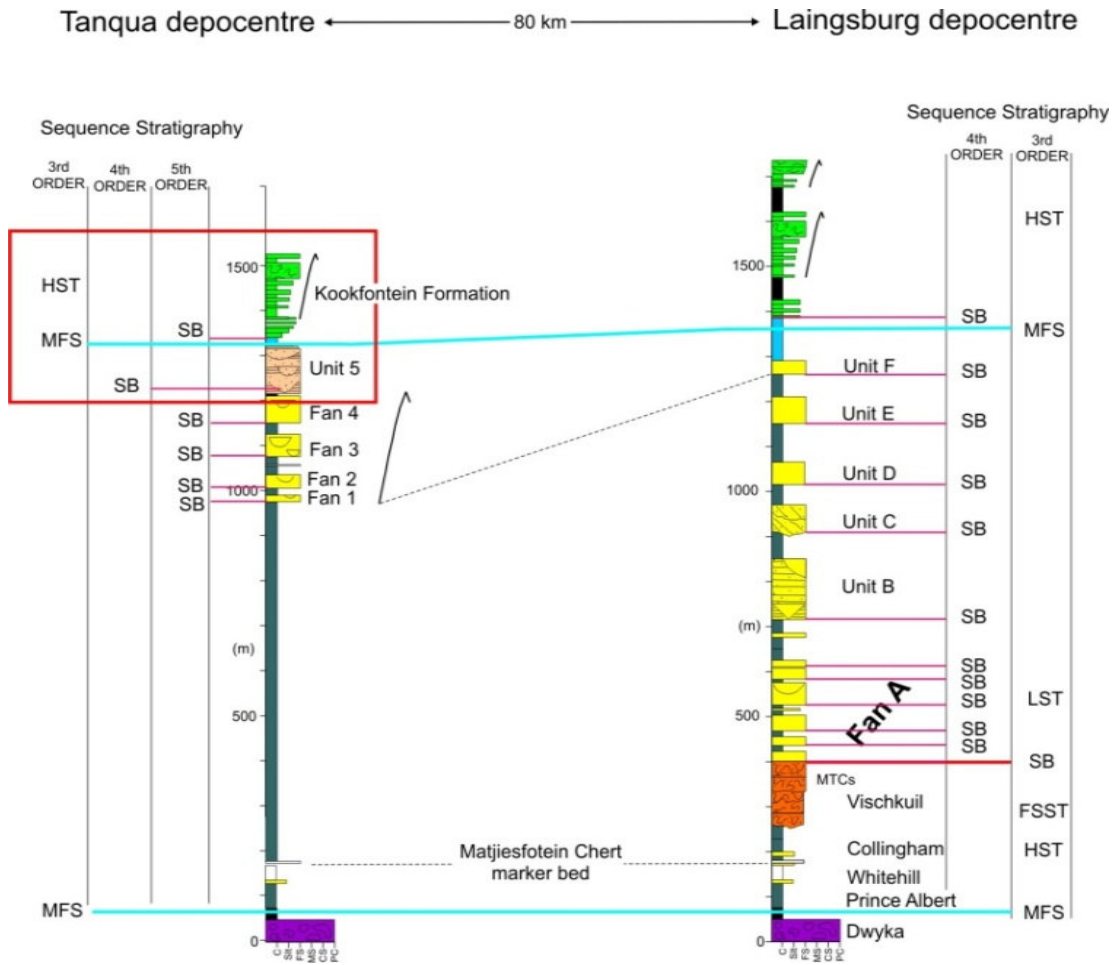


Figure 2.10: Correlation of the Laingsburg and Tanqua depocentre deepwater successions; the red box signifies shallow water successions of Tanqua depocentre, while simplified and idealised logs are shown (after Wild, 2005).

Tanqua depocentre

Laingsburg depocentre

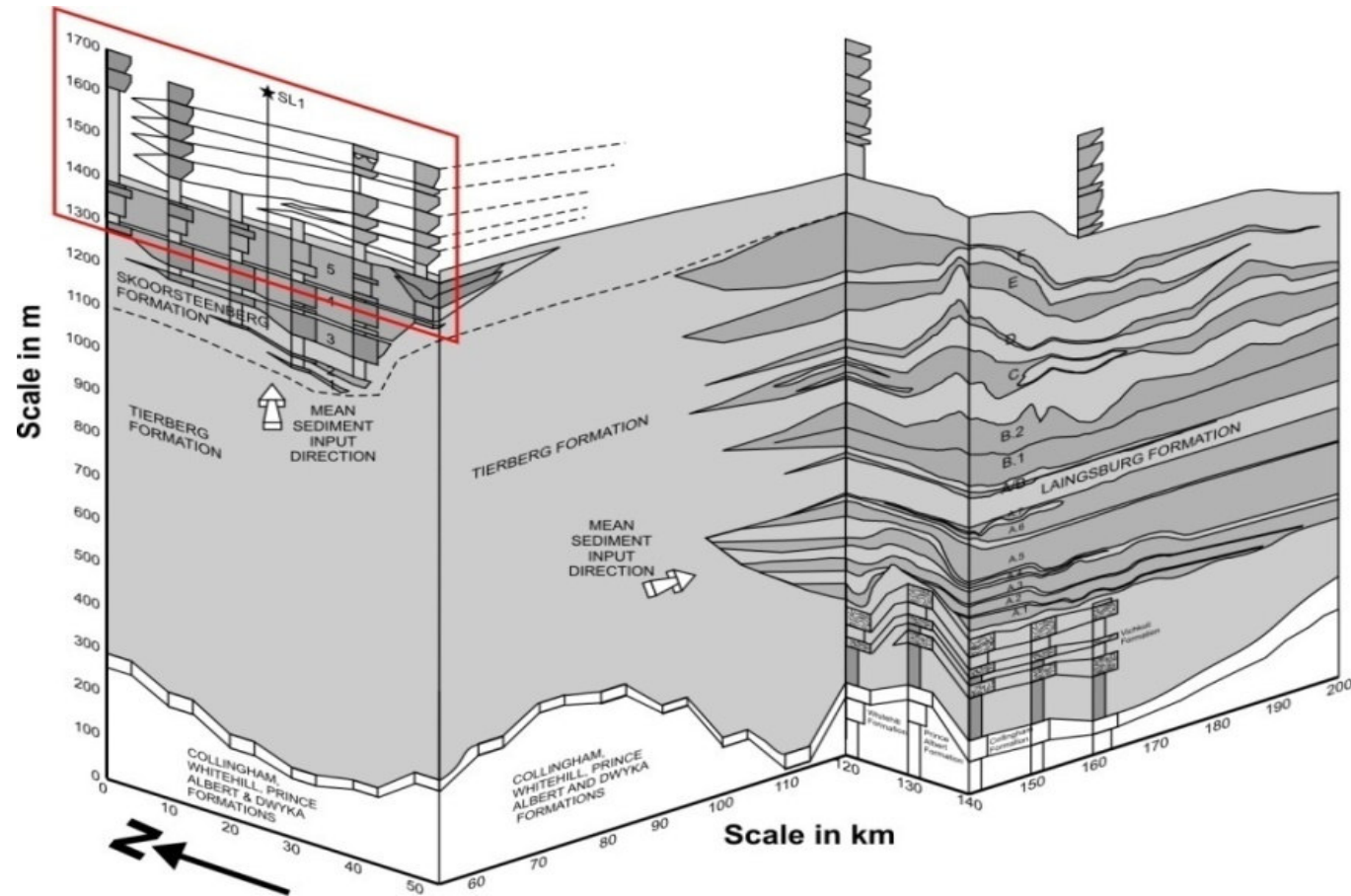


Figure 2.11: Fence diagram showing the revised correlation of the Karoo deepwater stratigraphy between the Laingsburg and Tanqua depocentres, the study area is boxed (after Hodgson, 2004).

## 2.5 LITHOSTRATIGRAPHY OF THE TANQUA DEPOCENTRE (STUDY AREA)

The Tanqua depocentre preserves an exceptionally well-exposed siliciclastic basin-floor to shelf-edge succession (Fig. 2.12 and 2.13). The Lithostratigraphic units of the Tanqua depocentre include the basal Dwyka Group glacial deposits, the three lowermost Ecca Group Formations (marine-shale of Prince Albert and Whitehill Formations, and the distal Collingham Formation mudrock deposited by mud-rich turbidity currents) deposited regionally in the SW Karoo Basin (Fig. 2.13). These SW regional units are overlain by the Tierberg Formation dark shale, which is succeeded by the Skoorsteenberg Formation i.e. a thick succession of five deep-water sand-rich submarine fan complexes separated by fine-grained intervals (Bouma and Wickens, 1991; Wickens, 1994; and Bouma, 1997). The Skoorsteenberg Formation is overlain by the Kookfontein, followed by the Koedoesberg Formations, both representing the deltaic portion of the basin-fill (Wild, 2005), and finally capped by the Abrahamskraal Formation fluvial system sandstones representing the palaeoshoreline.

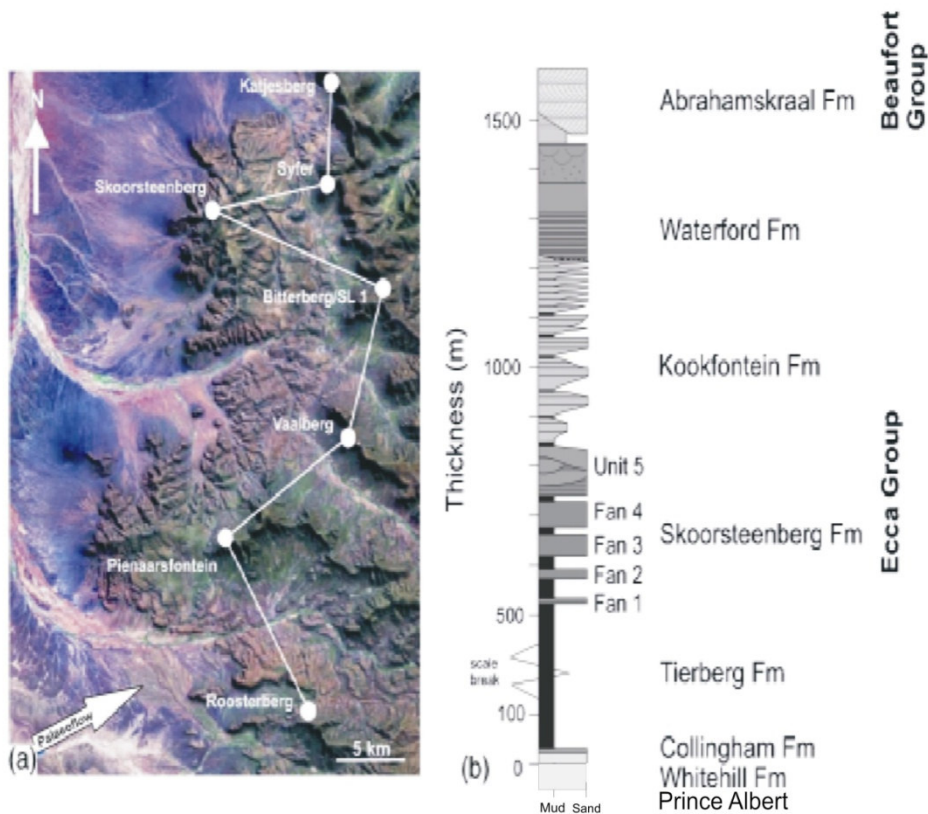


Figure 2.12: (a) Enlarged satellite image of the study area showing locations of key outcrops along the 40-km-long escarpment. Note depositional dip is towards the NE. (b) Schematic stratigraphic log of the Permian to earliest Triassic deep marine to fluvial fill of Tanqua depocentre. Note: the lithostratigraphic units are overlying the basal glacial deposits of the Dwyka Group (after Wild, 2005).

### 2.5.1 Dwyka Group

The basal glaciogene sedimentation occurred in a back-arc basin (Visser, 1990) during the late Carboniferous and early Permian, when the passive margin in the basin was depressed beyond a critical limit and no isostatic adjustment occurred (Visser, 1991). Therefore, this depression could possibly be what defined the Karoo Basin architecture. Final melting of the marine ice sheet resulted in a major transgression, and the subsequent infilling of the basin by prograding deltas was accompanied by a major regression. The deglaciation sequence recorded the first major marine transgression in the Karoo Basin at 302 Ma (Bangert *et al.*, 1999) probably due to sea level rise from melting ice sheets, while the Dwyka styles of subsidence continued into the Ecça period in an underfilled marine basin with anoxic bottom waters.

### 2.5.2 Prince Albert Formation

The lowermost Prince Albert Formation has a maximum thickness of 165 m and consists of dark grey shale, siliceous shale and subordinate silty rhythmites (Visser, 1991; Cole, 2005). The shale is the result of suspension settling of mud and the silty rhythmites represent turbidites i.e. sands deposited by tractional fall-out from turbidity currents (Visser, 1991). The lower part of the formation represents the final phase of deglaciation of the overlying Dwyka Group (Visser, 1997) and the presence of marine invertebrate fossils and phosphorite are indicative of marine conditions (Visser, 1992b). The water was relatively deep and the basin was considerably larger than its present size (Visser, 1993; Veevers *et al.*, 1994). A Sakmarian to Artinskian age is indicated (Bangert *et al.*, 1999; Turner, 1999; and Gradstein *et al.*, 2004).

### 2.5.3 Whitehill Formation

The Whitehill Formation has a thickness between 20 and 80 m in the SW Karoo Basin, with the latter being in the Tanqua and Laingsburg depocentre, and consists predominantly of black, carbonaceous shale, forming a conspicuous white-weathering marker horizon (Cole and McLachlan, 1991; and Visser, 1992). The black, organic-rich shale is thought to represent suspension-setting of mud under reducing conditions. Other fossils include palaeoniscid fish and a crustacean, *Notocaris tapscotti*. The palaeoenvironment remains unresolved with some researchers proposing a marine water body (Oelofsen and Araujo (1987) in Cole and Smith, 2008; Visser, 1992b), while others suggesting a non-marine, brackish water body with no connection to the world ocean (Cole and McLachlan, 1991; Veevers *et al.*, 1994).

The thin, black, fossiliferous mudrock horizon overlying the diamictite with an abrupt contact is interpreted as a marine condensed section (MCS) (Haq, 1991), which was deposited during a sea-level highstand. Although marine fossils are absent in the lower part of the Whitehill Formation, the Rb/K ratio of the shale suggests marine conditions (Visser, 1992ba). The lack of medium-grained sediment input into the basin and the strongly anoxic conditions can be attributed to a sea-level highstand.

#### **2.5.4 Collingham Formation**

The Whitehill Formation is succeeded by the Collingham Formation. The latter is up to 70 m thick and consists of alternating thin beds of dark grey siliceous mudrock and very thin beds of soft yellowish mudstone (K-bentonites), together with subordinate chert beds (Viljoen, 1994). The upper part of the formation ( $\pm$  40 m thick) comprises siltstone and very fine-grained sandstone, interbedded with mudrock and K-bentonites. The sediments were deposited by suspension settling of hemipelagic and pelagic detritus of aeolian origin, by underflow and overflow suspensions and from distal, low density, mud-rich turbidity currents (Viljoen, 1994). These deposits were periodically interrupted by the deposition of fall-out tephra (K-bentonites) and fine-grained turbidites, both being derived from the southwest. The latter are interpreted as basin plain and outer fan deposits that were derived from a source area to the southwest of the Karoo Basin (Viljoen, 1994). The lower part of the formation was deposited during a sea-level highstand (Visser, 1993), but deposition of the turbidites may have been associated with a local sea-level lowstand, which could have been caused by uplift of the southern edge of the Karoo Basin due to thrusting and folding of the Cape Fold Belt (Viljoen, 1994).

#### **2.5.5 Tierberg Formation**

The Tierberg Formation in the Tanqua depocentre is south of Calvinia and has a maximum thickness of 750 m (Wickens, 1984) and 600 m in SOEKOR borehole KLII65, thinning to about 400 m just north of Bloemfontein (Nolte, 1995). In SOEKOR borehole SA1166 a thickness of 1 252 m is present (Viljoen, 2005). The lithology is dark grey to greenish grey shale with interbedded thin siltstone and very fine- to fine-grained sandstone towards the top of the formation, forming coarsening upward cycles. Distinguished from overlying units by the lack of sandstone and from underlying units by the scarcity of altered tuffs (where it overlies the Collingham Formation) and/or absence of white-weathering, black carbonaceous shale (where it overlies the Whitehill Formation). Deposition of mud from suspension was the dominant sedimentary process and water depths most likely did not exceed 500 m (Visser and Lock, 1978) during a sea-level highstand (Visser, 1993).

### **2.5.6 Skoorsteenberg Formation**

The Skoorsteenberg formation is approximately 400 m-thick and composed of five deep-water turbidite fan system almost completely exposed over 650 km<sup>2</sup> consisting of sandstone-rich units up to 65 m thick separated by shale units (Wickens, 1994). The formation thins out in a northerly and easterly direction. A progradational trend can be seen in the approximately 400 m thick succession, from distal basin-floor (Fan 1) through basin-floor sub-environments (Fans 2, 3 and 4) to a slope setting for unit 5 (Wickens and Bouma, 2000). Deposition was unrestricted in the broad, open style N-S trending Tanqua depocentre and the sandstones are very fine- to fine-grained.

Fan deposition is believed to have been controlled by fluctuations in relative sea level, probably caused by local tectonic or isostatic factors rather than eustatic changes (Wickens, 1994). The duration of cyclic deposition for the entire basin-fill may be as little as 3 to 5 million years (Visser, 1990), favouring eustatic dominance over high-frequency or pulsating tectonics. The separate but simultaneous formation of the fans rather suggests a lowering of sea-level which, possibly together with tectonically induced unstable slopes, were the triggering mechanisms for fan development. The abrupt termination of each fan cycle indicates a sudden cut-off in sediment supply which could have been caused by switching of the input system or a sea-level rise (Wickens, 1990). Sparse tuff beds present in the shale units reflect continuous but very mild volcanic activity in the southern magmatic arc area.

### **2.5.7 Kookfontein Formation**

In the Tanqua depocentre, the succeeding Kookfontein Formation ( Fig.2.03) is about 250 m thick and consists of dark-grey shale and siltstones followed by alternating siltstone, shale and thin bedded, fine to very fine-grained sandstone beds that coarsen and thicken upwards and increase in frequency. This lithology represent proselyte sedimentation in a gradually shallowing water-body condition (Visser, 1993, Wickens, 1994), with the deltas prograding eastward the CFB from the west and southwest and filled in the rest of the depocentre. According to Wild



(2005) cycles 1-13 of the Kookfontein Formation are interpreted to represent individual sequences contained within a series of progradational and aggradational sequence sets that represent the deposits of a slope to shelf succession.

#### **2.5.8 Koedoesberg Formation**

The overlying the Kookfontein is the 200 m-thick Koedoesberg Formation which comprises fine-grained tabular sandstones alternating with grey shale or rhythmite beds. These represent deposition on large, highly constructive deltas that prograded from the west (Wickens, 1994). Deposition occurred during the Wordian i.e. mid Permian (Rubidge, 2005) under shallowing water/subaqueous conditions (Fig. 2.13), as sedimentation exceeded subsidence (Visser, 1993).

#### **2.5.9 Abrahamskraal Formation**

The Abrahamskraal Formation represents a transition regime involving a change from lower delta-plain (characterised by bay-fill sequences, channel-fill sequences, crevasse and levee deposits) to upper delta plain sedimentation (characterised by predominantly overbank/mudflat deposition) and therefore represents a palaeoshoreline (Figure 2.13). The exposed upper delta plain sediments were deposited behind the prograding delta lobes (Rubidge, 2005), and by now the Tanqua and Laingsburg depocentres had been filled with subaqueously-deposited sediments and were no longer effective as separate depositories. Hence, the Abrahamskraal Formation was deposited under subaerial conditions; and evidence of this is shown by the presence of calcareous nodules and desiccation cracks.



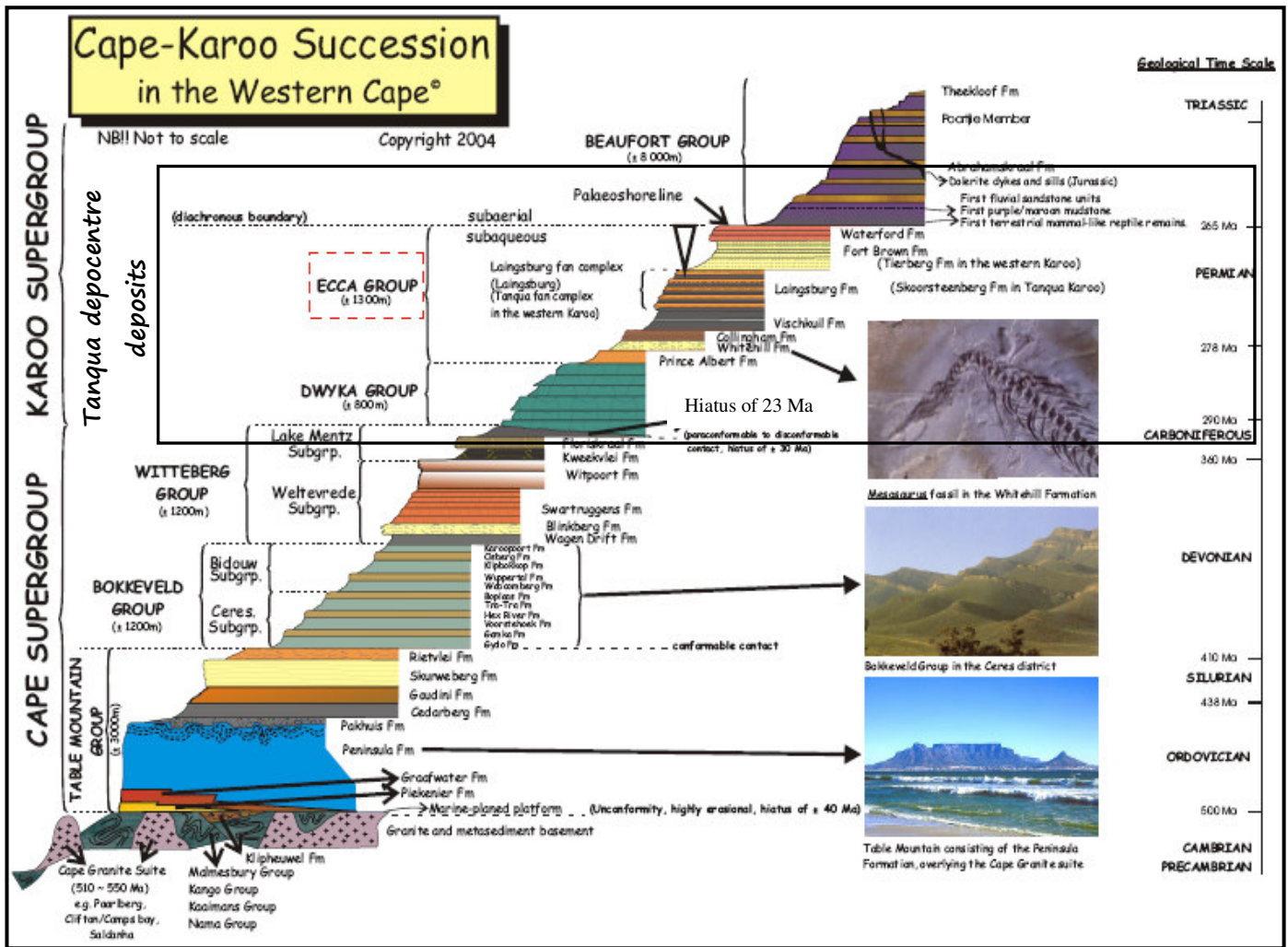


Figure 2.13: Schematic representation of the stratigraphy of the Cape and Karoo Supergroups (modified after Vander Merwe, 2003).

## CHAPTER THREE: METHODOLOGY AND DATABASE

### 3.1 CONCEPT OF THE BACKSTRIPPING TECHNIQUE

The main objectives of this project which is to determine the subsidence history of Tanqua depocentre, is best achieved through a tectonic subsidence analysis. The tectonic subsidence analysis technique was originally described by Sleep (1971) and extensively discussed by Watts (1978) and Van Hinte (1978). It is generally applied to recent or undeformed ancient sedimentary basins (Frostick and Steel, 1993). The subsidence of a sedimentary basin can be mainly attributed to three processes, namely: tectonic subsidence, water and sediment loading, and sediment compaction. Tectonic subsidence is the subsidence of the basement in the absence of water and sediments and it is controlled by tectonic forces associated with the basin formation and evolution; water and sediment loading refers to the effect of the weight of water and sediments in the basin; while sediment compaction refers to decrease in sediment volume as they are buried and compacted. The shape and magnitude of these three components of subsidence can be estimated from well logs, borehole and outcrop sections using the “backstripping” technique (Allen and Allen, 1990; Watts, 2001). This technique removes from each layer the effects of sediment compaction, water and sediment loading, thereby producing a tectonic subsidence curve on the time vs. sediment thickness graph.

The purpose of this methodology is to use stratigraphic and palaeobathymetric data to quantitatively estimate the depth that basement would be in absence of sediments and water loading. This depth provides a measure of the unknown ‘tectonic driving forces’ that are responsible for basin formation. This process involves the removal of the youngest sequence and correcting the next older one for compaction; the influence of isostasy is removed and iteration is done to generate time series. The steps used in the backstripping technique are further explained below.

### 3.1.1 Decompaction

Compaction is a very important parameter to be considered in tectonic subsidence and burial history analysis. Different lithologies will undergo different compaction during burial; hence, differential compaction is a function of varied porosities, overburden, and the ability of the individual grains to be re-arranged. Consequently, basin analysis or modelling from decompacted sediment age-thickness curves is a powerful tool to reconstruct the geodynamic evolution of sedimentary basins (Steckler and Watts, 1978; Beaumont, 1981).

Decompaction is the running of a unit's compaction history in reverse, and this is achieved by considering sedimentary rock as a mixture of sedimentary grains and interstitial pores. The volume of sediment grains remains constant while the water is squeezed out during compaction from the overlying sediment load. Initially, the subsidence history diagram is simply a graphical representation of the burial history, but the total subsidence is equal to the sum of all vertical movement, including tectonic and sediment load subsidence (Sediment load is derived from unit composition and porosity).

$$\rho_{\text{rock}} = \phi(\rho_{\text{pore H}_2\text{O}}) + (1 - \phi)(\rho_{\text{grains}}) \quad [1]$$

$$\rho_{\text{sed}} = \sum_{i=1}^n \frac{(\rho_{\text{rock } i})(\text{THI } i)}{S} \quad [2]$$

$$\text{Sed. load subsidence} = Z_t \left[ \frac{\rho_{\text{sed}} - \rho_w}{\rho_m - \rho_w} \right] \quad [3]$$

The equation and model components below are used to quantify sediment load:

*Where:  $\phi$  = porosity*

*$Z_t$  = column thickness,*

*$\rho$  = density*

*$S$  = total decompacted thickness =  $\sum$  (THI)*

$THI$  = decompacted thickness of interval

$$= [(1 - \varphi) / (1 - \varphi_{init})] * Z_i$$

With:  $\varphi_{init}$  for: Sandstone = 0.5, Shale = 0.6, and Limestone = 0.7

### **Density**

$\rho_{sed}$  = density of sediment column (weighted average)

$\rho_w$  = density of pore water = 1 g/cm<sup>3</sup>

$\rho_m$  = density of mantle = 3.33 g/cm<sup>3</sup>

### **Grain densities**

$\rho_{grains}$  for Sandstone = 2.65 g/cm<sup>3</sup>,

Limestone = 2.72 g/cm<sup>3</sup> and

Shale = 2.72 g/cm<sup>3</sup>

The parameters (initial porosity and solid density) of the different lithologies have been taken from Sclater and Christie (1980), as they suppose an exponential decrease in porosity with depth depending on the lithology of the rock in question. In addition, according to Van Hinte (1978), rock porosity is assumed to follow an exponential relationship with depth as given by the following porosity function:

$$\Phi = \Phi_0 e^{-cz} \quad [4]$$

Where  $\Phi$  = porosity at any depth  $z$ ;  $\Phi_0$  = porosity at the surface;  $c$  = lithological compaction coefficient; and  $z$  = depth in kilometres.

The equation used for the decompaction approximation method after Van Hinte, (1978) is given as:

$$T_d = [T_p (1 - \Phi) / (1 - \Phi_0)] \quad [5]$$

Where  $T_d$  is the decompacted thickness,  $T_p$  is the present thickness of the vertical section;  $\Phi$  is the final/present porosity and  $\Phi_0$  is the unconsolidated/initial porosity. The thickness of the decompacted unit depends on present day (i.e. compacted) thickness and porosity, and the porosity when the unit was near the surface at the time of deposition. Alternatively, an estimate of this porosity can be obtained by "sliding" a unit up an idealized porosity vs. depth curve (fig. 3.1).

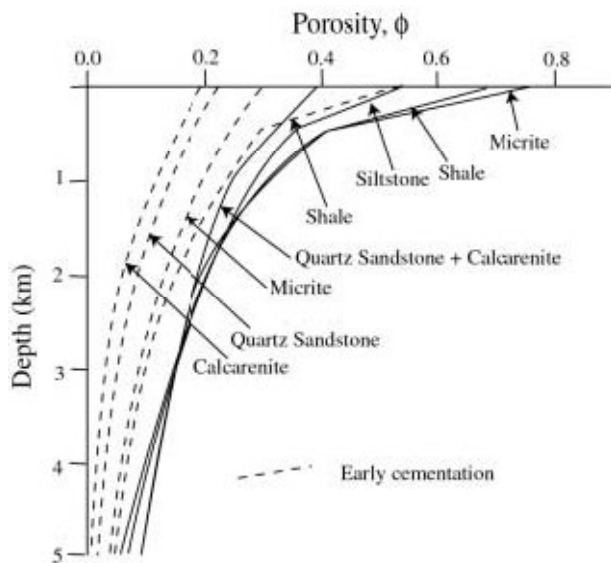


Figure 3.01: Summary of idealized porosity vs. depth curves for different lithologies. Note: the combination of sandstone and Calcarenite (a limestone with sand-grade sized grains) did not undergo early cementation; hence it's far away position (after Bond and Kominz 1984).

\*Syn depositional and early cementation commonly refers to changes occurring during burial up to a few hundred metres, where elevated temperatures are not encountered. The diagenetic system is partially open in this zone because of the exchange of dissolved constituents with the overlying water body and the underlying strata (Einsele, 2000).

To backstrip multiple layers there is need to "restore" all the stratigraphic units in a sequence for each time step - decompacting the younger units and compacting the older ones. The procedure is illustrated in Figure 3.2. The tectonic subsidence is calculated from the sediment thickness and the average density of the entire sedimentary sequence at a particular time.

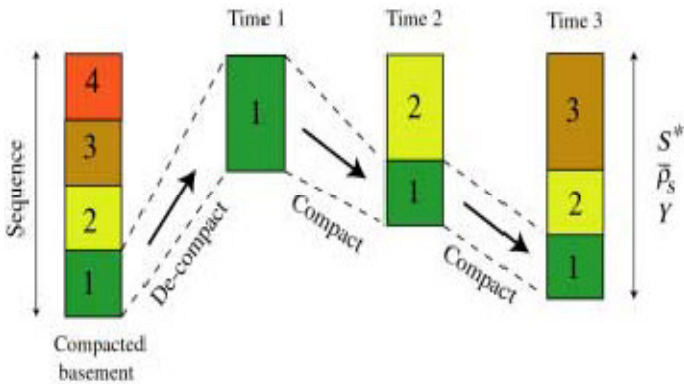


Figure 3.02: Schematic diagram explaining how multiple sediment layers can be backstripped

The total thickness  $S^*$  is easily obtained by summing all the individual thicknesses. In the case of the density, the mass of the total thickness must sum the masses of all the individual stratigraphic units within it and so that the equation below is obtained:

$$\bar{\rho}_s S^* = \sum_{i=1}^n \left[ \rho_w \phi_i^* + \rho_{gi} (1 - \phi_i^*) \right] S_i^* \quad [6]$$

Where  $n$  is the total number of stratigraphic units in the sequence at a particular time. It follows then that:

$$\bar{\rho}_s = \frac{\sum_{i=1}^n \left[ \rho_w \phi_i^* + \rho_{gi} (1 - \phi_i^*) \right] S_i^*}{S^*} \quad [7]$$

Finally, the total tectonic subsidence or uplift 'Y' can then be obtained by substitution in the backstripping equation.

$$\therefore Y = W_d + S^* \left[ \frac{(\rho_m - \bar{\rho}_s)}{(\rho_m - \rho_w)} \right] - \Delta_{sl} \frac{\rho_m}{(\rho_m - \rho_w)} \quad [8]$$

Where  $W_d$  and  $\Delta_{sl}$  are the water depth and sea-level height respectively at a particular time.

### 3.2 STUDY AREA AND DATA AVAILABILITY

The Tanqua depocentre SW Karoo Basin is extensive and well-exposed (Fig. 3.3). The main outcrops within the Tanqua depocentre are the Katjiesberg Mountain situated in the north, Skoorsteen Mountain in the northwest, Bitterberg Mountain in the northeast,

Pienaarsfontein in the southwest, Roosterberg Mountain in the South, and Hangklip Mountain at the extreme south (Fig. 3.4). These outcrops show distribution of facies and sand-body architecture.

### **3.2.1 Stratigraphic relationships and lithologies**

The Tanqua depocentre strata are structurally almost undisturbed, except for gentle folding, occasional reverse, and thrust faulting with minor displacements over the southern and central area, sedimentation is halted by prominent dolerite dykes and sheets of Early Jurassic age occur in the northern part of the outcrop area (Fig. 3.5). Interpretation of the depositional environments of the deltaic succession has been described initially using the Pienaarsfontein area as a type section (Wild, 2005). He documented a Permian siliciclastic lower slope to shelf succession in a delta-fed, relatively low relief margin with a grain size ranging from fine grained sand to clay. Sedimentological and stratigraphic studies done on the 250m thick Kookfontein Formation slope to shelf succession are interpreted to exhibit a shallow-water deltaic system, that builds out on the shelf until it reaches the shelf break and evolves into a deep-water deltaic system (Wild, 2005). A three-dimensional facies analysis (Patel – *in preparation*) should reveal the precise nature of the depositional system of the deltaic deposits. Furthermore, the underlying point-sourced basin floor fans (Fans 1 - 4) and the lower slope channel complex (Unit 5) in this system have been documented in detail previously (Wickens, 1994; Johnson et al., 2001; Van deer Werff and Johnson, 2003; Wild *et al.*, 2005; Hodgson et al., 2006; Luthi *et al.*, 2006).

### **3.2.2 Dating estimates**

Absolute dating of the lithostratigraphic units in the Tanqua depocentre is difficult, due to interpretation of the diachroneity of clastic sedimentation, diachronous evolution and subsequent foreland basin migration across the Karoo Basin. Below are some of the ages proposed by previous authors. For the basal glacial diamictites of the Dwyka Group, a Late Carboniferous age (302 - 290 Ma - Pennsylvanian to Early Sakmarian) was proposed by Gradstein *et al.* (2004) and Bangert *et al.* (1999). For the lower Ecca Group successions, Bangert *et al.* (1999); Turner,

1999; and Gradstein *et al.* (2004) further proposed a Sakmarian to Artinskian age for the Prince Albert Formation. Visser (1992, 1993) suggested that the Whitehill muds were deposited during a sea-level highstand under restricted oceanic circulation, whereas Cole and McLachlan (1991) suggested a maximum water depth of 80 m within the photic zone, with anoxic conditions being restricted to below the basin floor beneath benthic microbial mats.

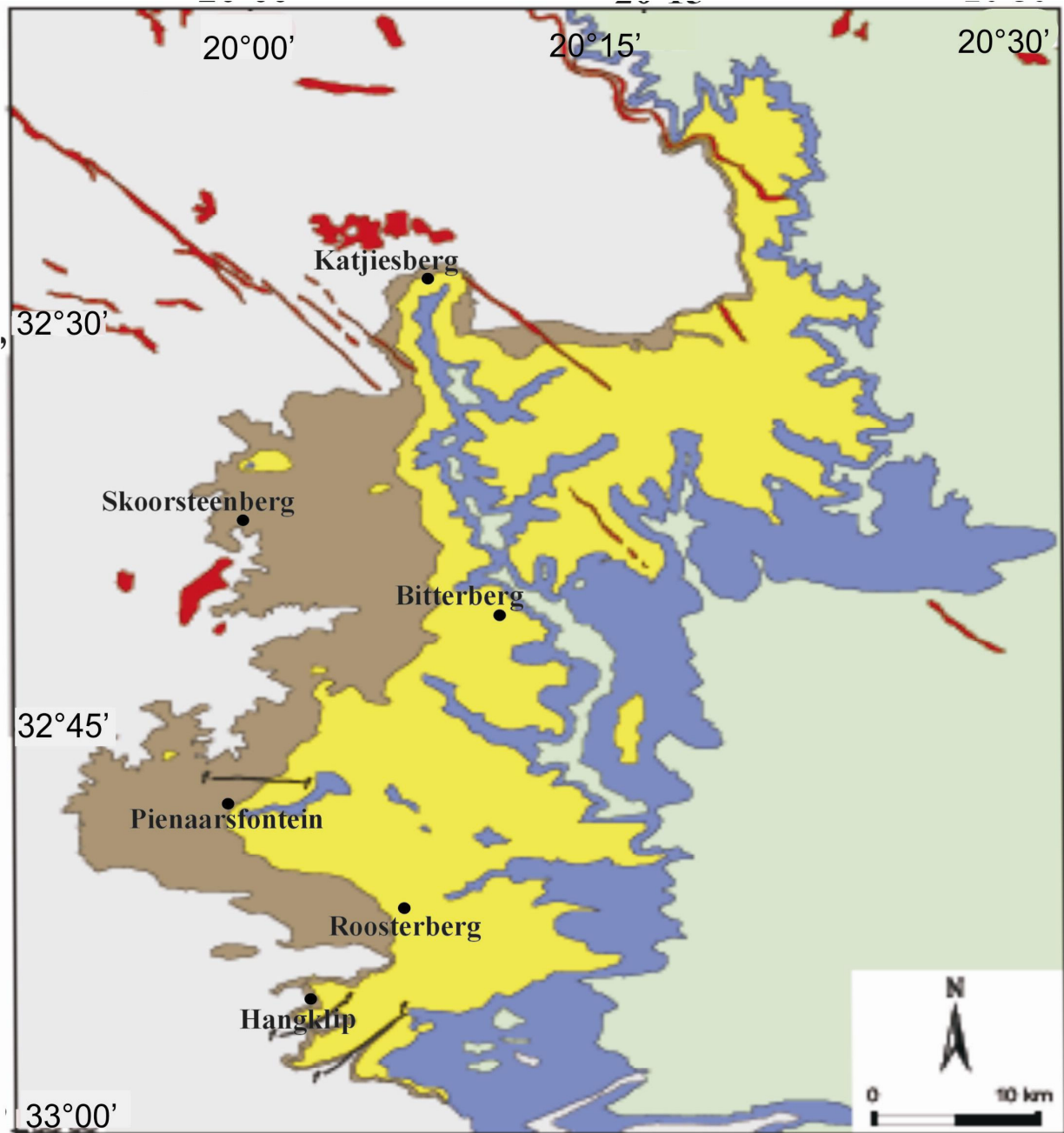
Turner (1999) dated zircons from tuffs (K-bentonites) in the lower part of the Collingham Formation, thereby suggesting a Roadian age of  $270 \pm 1$  Ma to the formation. In support of this age, a  $278 \pm 2$  Ma age was obtained on bentonitic layers in the equivalent Irati Formation, Paraná Basin, Brazil (Santos *et al.*, 2006). Therefore, the age of the Tierberg Formation is probably Roadian/Ufimian i.e. earliest Middle Permian (Viljoen, 2005) since the underlying Collingham Formation has been dated at  $270 \pm 1$  Ma, i.e., Kungurian (latest Early Permian), while a Kazanian/Wordian (middle Permian) age can be assigned to the Eodicynodon Zone at the base of the Beaufort Group (Rubidge, 1995).

There is a fair degree of error in the chronostratigraphic values, this is simply due to the ages being based on lithostratigraphic subdivisions (i.e. Formations), and as such are likely diachronous to some extent. However, the age ranges used in this study for the Tanqua depocentre shown in table 3.1 represent the best synthesis presently available. Therefore, it was decided that the age ranges assigned to units in the study should be chosen from Veevers *et al.*, 1994; Bordy *et al.*, 2004; Rubidge (2005) and Isbell *et al.*, 2008 for the purpose of accuracy of the thicknesses, ages and lithological descriptions (Table 2.1 and 3.1) for the SW Karoo and Tanqua depocentre rocks. This selection was based on personal communication with Dr Doug Cole at the Council for Geoscience, Bellville; who strongly criticised the accuracy of the above listed ages for the lithostratigraphic units in the Tanqua depocentre.





Figure 3.03: Photograph of the extensive and well exposed outcrops of the Tanqua depocentre, SW Karoo suitable for three dimensional facies analysis. Note the deepwater to shelf deposits of the Eccca Group exposed in Tanqua depocentre.



**Geological legend**

Mesozoic	Jurassic
	Permian
Paleozoic	

Lithostratigraphy		Lithology	
KAROO SUPERGROUP	BEAUFORT GROUP	Abrahamskraal Fm	Mudstone, Siltstone, Sandstone, thin cherty beds
	ECCA GROUP	Koedoesberg Fm	Sandstone, Siltstone, Mudstone, Shale
		Kookfontein Fm	Shale, Siltstone, thin Sandstone beds
		Skoorsteenberg Fm	Sandstone, Siltstone, Shale
		Tierberg Fm	Shale
		Dolerite	

Figure 3.04: Geological map of Tanqua depocentre, southwestern Karoo Basin. Note: Geological information are compiled from the Clamwilliam 3218 and Sutherland 3220 maps (1:250 000 scale), Geological survey of South Africa.

UNIT	THICKNESS* (m)	DEPTH (Km)	AGE* (Ma)	LITHOLOGIES
Surface	50	0.05		Fictitious
Abrahamskraal Formation	500	0.55	240–266	Sandstone
Koedoesberg Formation	200	0.75	266-268	60% sandstone / 40% shale
Kookfontein Formation (top)	250	1.00	268-269	60% sandstone / 40% shale
Skoorsteenberg Formation (Fan 1-4 & Unit 5)	400	1.40	269-270	90% sandstone
Tierberg Formation	750	2.15	270-271	90-95% shale / 5 -10% siltstone and sandstone
Collingham Formation	70	2.22	271-272	Siltstone/mudstone
Whitehill Formation	80	2.3	272-278	Shale
Prince Albert Formation	165	2.465	278-290	Shale
Dwyka Group	300	2.765	290-302	Glacial Diamictite

Table 3.1: The lithostratigraphic units deposited in the Tanqua depocentre; \*the ages and thicknesses of the units are from Veevers *et al.*, 1994; Bordy *et al.*, 2004; Johnson, *et al.*, 2006; Rubidge, 2005; Viljoen, 2005; and Isbell *et al.*, 2008.

### 3.3 DECOMPACTION OF LITHOSTRATIGRAPHIC UNITS IN TANQUA DEPOCENTRE

To calculate the decompacted thicknesses for each unit, average lithological compaction coefficients for five main lithologies (i.e. sandstone, shale, limestone, dolomite and shaley sand) from Frostick and Steel (1993) given in table 3.2 have been considered for the lithostratigraphic units in Tanqua depocentre. The percentage of decompaction for all the lithostratigraphic units is determined as the total decompacted thickness divided by the total compacted thickness of the section. The reason for this is to obtain which section decompacted more and which one less.

Sand/shale ratios of the main lithologies (sandstone, mudstone, siltstone and shale) were determined for each lithostratigraphic unit in Tanqua depocentre by dividing the total thickness of sandstone in a section by the total thickness of the section itself. Beds with silt and sand intercalations and having indistinct grain-size classification, are assumed to be about half sands, half silt - silty shale; and half the thickness of the sand/silt beds was added to the total sandstone thickness. The sand/shale ratio was determined for each individual package so as to define which facies to assign. The parameters (initial porosity, porosity scale height, and solid density) of these lithologies have been taken from Sclater and Christie (1980).

LITHOLOGY	INITIAL POROSITY $\bar{\alpha}_0$	COMPACTION COEFFICIENT $C(Km^{-1})$	DENSITY $\bar{\rho}$ (g/cm <sup>3</sup> )	REFERENCE
Shale	0.63	0.51	2.72	Sawyer et al. (1982)
Sandstone	0.56	0.39	2.68	Schmoker and Halley (1982)
Limestone	0.51	0.52	2.71	Sclater and Christie(1980)
Dolomite	0.31	0.22	2.85	Sclater and Christie(1980)
Shaley sand	0.56	0.45	2.70	Sclater and Christie(1980)

Table 3.2: Compaction coefficients and parameters for main lithological types (after Frostick and Steel, 1993).

### 3.4 DEPOSITIONAL WATER-DEPTH

Bathymetric estimations are mainly made from palaeontological and palaeoecological data, petrographical composition and sedimentary structures of rocks (Frostick and Steel, 1993). Relative global sea-level was low during the mid-Carboniferous ( $\pm 330 - 315$  Ma) (Vail et al., 1977), thereby terminating shelf deposition in the south-western Gondwana, the shelf areas were also exposed to erosion resulting in the dissection of the continental uplands by major river systems and the formation of an adjoining fairly flat-lying basinal plain (Visser 1992b). The bathymetric conditions of interior seaway into the Karoo Basin changed from deep marine (100 m), during the Dwyka–lower Ecca interval, to shallow marine (10 m) during the upper Ecca time (Visser and Lock, 1978). However, the data from literature are somewhat sparse or of insufficient reliability to enable sound evaluations of bathymetry.

The lack of marine body fossils in the southwest Karoo led some workers to propose a lacustrine setting for the Skoorsteenberg and Kookfontein Formations (Wickens, 1994; Scott *et al.*, 2000); however, the presence of marine trace fossils (Chondrites, Planolites, Palaeophycus, Thalassinoides, Ophiomorpha, Thalassinoides and Skolithos) and tidally influenced sandstones identified by Wild (2005) suggests a marine setting. The lack of marine faunas may signify a partially enclosed basin, and also that restricted oceanic circulation within a morphologically complex basin created anoxia conditions within the water column (Visser, 1992). Thus, it is proposed that the basin was not a fully open marine system (Wild, 2005). Furthermore, within the Karoo Basin, it is believed that mainly organic carbon-rich muds were deposited under anoxic conditions, and sedimentation within the Karoo foredeep was extremely slow ( $< 10$  m/Ma), thereby suggesting starved conditions. Also, the brackish to fresh Ecca basin ( $\pm 258 - 253$  Ma) formed a transition from an open to enclosed depository.

The water-level fluctuations in the southwest Karoo may be largely controlled by variations in the ice-volume covering this part of southwest Gondwana during the Palaeozoic. Therefore, data from the literature are sparse or of insufficient reliability to provide good estimates of the bathymetry for the Tanqua depocentre. Thus, in this study the effects of palaeobathymetry and

water-level fluctuations on the tectonic subsidence calculations are disregarded. Also not considered is the non-tectonic subsidence due to loading so was non-tectonic isostatic rebound due to removal of water; as these effects will contribute only small variations to the computed subsidence curves.

### **3.5 1- D AIRY BACKSTRIPPING**

In this study, the 1D Airy backstripping was done using a computer program based on the approach described in Allen and Allen, 1990; and Watts, 2001. The program is the OSXBackstrip developed by Professor Nestor Cardozo (University of Stavanger, Norway) and runs on Apple Macintosh<sup>®</sup>. It works for predicting subsidence (a combination of basement and sediment load-driven subsidence with an exponential reduction of porosity).

#### **3.5.1 Program description and work flow**

The OSXBackstrip program works with three modules for data input (program structure Fig.3.5): namely:

1. Lithobase: This comprises lithology-dependent values, including parameters for the decompaction exponential function, such as the initial porosity  $\Phi_0$  and the porosity reduction coefficient C.
2. Strata: These are the general properties of the stratigraphic units, which are independent of the actual well (outcrop) location, such as sedimentation depth, age, sea level, name of a stratigraphic unit, well or outcrop data, such as local thickness of strata and lithological composition.
3. A backstrip plot where the progressive decompaction of the sediments can be observed and a tectonic subsidence plot where the total thickness curve, the total subsidence (decompact) curve, the decompact curve corrected for sediment

loading, and the tectonic subsidence (decompacted) curve corrected for sediment and water loading are shown.

The OSXBackstrip program makes backstripping easy, whereby parameters can be entered in the “input units”, and the stratigraphic units are entered from the oldest (deepest) to the youngest (shallowest) unit. Although backstripping requires knowledge of stratigraphy, water depths of deposition, paleo-sea level and porosity changes with depth, the OSXBackstrip program’s correction for water loading in a continental basin (type 1 – see appendix C) assumes that sea-level change is the palaeoelevation of the basin top with respect to present-day sea-level.

Because each elevated layer was deposited over an interval of time, the computer program uses the median time of interval assigned to each unit in table 3.1 for backstripping computations. Also, for computational simplicity, sedimentation and associated basement subsidence were assumed to be constant over the specific time interval under study i.e. Permian period, even though sedimentation rates may have been variable during that time span.

In addition, it was assumed that sediment rates kept pace with tectonic subsidence rates, although during times of both basin starvation and of progradational filling of deep basins, even this might not be true. Despite the above-mentioned assumptions and limitations, tectonic and sedimentation trends can be obtained from the tectonic subsidence curves produced using the OSXBackstrip program, with the results representing an inverse model and not direct observation.

### **3.5.2 Error sources**

- Normally, layer thickness is derived from well data or outcrops (e.g. stratigraphic sections). Uncertainties are derived from the unknown amount of erosion or from an erroneous stratigraphic classification. This leads to inaccuracy in age, which is based on either biostratigraphy, or chronostratigraphic correlations or geochronology.



- Sedimentation depth (uncertainties in palaeobathymetry, however, if sedimentation (usually a quarter of palaeo-water) depth is the most significant uncertainty then the nonlinear decompaction curve is not affected (Waltham et al., 2000).
- Sea-level or eustatic corrections are mostly assigned to curves of eustatic changes, but regional sea-level histories often differ considerably from global curves. Thus, whether or not eustatic corrections are necessary has to be considered from case to case.
- Quantification of lithological parameters (e.g. lithology, porosity) is often derived from geochemical and sedimentological analyses or from geophysical well logs. Thus, these factors are dependent on the quality of the analysis or measurements.
- Decompaction of each strata interval utilises porosity versus depth curves (initial porosity  $\Phi_0$ ; decompaction coefficient  $c$ ) for each lithology based on empirical subsurface porosity data from regional (Sclater and Christie, 1980) or global data sets (Magara, 1980; Bond and Kominz, 1984; Baldwin and Butler, 1985). From these spectra of curves, estimates for the best-fitting curve should be determined



## CHAPTER FOUR: TECTONIC SUBSIDENCE ANALYSIS

### 4.1 COMPARISON BETWEEN COMPACTED AND DECOMPACTED LITHOLOGICAL UNITS OF TANQUA DEPOCENTRE

This chapter is concerned with decompaction of the lithostratigraphic units in Tanqua depocentre, SW Karoo Basin and the backstripping of these units to obtain the tectonic subsidence of the study area through time. In order to achieve the above listed aims, decompaction of these compacted units is undertaken by calculation and the backstripping with the aid of a computer program.

In addition, compaction estimates are carried out for all the ten lithostratigraphic units in Tanqua depocentre. This procedure is necessary to determine the effect of sediment compaction by porosity reduction, often defined as a homogenous volume loss, where original angular relationships would be unaffected. Likewise, decompaction estimates were also made on the lithostratigraphic units, and several steps were adopted to achieve this:

- The first step in the decompaction estimates for each unit (Table 3.1) in the Tanqua depocentre was determining porosity of each lithology at its specific depth. This procedure included using Van Hinte's (1978) equation on porosity–depth relationship, which states that rock porosity is assumed to follow an exponential relationship with depth, refer to equation [4].
- The second step in the decompaction calculation involved Van Hinte's (1978) equation for decompaction estimates; refer to equation [5]. Note:  $\Phi_0$  is the unconsolidated/initial porosity obtained from table 3.2 for each unit in their specific depositional environment (i.e. deepwater to shallow water).
- Lastly, the third step involved determining the percent decompaction for all the lithostratigraphic units in Tanqua depocentre. This value is useful when determining

which section decompacted more and which one less (Fridge and Bouma, 2003), and is expressed as:

$$\frac{\text{Total decompacted thickness of the vertical section}}{\text{Total compacted thickness of the vertical section}} \times 100$$

## 4.2 RESULTS AND INTERPRETATION

The calculated compaction and decompaction estimates obtained using Van Hinte's (1978) equation [4] for porosity at any depth are presented in Table 4.1. The percent compaction and critical porosity was calculated to demonstrate an average porosity reduction with depth in the sandstones and shales of Tanqua depocentre. This critical porosity is the porosity of random assemblages of more or less spherical grains and depends on the grain-size distribution of the sand grain assemblage. Furthermore, this quantitative technique involved plotting of graphs showing the difference in thicknesses between the compacted and decompacted sections of the eight lithostratigraphic units with their interpreted sub-environments in Tanqua depocentre, a direct comparison between the two (Fig. 4.01), and the percentage of decompaction per section (Fig. 4.02).

### 4.2.1 Compaction estimates

A percentage compaction ranging from 80 – 64.7% is calculated for the Tanqua depocentre sandstones, and the porosity is observed to decrease with increasing depth of burial (ranging from 0.45 – 0.32) until a critical porosity is reached. These compaction percentage and porosity value ranges correspond to the Abrahamskraal Formation (top lithostratigraphic unit) and Skoorsteenberg Formation (turbidite fan units) respectively. On the other hand, a compaction percentage ranging from 45.12 – 46.83% is calculated for the shale units (Tierberg, Prince Albert, and Whitehill Formations), which can be regarded as averagely the same percent compaction. The Prince Albert Formation shale has the lowest percent compaction of 45.12%,

whereas, the Abrahamskraal Formation sandstone has the highest, and the Koedoesberg and Kookfontein Formation are seen to have a percent compaction of 73.33 and 68.76% respectively (Fig. 4.02). Overall, the percentage compaction was seen to decrease with depth.

#### **4.2.2 Decompression estimates**

The percentage decompaction graph (Fig. 4.02) showed that the basin plain shale i.e. Tierberg, Whitehill and Prince Albert Formations decompacted the most at 213.51%, 218.91% and 221.6% respectively. Whereas the sandstones lithostratigraphic units are seen to have a lower % decompaction of 125% and 145.44% for the Abrahamskraal and Skoorsteenberg Formations respectively. Unlike the results obtained for the calculated percent compaction (table 4.2), The Prince Albert Formation shale decompacted the most while the Abrahamskraal Formation sandstone decompacted the least (Fig. 4.01). Overall, the percentage decompaction is seen to increase with depth.

SERIAL NO	UNITS	COMPACTED THICKNESS (m)	LITHOLOGY	POROSITY AT SURFACE $\Phi_0$	POROSITY AT ANY DEPTH $\Phi$	DECOMPACTED THICKNESS (m)	% COMPACTION	% DECOMPACTION	THICKNESS DIFFERENCE (m)	
1	Abrahamskraal Formation	500	Sandstone	0.56	0.45	625	80	125	125	Palaeoshoreline (Fluvial)
2	Koedoesberg Formation	200	60% Sandstone/40% shale	0.56	0.4	272.73	73.33	136.36	72.73	
3	Kookfontein Formation (top)	250	60% Sandstone/40% shale	0.56	0.36	363.6	68.76	145.44	113.6	Slope
4	Skoorsteenberg Formation	400	90% Sandstone	0.56	0.32	618.18	64.7	154.54	218.18	Basin plain
5	Tierberg Formation	750	95% Shale	0.63	0.21	1601.35	46.83	213.51	851.35	
6	Collingham Formation	70	Siltstone/Mudstone	0.63	0.18	130.45	53.66	186.36	60.45	
7	Whitehill Formation	80	Shale	0.63	0.19	175.13	45.68	218.91	95.13	
8	Prince Albert Formation	165	Shale	0.63	0.18	365.67	45.12	221.62	200.67	
9	Dwyka Group	300	Glacial Diamictite	0.56	0.14	586.36	51.16	195.45	286.36	

Table 4.1: Calculated results for porosity at specific depths, decompacted thickness, % compaction and decompaction; and thickness difference for lithostratigraphic units in Tanqua depocentre. \*  $\Phi_0$  values are from table 3.2; and Veevers *et al.*, 1994; Bordy *et al.*, 2004; Johnson, *et al.*; 2006; Rubidge, 2005; Viljoen, 2005; and Isbell *et al.*, 2008.

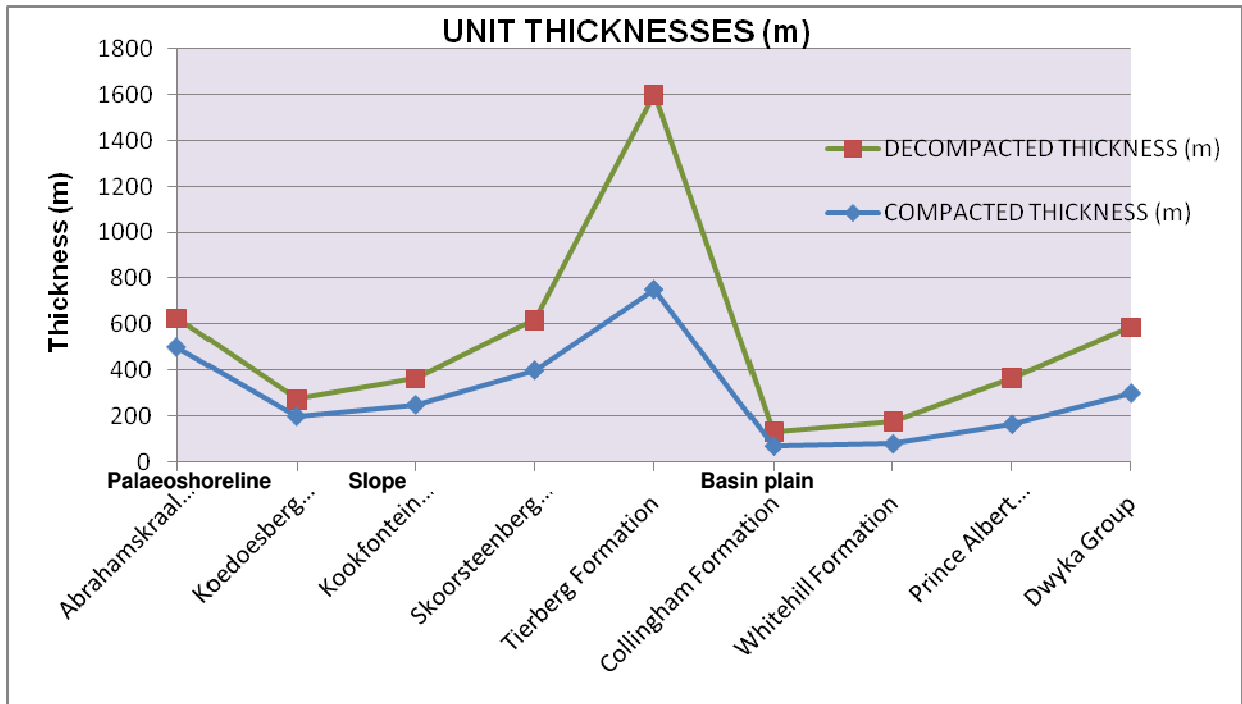


Figure 4.01: The thickness of compacted sections compared to decompact sections. Note: the lithostratigraphic units except for the Tierberg Formation shale did not compact much.

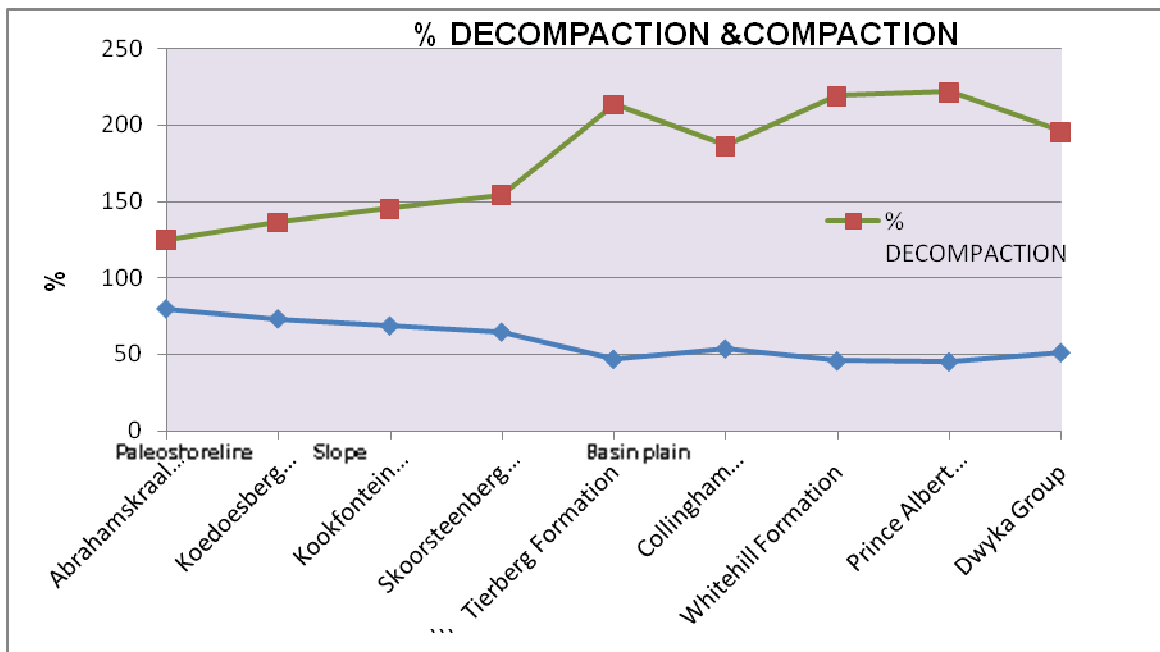


Figure 4.02: The percent decompaction compared to percent compaction per section in Tanqua depocentre. Average values were taken for each sub-environment, and the result of this graph shows inverse patterns for the percent decompaction and compaction of each lithostratigraphic units. Note the sharp peaks in the % decompaction for the shale unit of the Tierberg Formation.

### 4.3 COMPACTION OF SEDIMENTS

The properties of the sediment upon compaction are influenced by the initial arrangement of the mineral grains. In addition, overburden pressure seemingly causes preferred orientation of the mineral grains, and the pore structure of compacted sediments is useful in defining the details of the compaction process and in determining the degree of compaction (Rieke and Chilingarian, 1974). The extent of compaction is strongly influenced by burial history and sediment lithology, as overburden increases the differential stress on the sediments increases and pore fluid will gradually be eliminated, and as more stress is applied, the grains of the sediment will re-arrange.

Both processes (dewatering, and re-arranging) serve to reduce the rock volume and porosity is also significantly reduced. The reason for this being that the freshly deposited loosely packed sediments tend to evolve like an open system towards a closely packed grain framework during the initial stages of burial compaction. This is accomplished by the processes of grain slippage, rotation, bending and brittle fracturing. Such reorientation processes are collectively referred to as *mechanical compaction*, and generally take place in the first 1–2 km of burial. After this initial porosity loss, further porosity reduction is accomplished by processes of *chemical compaction* such as pressure solution (Rutter, 1983; Tada and Siever, 1989).

#### 4.3.1 Petrographic descriptions

Petrographic study is done on the Permian sandstone and silty sand samples taken from the deltaic slope succession of the Kookfontein Formation of Tanqua depocentre (see Appendix A for sedimentological log description and co-ordinates for the sample locations). The reason for sampling the Kookfontein Formation is due to the sequence being tectonically undisturbed, removed from areas of major tectonic disturbance, and having a nearly horizontal bedding plane of  $\sim 5^\circ$ . In addition, the absence of major unconformities in this section made it possible to assume that existing overburden stresses are essentially the maximum overburden loads experienced by the sediment grains.

Ten polished thin-sections were made of the samples collected from the Kookfontein Formation of Pienaarsfontein Se Berge (Fig. 4.03), and only six of these samples were selected for petrographic and Scanned Electron Microscopic (SEM) analysis using a petrographic microscope and a Leo®1430 VP Scanning Electron Microscope respectively at the University of Stellenbosch (as the remaining four were not studied due to it being very fine-grained and the minerals unidentifiable under the microscope). SEM analysis with a field of view under Cathode Luminescence (CL) was done on the polished surface of thin sections after initially identifying the mineral grains under the petrographic microscope, in order to identify the extent of quartz growth and fracturing that was difficult or not possible to observe under the petrographic microscope. The operating conditions of the SEM are given in Appendix D.

Inspection of four thin sections of samples from massive and bedded sandstone outcrops and two thin sections of silty sand samples of the Tanqua depocentre showed no visible porosity and permeability. In addition, petrographic and Scanned Electron Microscopic (SEM) analysis of the Tanqua depocentre sandstone showed that the mineral grains were affected by compaction. Table B1 in Appendix B gives a detailed petrographic description from the microscopic study of the two polished thin sections made from silty sand samples 'SWA6 and SWA7' and four polished thin sections from sandstone samples 'SWA13, SWA14, SWA15-2 (slump bed) and SWA20' that were collected from location 'PVF1' and 'PVF2' respectively from the Kookfontein Formation in Tanqua depocentre.

#### **4.3.2 Scan Electron Microscopic (SEM) analysis**

The SEM Cathode Luminescence images (Fig. 4.04 and 4.05) of the Tanqua depocentre sandstone from the Kookfontein Formation shows that:

- The quartz grains were deposited as rigid, single and interlocked grains (i.e. having intergranular contact) rather than porous.

- Upon deep burial i.e. at ~ 7.5 Km depth (see depth of Kookfontein Formation in Fig. 4.10) where the samples were collected, the ground matrix is of a diagenetic origin (which might explain the fine-grain size of the sandstones) and is moderately filled with cement (see Fig. 4.04 and 4.05).
- The mineral transformations mostly involved quartz/feldspar overgrowth at depth, followed by secondary matrix and clay mineral transformations like albite replaced by illite.
- Tight, subparallel felt-like fabric of clay minerals admixed with silt, pellets and negligible/non-existent permeability.
- No porosity is observed except for microfractures on the quartz grains.



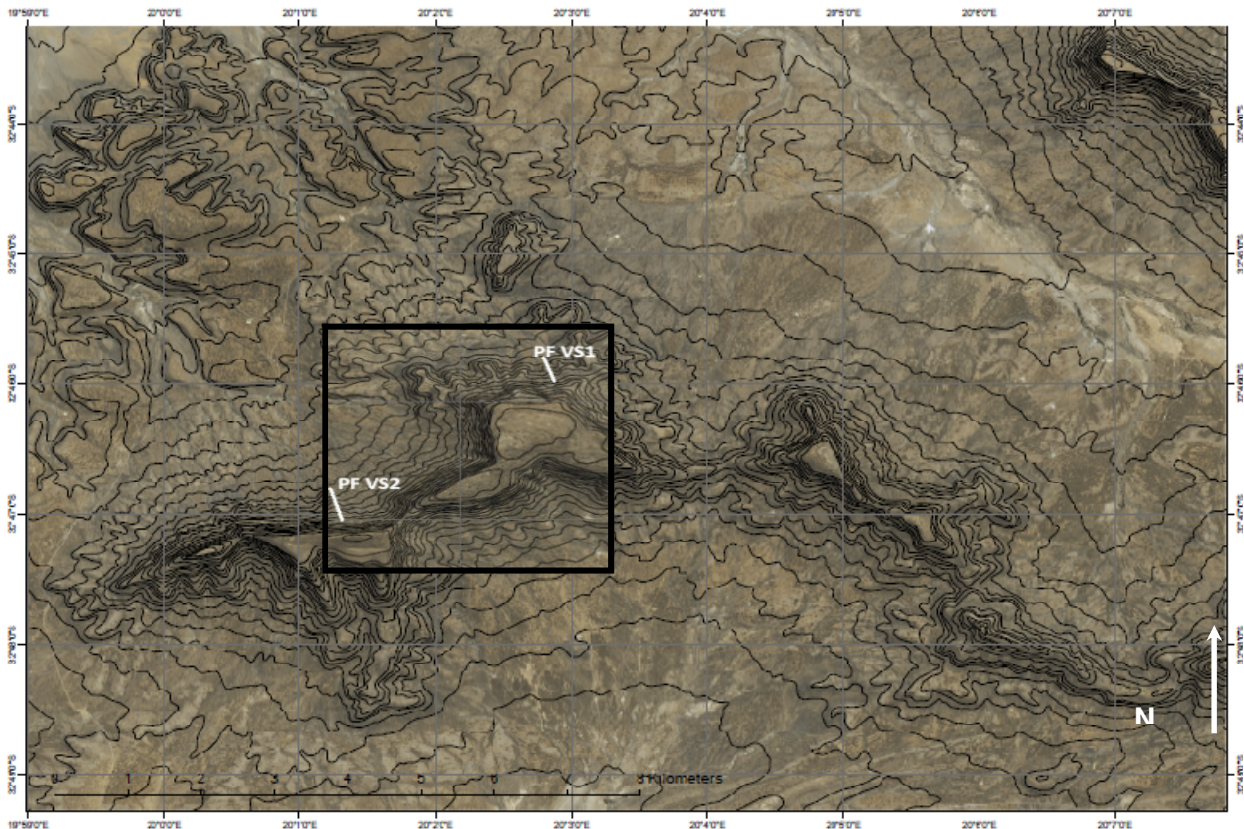
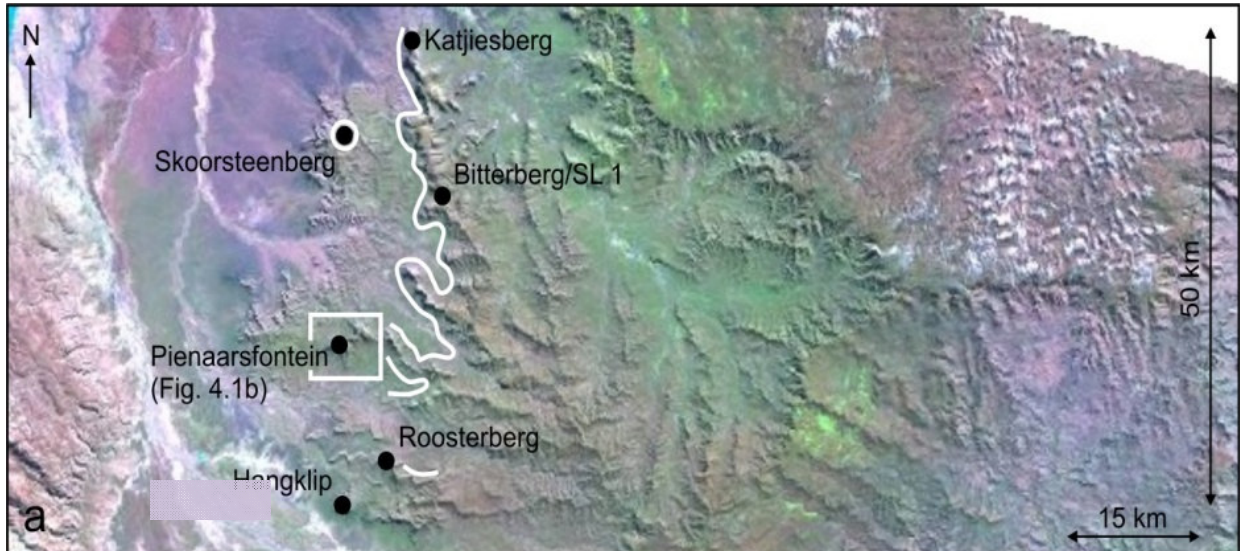


Figure 4.03: Location map. (a) Landsat image of the Tanqua depocentre showing the position of the Pienaarsfontein study area where samples were collected (boxed). The regional mapped extent of the base of the Kookfontein Formation is highlighted (white line). Landsat image from: <https://zulu.ssc.nasa.gov/mrsid/>. (b) Satellite image of the Pienaarsfontein study area showing the positions of the sections PF VS1 and PSVF2 where the sandstone samples were collected (see Appendix A for sedimentological log and co-ordinates for the sample locations).

### 4.3.3 Diagenesis

The origin of the silica for quartz overgrowths has frequently been attributed to pressure solution. Pore solutions become enriched in silica, which is then re-precipitated as overgrowths when super saturation is achieved (Tucker, 1991). This relation of pressure solution to rock deformation calls for particular interest in the role of pressure solution mechanisms in the diagenesis of sedimentary rocks. Diagenesis begins at the moment sediments are deposited, and it continues to a point in history when (1) either deep burial or orogenic buckling cause the initiation of metamorphism, or (2) when excavation initiates weathering and erosion. Thus, three diagenetic phases exist (Larsen and Chilingar, 1983):

Syndiagenesis: involving the sedimentation phase, depositional and early burial.

Anadiagenesis: involving the compaction – maturation phase, with deep burial, during which the particulate sediment grains become lithified.

Epidiagenesis: involving the emergent – pre-erosion phase

The diagenetic alterations observed to have occurred in Tanqua depocentre can be sub-divided into two phases: an early-shallow syndiagenetic phase, and a deep anadiagenetic phase. Hence, for the purpose of investigating the effect of compaction on the sediments of Tanqua depocentre, only the anadiagenetic phase of diagenetic evolution will be considered.

#### ***Anadiagenetic phase***

Characteristically, the anadiagenetic phase is one of slow compaction and concomitant expulsion of connate water (a de-watering stage), whereby some of the water becomes trapped permanently in the sediments as a result of compaction and cementation to the point of impermeability. The diagenetic fabric of sediments that have undergone anadiagenesis are therefore characterised by cementation (mostly siliceous or calcitic cements).

#### 4.3.4 Diagenetic evolution

The physical changes occurring in sediments during subsidence of a depositional basin are directly related to the evolution of stress within the basin. As long as the basin is subsiding, the expulsion of interstitial fluids from the fine-grained clastic takes place and the extent of compaction is strongly influenced by burial history and the lithology of sediments. In this context, the petrographic and SEM studies of the Tanqua depocentre sandstone at depth of ~ 7.5 Km indicate that mechanical and chemical compaction (i.e. grain deformation and pressure solution respectively) occurred on the sediments.

Figures 4.04 - 4.07 shows that the Tanqua depocentre sandstone underwent mechanical compaction as the dominant cause of porosity reduction of the quartz-rich sediments; this phenomenon is displayed by:

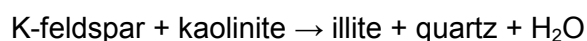
- The presence of lithic fragments
- The mica grains being squeezed between grains
- Fracturing in the quartz grains and squeezing of the mud clasts, micas and rock (lithic) fragments into the remaining pore spaces (Fig. 4.04 and 4.05) and this was the most important process to diminish porosity and permeability.

While chemical compaction on the other hand, is also observed to have played a role in the total compaction of Tanqua depocentre sandstone; this is displayed by the following characteristics:

- The mineral grains dissolved at intergranular contacts under non-hydrostatic stress and re-precipitated in pore spaces, thereby resulting in compaction.
- The occurrence of early cementation (Fig. 4.04 and 4.05) is inferred from the presence of sutured contact between the rock fragments and clay minerals (minor

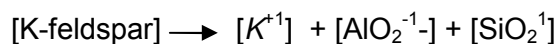
cements include calcite and some iron oxides); this could be described as a kind of deformation caused by chemical compaction.

- Chlorite and illite replaced kaolinite and smectite, since K-feldspar and kaolinite are metastable as expressed by the following chemical reactions:

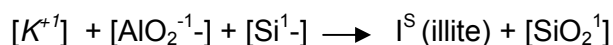


- The recrystallization and illite crystallinity expressed above had no effect on the porosity; rather the initial porosity was increased by feldspar dissolution (Feldspar grains have been altered, and in some cases completely replaced by illite and chlorite) and reduced by pressure solution/quartz overgrowth and illite growth (see reaction equations below):

*K-feldspar dissolution*



*Illite precipitation*



The chemical reactions above are due to the fact that the solubility of minerals increases with increasing effective stress at grain contacts; therefore, pressure dissolution at grain contacts is therefore a compactional response of the sediment during burial in an attempt to increase the grain contact area so as to distribute the effective stress over a larger surface (Yang, 2001).

The different diagenetic phenomena above can be placed on a relative diagenetic sequence, giving an overview of the diagenetic history of rocks in the Tanqua depocentre (Fig. 4.08). Conclusively, at the great depth where the Tanqua depocentre silty sand and sandstone samples were collected i.e. ~7.5 Km, the following sequence of processes is inferred:

1. Cementation (calcite and quartz cement) and dissolution of the grains is seen to have occurred, and the latter caused further compaction.
2. At greater depths still, cementation began to occur between the grain boundaries, and gradually the pores closed resulting in permeability reduction.
3. As cementation was taking place, pressure solution decreased due to the reduction of interstitial fluids, and the Tanqua depocentre became more or less sealed. This caused reversion of the rheology of the medium to an elastic one, and probably only to be partly reopened by further subsidence.
4. From the point of view of the sediments, compaction ceased completely and the medium possibly became virtually rigid, and diagenesis initiated.
5. Geochemically, anadiagenesis caused dewatering of the silty sand and sandstone, whereby interstitial fluids were progressively expelled from the deeper levels, moving upwards and outwards through the overlying strata, and following within dip of the depocentre.



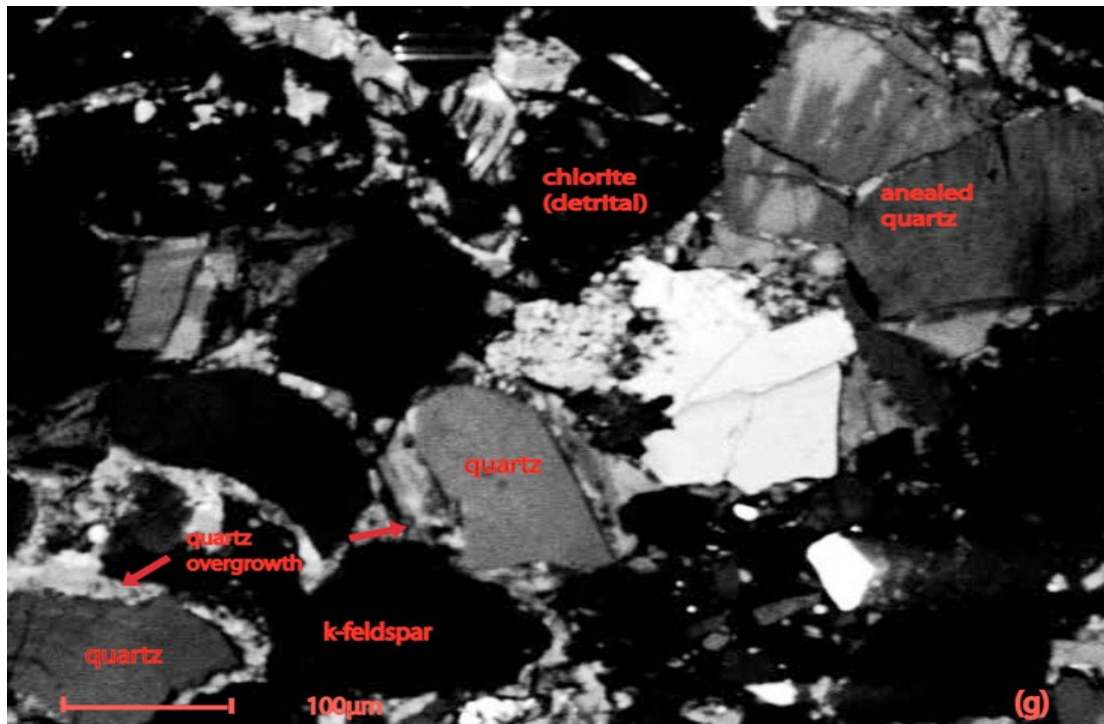
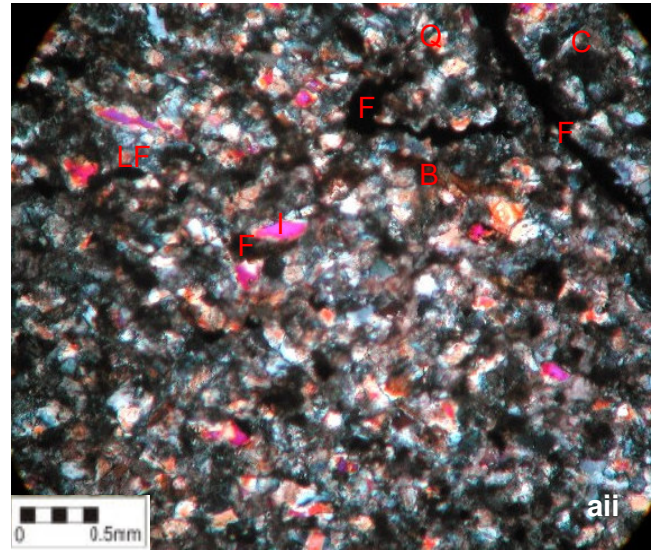
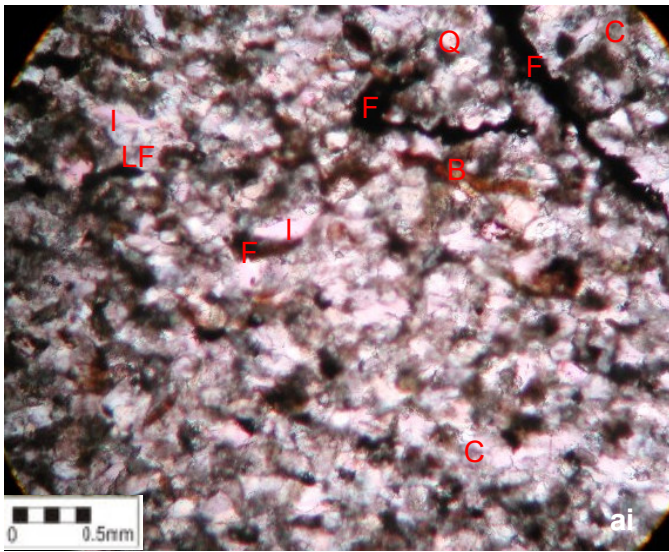


Plate 1: Sample Microphotographs of thin sections SWA6 from a carbonaceous silty clay bed at a depth of 44m from a carbonaceous silty sand bed collected from PFVS 1 location in Tanqua depocentre. Note: (i) view under plane polarized light (ii) view under crossed nicols. C – Clay; F - Feldspar; I - Illite; LF- Lithic fragment; Q - Quartz; B - Biotite. The corresponding SEM image (g) displays a field of view under CL showing an annealed quartz grain and quartz overgrowth.

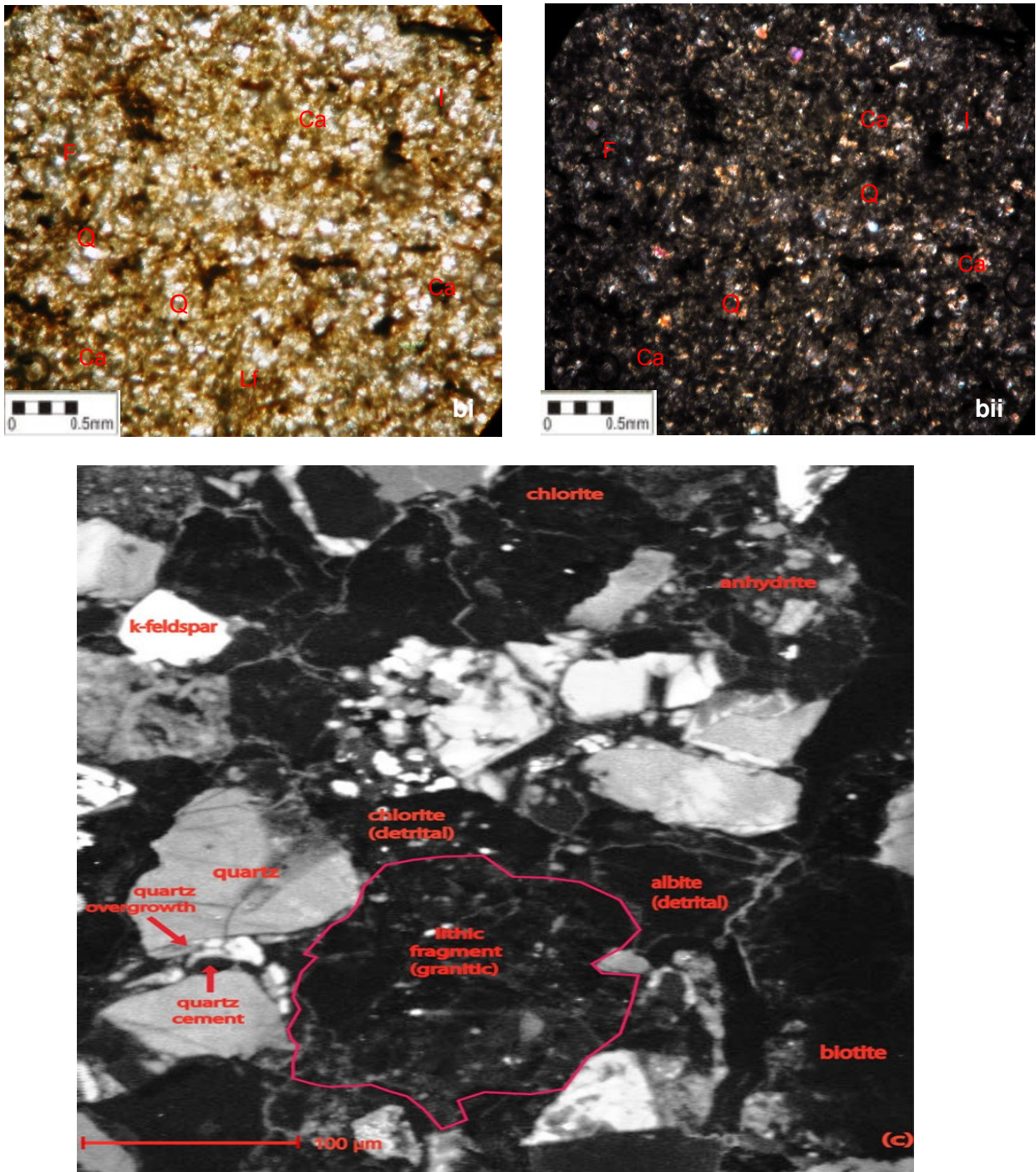


Plate 2: Sample Microphotographs of thin sections SWA15-2 from slump bed with wavy lamination at 20 m depth collected from PFVS 1 and PFVS 2 locations in Tanqua depocentre. Note: (bi) view under plane polarized light (bii) view under crossed nicols. F - Feldspar; I - Illite; LF - Lithic fragment; Q - Quartz; Ca - Calcite cement with greenish colour. The corresponding SEM image (c) displays a field of view under CL showing a lithic grain with fractures and annealing, and quartz overgrowth with cement.



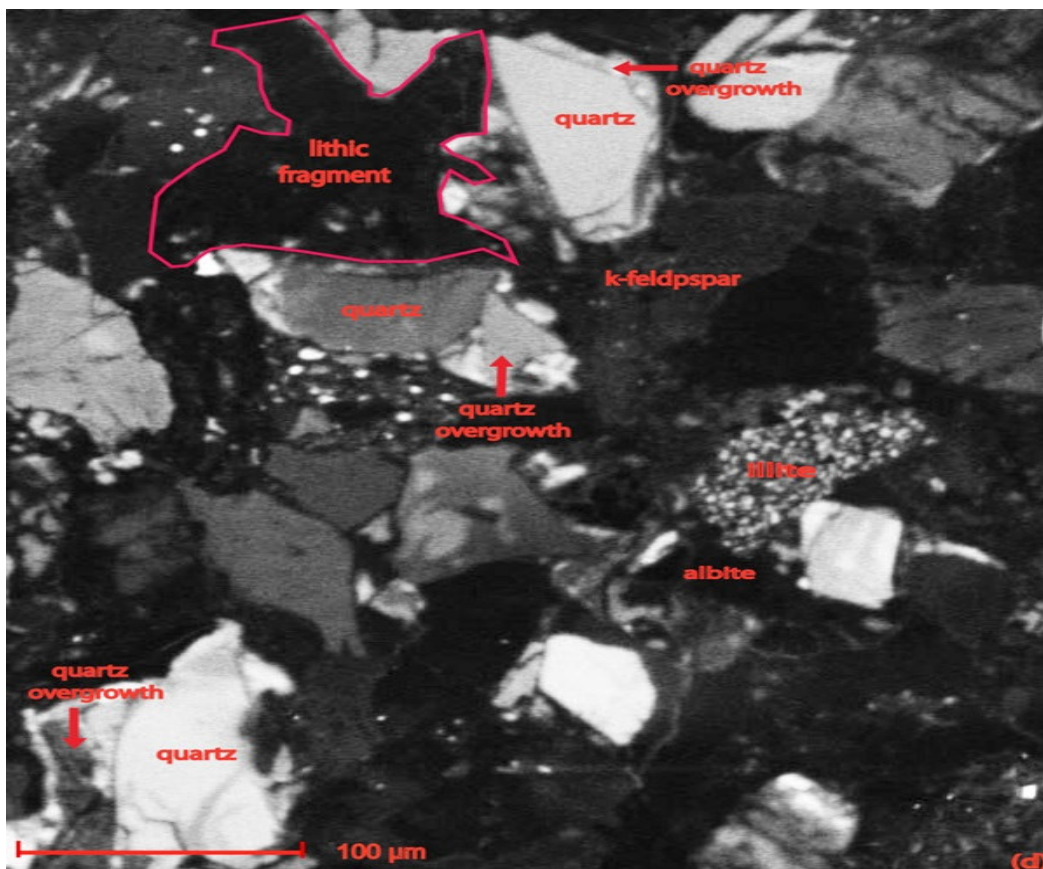
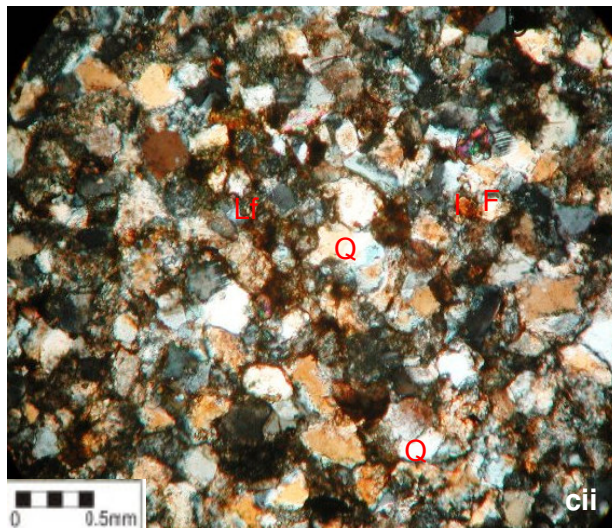
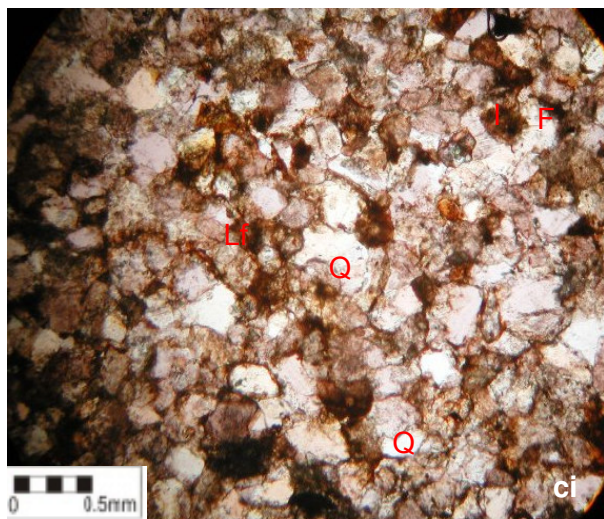


Plate 3: Sample Microphotographs of thin sections SWA20 from massive sandstones bed at 70 m depth collected from PFVS 1 and PFVS 2 locations in Tanqua depocentre. Note: (ci) view under plane polarized light (cii) view under crossed nicols. F - Feldspar; I - Illite; LF - Lithic fragment; Q - Quartz. The corresponding SEM image (d) displays a field of view under CL showing albite grain replaced by the illite, and k-feldspar (darker grain colour shows lower K content).



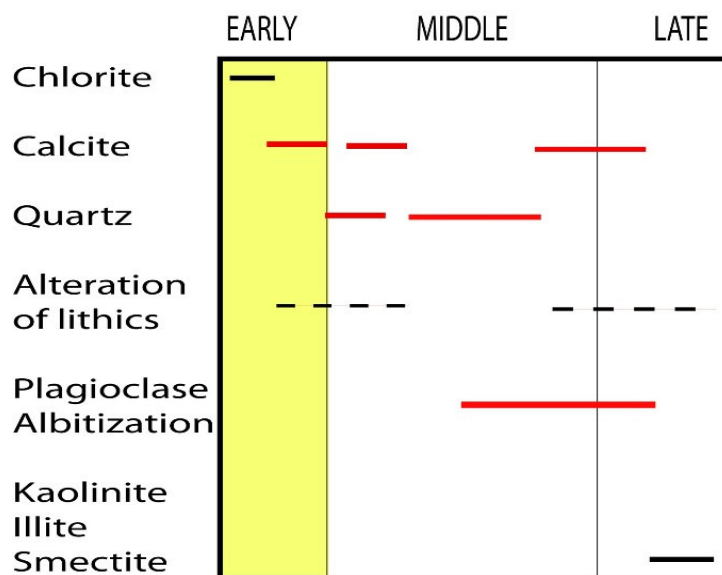


Figure 4.04: Generalized diagenetic sequence for the Tanqua depocentre sandstone shows periods of sediment compaction (yellow zone), cementation (red lines), dissolution of grains and cements (dashed lines), and replacement of feldspars by clays (black line). The changes in petrology affected porosity and permeability.

#### 4.4 SUBSIDENCE CURVES

In this study, the Airy model is adopted, and changes in sediment-supply and water-loading in the Tanqua depocentre are simply accounted for by assuming a homogeneous local, airy-type isostatic adjustment for the lithosphere. Such an isostatic model can only be valid in early stages of basin development; whereas for later stages, a flexural compensation with increasing lateral strength due to cooling of the lithosphere needs to be incorporated (Frostick and Steel, 1993). Since the sediment density is variable and compaction also must be taken into account, such flexural compensation must be carried out separately for each lithostratigraphic unit (McKenzie, 1978).

##### 4.4.1 Results of the 1D Airy subsidence model

Backstripped and subsidence curves for the nine lithostratigraphic units in the Tanqua depocentre (Table 3.1) during the Permo-Carboniferous time are shown in figures 4.09 and

4.10. Note that the subsidence curves are the results from an inverse model and not direct observation, and should be interpreted accordingly with more emphasis on relative rather than absolute values.

Interpretations made are based on the shape and timing of representative subsidence curves. The consistency of these subsidence curves are then checked by making comparison with a previous 1D subsidence model for the SW Karoo Basin by Cloetingh *et al.* (1992).

### **I. Ordovician – Early Carboniferous subsidence**

The compacted, backstripped and total subsidence curves (Fig. 4.10) during the interval of 495 – 335 Ma are linear in profile. This linear subsidence curve shape is characteristic of tectonic and thermal stages of lithospheric extension (McKenzie 1978), and in the Tanqua depocentre it resembles that of a passive continental margin characterised by slow to medium subsidence rate at  $51.3 \text{ mMa}^{-1}$  i.e. they generally display decelerating subsidence rates from Ordovician to Early Carboniferous time corresponding to deposition of the Cape Supergroup deposits. The tectonic and basement subsidence curves for the Tanqua depocentre obtained in this study correlates with subsidence curves of the Western Cape Province by Cloetingh *et al.*, 1992 (see Fig. 4.11). The latter much like the former also interprets this interval as an extensional regime displays decelerating subsidence rates from Ordovician to Early Carboniferous time (expressed in subsidence phase 1 and 2 between ~460 - 330 Ma in Fig. 4.11).

### **II. Hiatus**

The horizontal profile on the subsidence curve (Fig. 4.10) suggests a hiatus in sedimentation that extended for ~23 Ma i.e. between the interval of 335 – 312 Ma. This time interval reflects a local unconformity in the lithostratigraphy of the Tanqua depocentre. A horizontal profile is also expressed on the subsidence curve for the Western Cape obtained by Cloetingh *et al.*, 1992 (Fig. 4.11).

### III. Late Carboniferous – Early Permian subsidence

The end of the hiatus is marked by deposition of the Dwyka Group glacial deposits during the Late Carboniferous and into the Early Permian. This is expressed on the subsidence curves as a concave-up profile during the interval of 302 - 290 Ma, and this subsidence phase continued into the Early Permian with a decreasing subsidence rate of  $27.92 \text{ mMa}^{-1}$  (see Fig. 4.10). This subsidence phase corresponds to deposition of the Prince Albert and Whitehill Formations during the interval of 290 – 278 Ma and 278 - 272 Ma respectively, with a decreasing subsidence rate of  $11.17 \text{ mMa}^{-1}$ . This subsidence profile for the Late Carboniferous - Early Permian correlates directly with the subsidence curve of the Western Cape from the study of Cloetingh *et al.*, 1992 (i.e. the linear profile at the onset of subsidence episode 3 in Fig. 4.11).

### IV. Mid Permian subsidence

The mid-Permian subsidence induced a change in the basin configuration as expressed on the subsidence curves by a two-fold change in subsidence pattern: (1) a convex-upward profile denoting a short and rapid subsidence phase and a subsidence rate that increases through time at  $134 \text{ mMa}^{-1}$  (Fig. 4.10) corresponding to deposition of the Tierberg Formation during the interval of 272 – 271 Ma; and (2) another convex-upward profile is noticed on the subsidence curve during the interval of 271 - 270 Ma expressing a short phase of rapid subsidence with a subsidence rate that increases through time at  $469 \text{ mMa}^{-1}$  corresponding to deposition of the Collingham Formation. These interpretations are based on a characteristic feature mentioned in Allen *et al.* (1986) that at a rapid subsidence stage, curves are either straight or convex upwards. This mid Permian subsidence phase in the Tanqua depocentre correlates with the subsidence model of the Western Cape produced by Cloetingh *et al.*, 1992 (the short rapid subsidence phase that marks the onset of episode 3 in Fig. 4.11).

The onset of flexurally controlled subsidence (Fig. 4.10: phase 4) is displayed in Tanqua depocentre through the mid Permian Period. Upon comparison with the subsidence model of the SW Karoo Basin by Cloetingh *et al.* (1992), the mid Permian subsidence obtained in this

study can be attributed to basin over-deepening, associated with a peak average subsidence rate calculated (see Fig. 4.10). At the onset of this episode of rapid subsidence, the inflection on the subsidence curve denotes a change in basin configuration whereby marine conditions became more restricted due to impeded oceanic circulation causing an abrupt change from marine to brackish conditions, all of this accounts for deposition of the Collingham Formation mudstone.

#### **V. Mid – Late Permian subsidence**

During the Mid – Late Permian another convex-upward profile is expressed on the subsidence curve during the interval of 269 – 266 Ma, and interpreted as rapid flexural subsidence with a rapid subsidence rate of 268  $\text{mMa}^{-1}$ , 134  $\text{mMa}^{-1}$ , and 67  $\text{mMa}^{-1}$  corresponding to deposition of the Skoorsteenberg (269 Ma), Kookfontein (268 Ma) and Koedoesberg Formations (266 Ma) respectively.

This subsidence phase in the Tanqua depocentre correlates with the subsidence (see phase 3 in Fig. 4.11). In addition, this rapid subsidence pattern is comparable to predictive models of foreland basin subsidence. Generally, foreland basins show convex-upwards subsidence curves due to subsequent increasing subsidence rates through time resulting from migration of a supra-crustal orogenic load toward the foreland basin (Decelles and Giles, 1996). Furthermore, subsidence rates in foreland basins decrease away from the orogenic load, and are generally higher than those in extensional basins (Allen *et al.*, 1986). Therefore, a compressional setting is interpreted for this interval, with subsidence due to the development of a significant supra-crustal load that is presumably, related to thrust tectonics from the adjacent CFB, and the Karoo foreland basin system development during the late Permian.

#### **VI. Late Permian - Early Triassic subsidence**

At the interval of 266 - 240 Ma, a subsidence phase with a decelerating subsidence rate of 7.73  $\text{mMa}^{-1}$  through time (Fig. 4.10) is expressed. This subsidence phase is most probably related to tilting of the Namaqua basement block (Tankard *et al.*, 2009). This change in subsidence profile

can only be described as a strike-slip transtensional setting within the Tanqua depocentre. The subsidence model of the Western Cape by Cloetingh *et al.*, 1992 also expresses between this time intervals 266 – 240 Ma a subsidence phase.

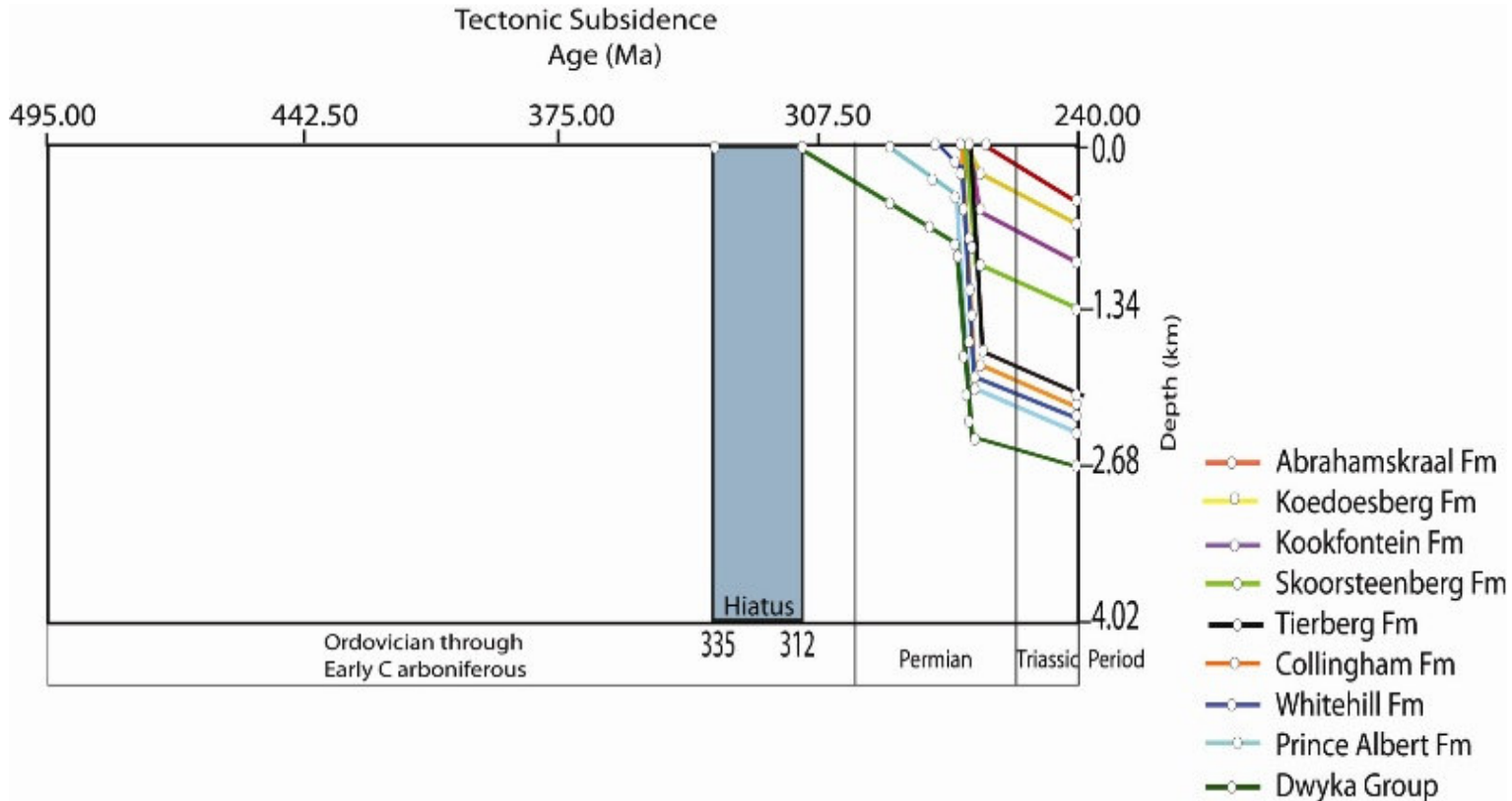


Figure 4.05: Subsidence curves for Tanqua depocentre. Boundaries of nine selected horizons are recognized on the subsidence curves with ages corresponding to the age of the top surface of each horizon; the blue zone signifies the hiatus between the Cape and the Karoo Supergroup sedimentation.

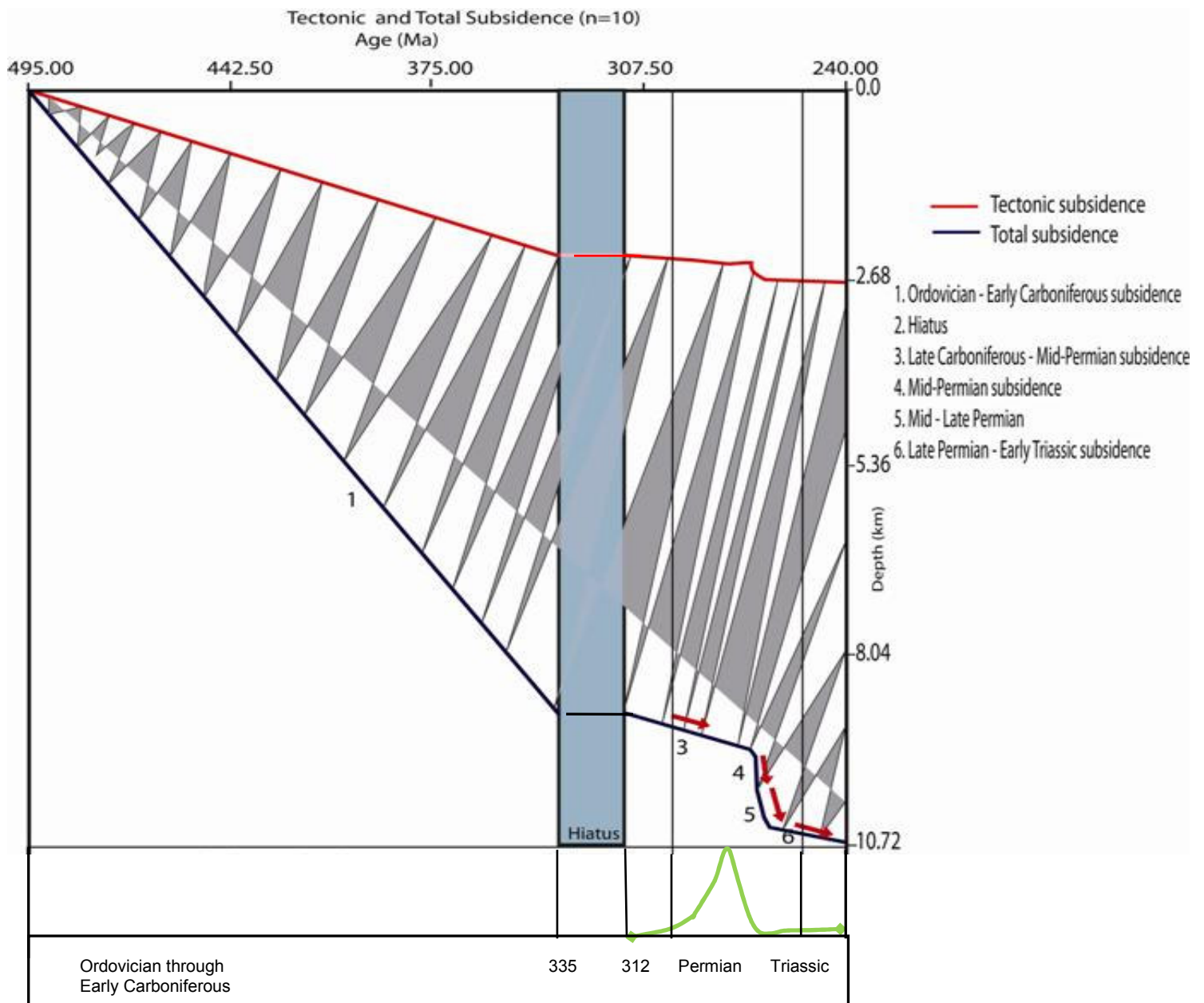


Figure 4.06: Difference between backstripped tectonic and basement/total subsidence. Incorporated as the green curve is the calculated tectonic subsidence rate; the blue zone signifies the hiatus between the Cape and Karoo Supergroup sedimentation, and the shaded region show the subsidence (~8 km) due to sediment and water load assuming Airy isostasy. Note the inflections (red arrows) in the subsidence.

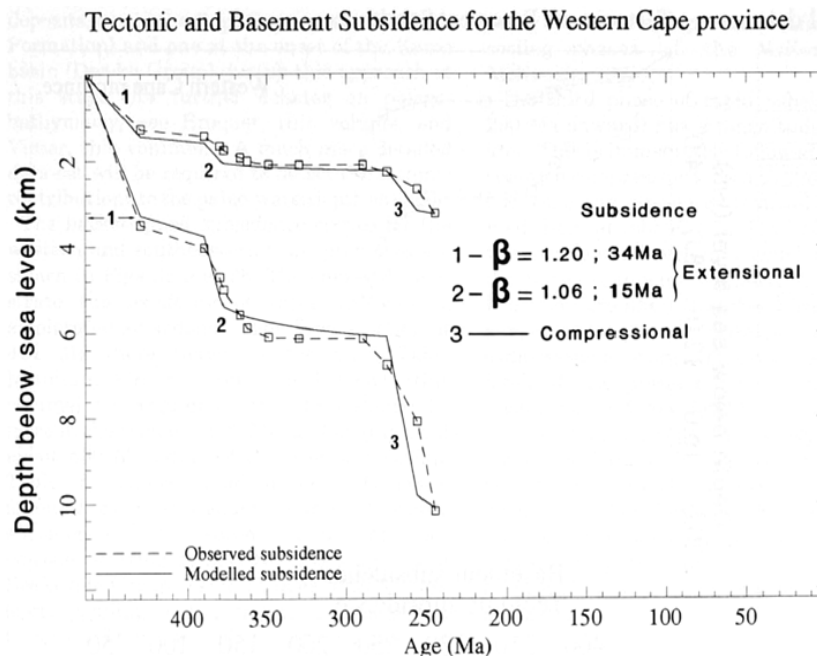


Figure 4.07: Tectonic and basement subsidence for the Western Cape province obtained from the subsidence analysis study of Cloetingh *et al.*, 1992.

An illustration of the subsidence rate over time for the lithostratigraphic units in Tanqua depocentre is presented in figure 4.11. The peak average subsidence rate corresponds directly to deposition of the Collingham Formation which contains regional marine shale unit, attributed to basin over-deepening and increase in marine influence in the depocentre. This event occurred immediately as renewed thrust loading at the CFB orogen elicits an elastic flexural response.

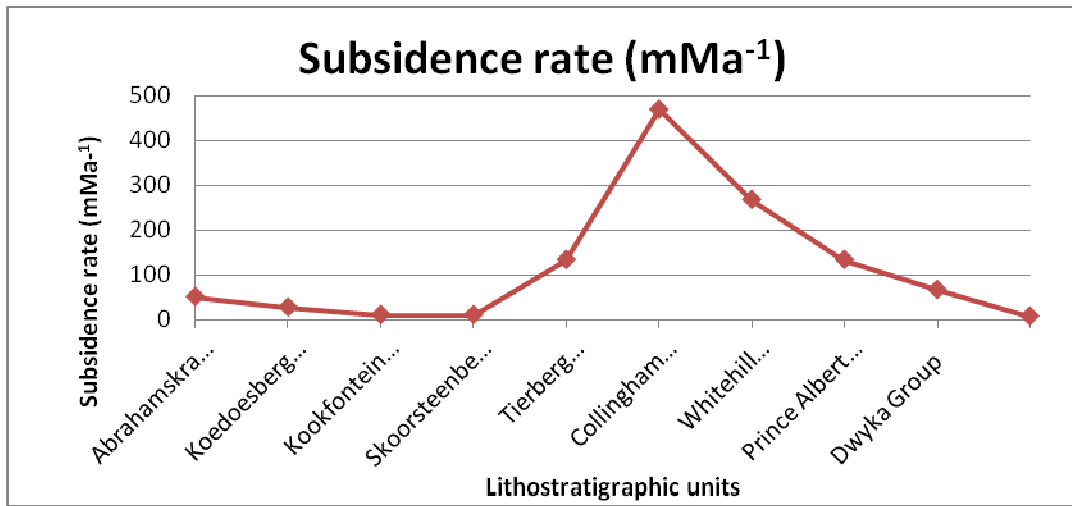


Figure 4.08: Graph illustrating the subsidence rates over time and corresponding to deposition of the lithostratigraphic units in Tanqua depocentre. Note the peak average subsidence rate for the duration of 271 – 270 Ma; see text above for explanation.

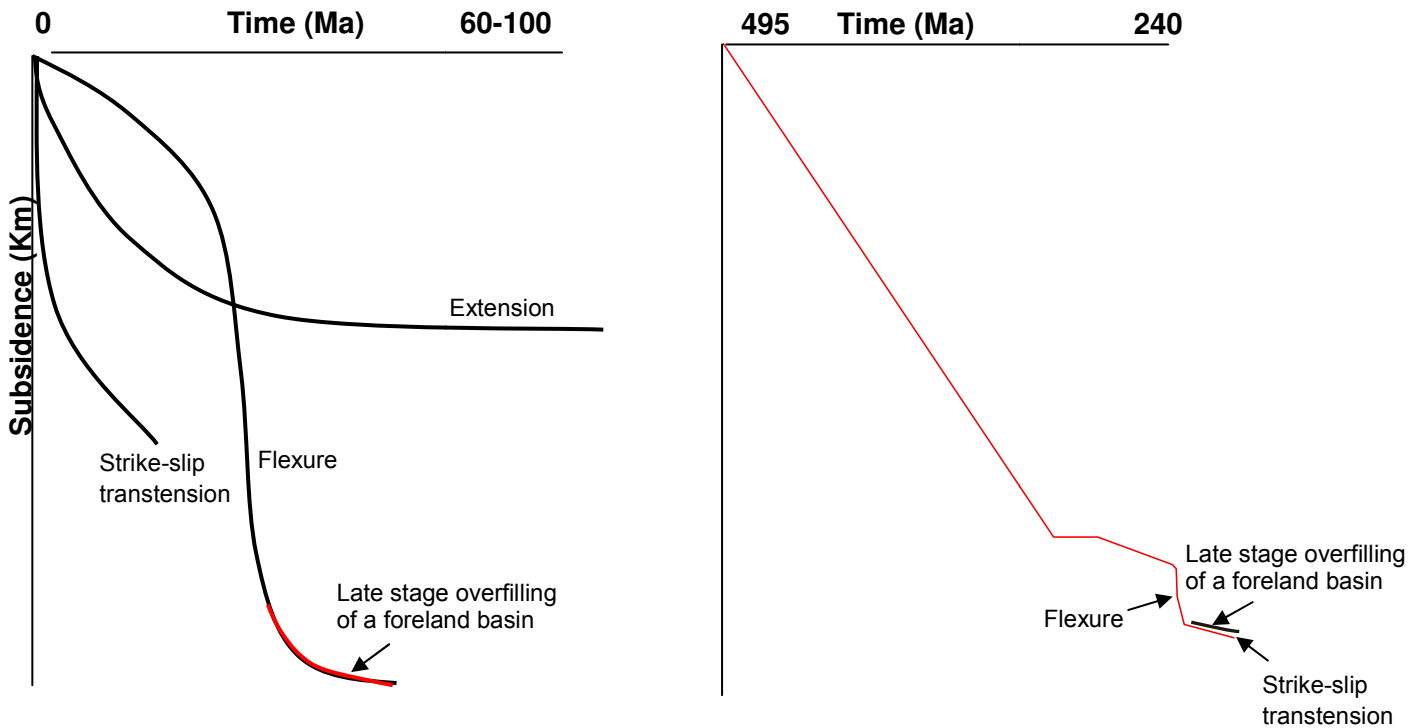


Figure 4.09: Comparison between the tectonic subsidence curves obtained in this study and a simplified diagram depicting the visual expression of basin-generating mechanisms on various subsidence curve shapes. No absolute vertical scale is implied, although relative timescales (horizontal) vary but are often found as shown. (Modified after Kneller, 1991; and using data from Pitman and Andrews, 1985; for the simplified diagram.)



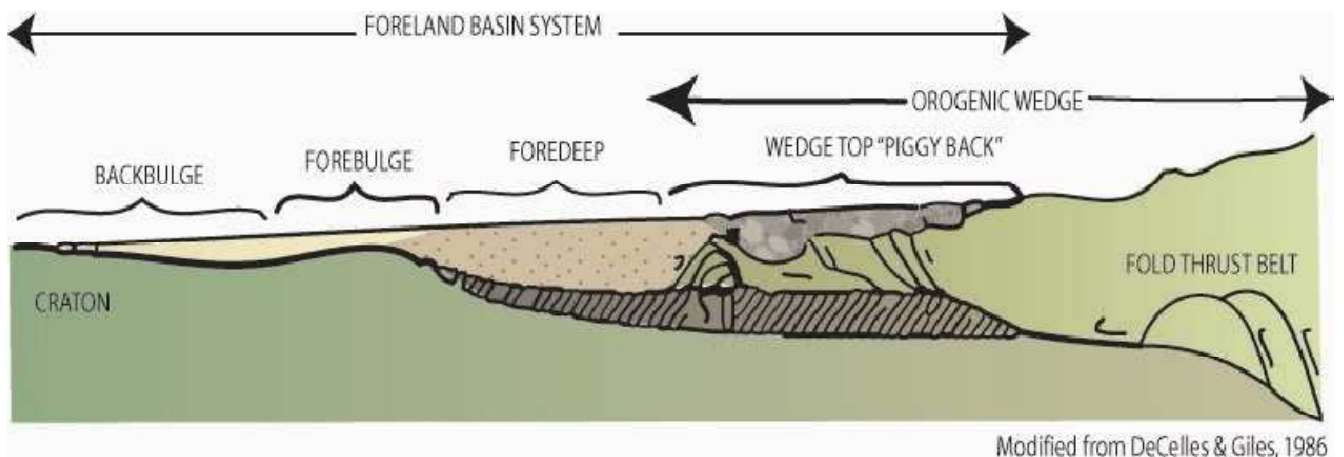


Figure 4.10: Schematic illustration of a foreland basin system (modified after Decelles and Giles, 1996).

#### 4.4.2 The relative timing of inflections on the Tanqua depocentre subsidence curves

Subsidence patterns and positive inflexions can provide information concerning the timing of basin development; in this regard, the subsidence curves for Tanqua depocentre (Fig. 4.10) show a number of features:

- Contemporaneous decelerating subsidence of low gradient and linear profile occurred in Tanqua depocentre. Subduction of the Palaeo-Pacific oceanic plate under the Gondwana plate possibly during the mid-Carboniferous thereby forming a magmatic arc may have caused stretching and then slow thermal subsidence of the lithosphere. Furthermore, in the mid-Carboniferous time, thermal thinning of the lithosphere resulted in the formation of a back-arc basin. The back-arc activity must have caused significant extension followed by thermal subsidence, and such tectonic activity may therefore explain the Ordovician to Early Carboniferous subsidence profiles.

- There appears to be a positive inflexion within the concave profile of the subsidence curves for Tanqua depocentre during the Late Carboniferous – Mid Permian Period (312 -290 Ma) with deposition of the Dwyka Group (Fig. 4.10, phase 3).
- The onset of flexurally controlled subsidence (Fig. 4.10, phase 4) is displayed in Tanqua depocentre through the mid Permian Period. At the onset of rapid subsidence, this positive inflexion denotes a change in basin configuration whereby marine conditions became more restricted due to impeded oceanic circulation causing an abrupt change from marine to brackish conditions. All of this accounts for deposition of the Collingham Formation mudstone which has often been interpreted as a possible condensed section (Flint *et al.*, 2004).

#### **4.4.3 The implications of flexural subsidence in Karoo foreland basin**

The flexural subsidence during the interval of 270 – 266 Ma observed on the subsidence curves (Fig. 4.10) is in agreement with the tectonic model of Visser (1993) about the transition from a back-arc to a foreland basin during the late early Permian, and this resulted in a major change in basin configuration. This flexural subsidence phase is associated with the post-glacial open sea that inundated large parts of the continental interior, whereby the inundated region formed a gently sloping foreland ramp in the palaeo-west.

On the subsidence curves, the total subsidence during the foredeep formation is 8.5 km, with a net tectonic subsidence of 8 km. This isostatic model can only be valid in early stages of basin development; and for later stages, a flexural compensation with increasing lateral strength due to cooling of the lithosphere needs to be incorporated (Frostick and Steel, 1993). To produce a basin without crustal stretching, materials must be removed on a large scale by erosion when uplift occurs (McKenzie, 1978). Dingle *et al.* (1983) proposed that ~ 3.5 – 4.5 km of Karoo sediment (Upper Permian to Middle and Upper Triassic) in the southern Cape has been removed by erosion. If the entire Karoo sequence up to and including the Karoo volcanics

originally covered the southern Cape region, then a potential maximum of ~ 6 – 7.5 km of sedimentary and volcanic rock may have been eroded from this area since ~ 181 Ma (the age of the Karoo volcanics). Apatite fission track modelling by Tinker, *et al.* (2004) suggests an eroded thickness of 3.3 – 4.5 km since the mid-late Cretaceous which falls well within this range, in addition suggesting that Early Cretaceous denudation may account for the extra 1.5–4 km.

However, foreland basins are generally accepted to express down-flexing of the lithosphere in front of supra-crustal loads (Beaumont, 1981; Jordan, 1981; Karner and Watts, 1983; Lyon-Caen and Molnar, 1985; Stockmal *et al.*, 1986; Flemings and Jordan, 1989; Sinclair *et al.*, 1991; Watts, 1992). Therefore the evolution of such basins should be tightly linked to, and contain significant information about, the evolution of the thrust-sheet loads. This information can provide insights into the development of the adjacent orogenic thrust belts that may be otherwise difficult to obtain, especially when much erosion or subsequent deformation obliterated the situation that existed during basin formation.

#### **4.5 SIGNIFICANCE OF PETROGRAPHIC CONSTRAINTS ON DIAGENETIC PROCESSES TO COMPACTION ESTIMATES, AND SUBSEQUENTLY ON THE SUBSIDENCE CURVES**

In the process of foredeep formation a first phase of slow to moderate subsidence ends by a hiatus, and then followed by a series of episodes of rapid subsidence. Based on these observations on the subsidence curves, it is possible to infer that the first stage of relative inflexion (~ 290 Ma) is therefore recognised as the first stage of Tanqua depocentre formation. In the process of Tanqua depocentre formation, the first tectonic event (passive margin stage *sensu-stricto*) and subsequent phases of subsidence occurred during an extensional setting and later continued in a compressional setting (associated with the substratum -upper plate, whereby thrust-faults loading of the CFB induced subsidence of the substratum which in turn influenced the elastic thickness of the underlying lithosphere) respectively.

Therefore tectonic subsidence of the Tanqua depocentre can be broken into two major episodes: (i) an extensional and (ii) a compressional phase. The tectonic subsidence curves show the onset of the compressional phase i.e. the bulge effect during the flexural subsidence. A hypothetical schematic illustration of the tectonic phases in the subsiding Tanqua depocentre is presented in Fig. 4.14.

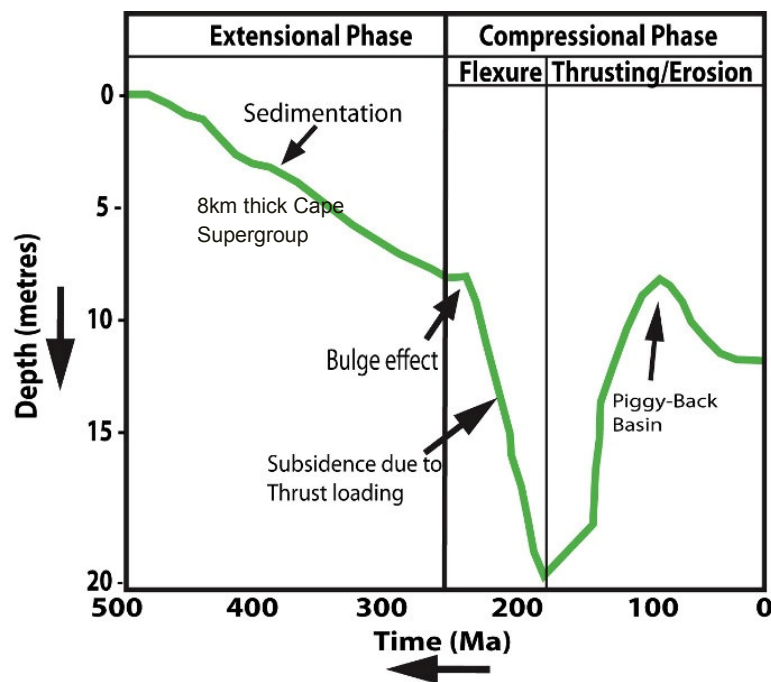


Figure 4.11: Hypothetical illustration of tectonic subsidence of the Tanqua depocentre during the Permo-Carboniferous time can be broken into two major phases: (i) an extensional phase involving subsidence caused by sedimentation and (ii) the onset of the compressional phase causing the occurrence of the bulge effect. Note: the piggy-back basin caused by uplift and erosion later on during the compressional phase as expressed would occur craton-ward i.e. NE and distal to the CFB (this would happen in the Late Triassic, which is outside the scope of this study).

#### 4.6 PROPOSED BASIN-FILL MODEL FOR THE TANQUA DEPOCENTRE

The subsidence plot in Fig. 4.10 displayed linear and convex-upward curves with the subsidence rates de-accelerating early on and then accelerating through the Permo-Carboniferous period. The tectonic subsidence curves show a pre-molasses phase resembling

that of a passive continental margin characterised by slow to medium subsidence rate, and a molasses phase of rapid subsidence with the onset of foreland basin evolution (Einsele, 2000). The development of a passive margin along the southern margin of the Kalahari craton resulted from the occurrence of extensional tectonics in the Early Palaeozoic. Subsequently, continental shelf deposition of the Cape Supergroup (Ordovician to Early Carboniferous in age) occurred. Therefore, this tectonic setting suggests that the Cape Supergroup probably underwent extensive reworking by shallow-marine processes on a stable shelf to produce quartz-rich sands (Tankard *et al.*, 1982; Johnson, 1991; Thomas *et al.*, 1993), and the provenance proposed as a cratonic source to the north during the late Devonian.

Recorded data in the form of structures to further support the stated above tectonic setting for the Cape Supergroup are:

1. Thrust stacking is a common characteristic in the arenaceous units of the Witteberg and Table Mountain Group of the Palaeozoic Cape Supergroup rocks (Booth and Shone, 1992; 2004; and Newton, 2006). Bedding-parallel thrusting, duplexing, and piggy-back thrusting are seen to have disrupted strata, giving rise to variable bed thicknesses of the stacked.
2. These thrust stacking resulting in tectonically thickened arenaceous units are observed in areas of thrust faulting. The thrust faulting is interpreted to have taken place during the late Palaeozoic, whereas normal and strike-slip faults (with the latter seen to occur approximately parallel to the strike of the former) are products of Gondwana break-up during the Mesozoic (Booth, 2009).
3. Rocks of the Witteberg Group observed to be folded into asymmetric folds and thrust faulted during the late Palaeozoic (Booth 1992).
4. A complex pattern of ductile and brittle deformation occurs in the Table Mountain Group, whereas in the overlying Bokkeveld and Witteberg Group there is a close association of folding with the development of thrust faults (Booth, 2009).

In this context, the internal part of the Karoo foredeep was superimposed on a passive continental margin, i.e. on lithosphere which was already mechanically extended and had thermally subsided. Relating this theory to the SW Gondwana, subduction of the Palaeo-Pacific oceanic plate under the Gondwana plate possibly during the mid-Carboniferous, which formed a magmatic arc may have caused stretching and then slow thermal subsidence of the lithosphere. In agreement to this theory, Visser and Praekelt (1996) proposed thermal subsidence associated with release of Gondwana heat as the main process responsible for the formation and location of the foredeep. In addition, Catuneanu *et al.* (2005) proposed that interplay of these tectonic mechanisms, combined with the influence exerted by the inherent structures of the underlying Precambrian basement, resulted in the formation of discrete depozones that follow regional tectonic trends.

The initial occurrence of extensional tectonics and the development of a passive margin along the southern margin implies the subsidence was initiated and mainly controlled by mechanical (i.e. detachment faults of basement blocks that occurred during rifting) rather than thermal geologic events (i.e. sediment burial). Furthermore, as overthrusting continues, the orogenic belt progressively loads more rigid lithosphere on the landward side of the former passive margin. In addition, variations in the flexural rigidity along the strike of the basin possibly led to unpredictable lateral changes in the subsidence history (Fig. 4.16). The suggested model showed a good agreement with the lithostratigraphic data, in particular, it explains the thickness of sediments in the Tanqua depocentre, the depocentre's formation at the front of the Cape Fold Belt, and rapid subsidence. Conclusively, the Tanqua depocentre subsided rapidly as orogenic loading increased, leading to the conclusion that periods of thrusting in the CFB and periods of subsidence of Tanqua depocentre are simultaneous. The computed tectonic subsidence is consistent with tectonic models that propose a Permo - Carboniferous basin formation.

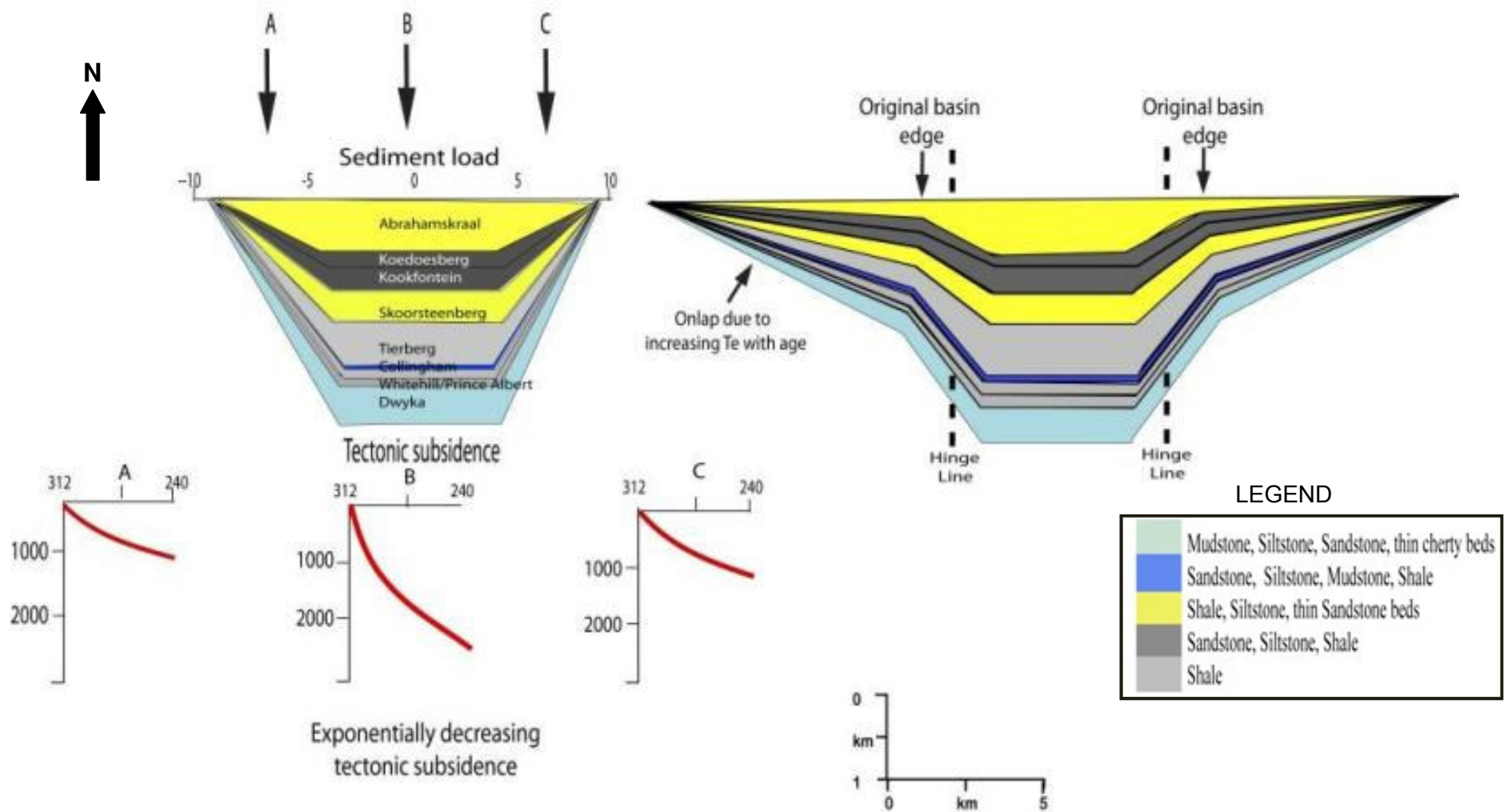


Figure 4.12: Cross-section through Tanqua depocentre showing the approximation of the tectonic subsidence due to sediment load obtained from the observed lithostratigraphic units backstripped using the method by Allen and Allen, 1990; Watts, 2001.

## CHAPTER FIVE: TECTONIC LOADING AND SEDIMENTATION IN TANQUA DEPOCENTRE

### 5.1 SEDIMENTATION RATES AND SEDIMENT TRENDS

In this chapter the link between tectonic loading history in the CFB, eustatic (global) sea-level changes and sedimentation pattern in the Tanqua depocentre is established with the purpose of describing how mass accumulation rates and sediment volume correlates with major terrain accretion events. The method used to calculate sedimentation rate is described by Magara (1978) and relies on the decompaction of a lithological unit to its original thickness as done in the previous chapter using Van Hinte's (1978) equation for decompaction estimates. The resultant thickness is divided by the time interval associated with deposition of that particular unit. Unfortunately, uncertainties often associated with absolute age dates, and more critical factors such as over pressuring, changes in rock type, and the existence of unconformities, which have an influence on decompaction modelling (Pate, 1986) all lead to large uncertainties in the final sedimentation rate calculated. In addition, the decompaction process is generally applied on a well-by-well basis making it difficult to obtain a basin-wide characterisation of sedimentation rates.

According to Underschultz (1991), to measure how quickly a particular unit accumulated in the basin for a specific rock unit, the mass accumulation rate  $Rm$  ( $\text{kgm}^{-2} \text{Myr}^{-1}$ ) is given by the formula below:

$$Rm = \frac{(1 - n)D\rho}{\Delta T} \quad [10]$$

Where  $n$  is porosity,  $D$  is thickness (in metres),  $\rho$  is grain density ( $\text{kg m}^{-3}$ ) and  $\Delta T$  is the time interval (Myr) during which the unit was deposited.

Furthermore, the accumulated sediment volume is easy to calculate from the mass accumulation rate below:



$$\frac{\rho_m \times A \times \Delta T}{\rho} = V \quad [11]$$

i.e. 
$$\frac{\text{Kgm}^{-2} \text{Ma}^{-1} \times \text{m}^2 \times \text{ma}}{\text{Kg m}^{-3}} = \text{m}^3$$

Where A is area in m<sup>2</sup>

Calculation of the mass accumulation rate and sediment volume in Tanqua depocentre use dataset that lists successions from the depths of basement to the surface. The successions of the Tanqua depocentre were divided into nine regional lithostratigraphic units (Table 5.1). The time-scale and radiometric date from Veevers *et al.* (1994), Bordy *et al.* (2004), Rubidge (2005) and Isbell *et al.* (2008) were used to estimate ages for the lithostratigraphic units. The values assigned to the duration of each unit are thus the best available estimate given the present state of knowledge of regional stratigraphic correlations and limited biostratigraphy of the depocentre.

The Tanqua depocentre is bounded in the west and east by the N-S arm of the CFB i.e. 50km along Cederberg and the Bontberg antiform i.e. a width of 15km along an extension of where the Hex river antiform (a basement high) begins respectively (Fig. 5.01), which would have acted as barriers to sediment transport. The mass accumulation rates are averaged over the period of sediment accumulation. In addition, sedimentation rates in km<sup>3</sup>/Ma were calculated as volume divided by the time span. The volume of accumulated sediment is calculated for nine time intervals for each of the nine lithostratigraphic units depocentre (~302 – 290 Ma; ~290 – 278 Ma; ~278 – 272 Ma; ~ 272 – 271 Ma; ~ 271 – 270 Ma; ~ 270 – 269 Ma; ~269 – 268 Ma; ~268 – 266 Ma; ~266 – 240 Ma) by subtracting the depth of each unconformity from the depth of the unconformity stratigraphically below. These volumes are then corrected for compaction using the formula:

$$V_{\text{surf}} = V_{\text{bur}} + (\Phi_{\text{surf}} - \Phi_{\text{bur}}) \quad [12]$$

Where  $V_{\text{surf}}$  = volume at surface

$V_{bur}$  = volume at a given depth

$\Phi_{bur}$  = porosity at depth

$\Phi_{surf}$  = porosity at surface

Porosity and grain-density data were taken from Frostick and Steel, (1993). Therefore, all parameters needed to calculate mass accumulation rates for the Tanqua depocentre were easily accessible. The results are presented in Table 5.1 and a bar chart of the sediment volume and the corresponding sedimentation rate of the lithostratigraphic units in the Tanqua depocentre is presented in figure 5.02.

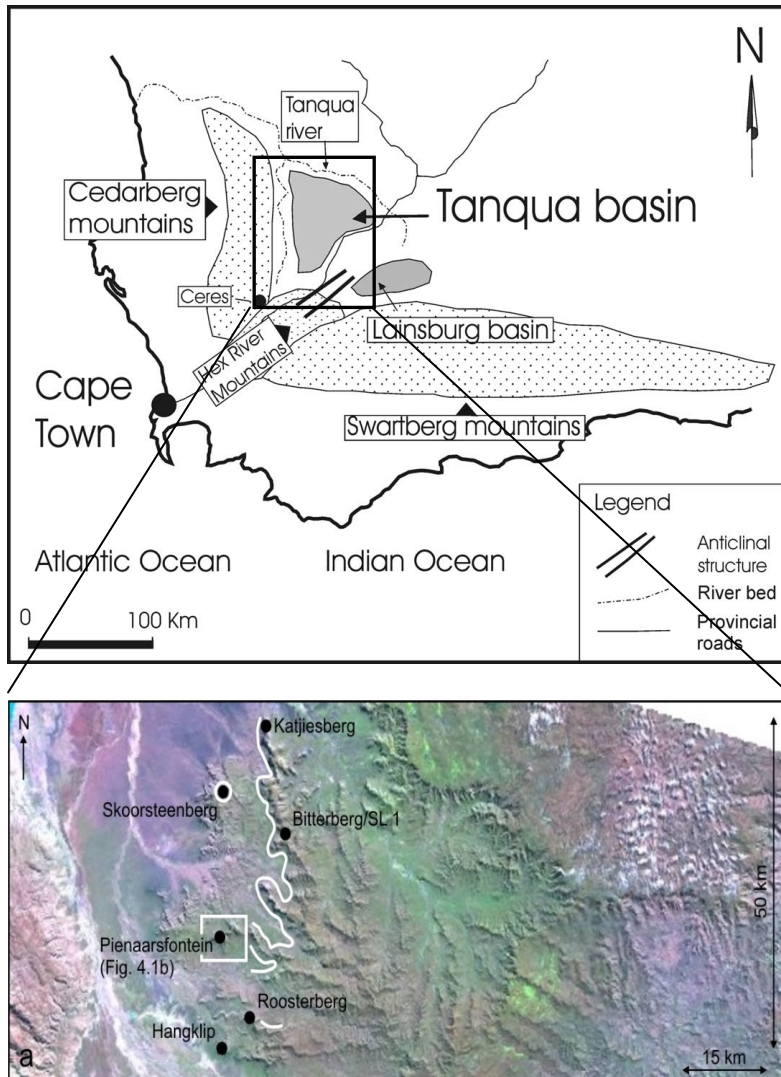


Figure 5.01: Location map showing Tanqua depocentre (study area) and Laingsburg depocentre (adapted after W. Van der Werff *et al.*, 2003), the landsat image is showing the area extent of the Tanqua depocentre.

## 5.2 RESULTS

A low accumulation rate is observed (Fig. 5.02) during deposition of the Dwyka Group (0.44  $\text{Km}^3$  at 0.037  $\text{Km}^3/\text{Ma}$ ). Subsequently, a rapid increase in sedimentation rate occurred up until the mid Permian where it reached a peak with deposition of the Tierberg Formation (0.75  $\text{Km}^3$  at 0.75  $\text{Km}^3/\text{Ma}$ ). Then there was a rapid decrease in sedimentation rate through to the Late Permian period until it reached the Early Triassic with during deposition of the Abrahamskraal Formation (0.18  $\text{km}^3$  at 0.0069  $\text{km}^3/\text{Ma}$ ).

Units	Age span (Ma)	Time span $\Delta T$ (Ma)	Compacted thickness (m)	Density $\rho$ ( $\text{kgm}^{-3}$ )	Ave. Mass accumulation $R_m$ ( $\text{kg/m}^2/\text{Ma} \times 10^3$ )	Actual length (km)	*Area A ( $\text{km}^2$ )	Volume V ( $\text{km}^3$ )	Sedimentation rate $V/\Delta T$ ( $\text{km}^3/\text{Ma}$ )
Abrahamskraal Formation	240–266	26	500	2680	28.35	0.5	0.25	0.18	0.0069
Koedoesberg Formation	266-268	2	200	2700	162	0.2	0.04	0.16	0.08
Kookfontein Formation (top)	268-269	1	250	2700	432	0.25	0.0625	0.21	0.21
Skoorsteenberg Formation Fans 1-4 & unit 5	269-270	1	400	2680	728.96	0.4	0.16	0.28	0.28
Tierberg Formation	270-271	1	750	2720	1611.6	0.75	0.5625	0.75	0.75
Collingham Formation	271-272	1	70	2700	154.98	0.07	0.005	0.38	0.38
Whitehill Formation	272-278	6	80	2720	29.38	0.08	0.0064	0.44	0.07
Prince Albert Formation	278-290	12	165	2720	30.67	0.165	0.027	0.45	0.038
Dwyka Group	290-302	12	300	2600	55.9	0.30	0.09	0.44	0.037
<b>TOTAL</b>		62	2715			2.715	1.2034	3.29	

Table 5.1: Total sediment volumes and accumulation rates for Tanqua depocentre. \*Area for each lithostratigraphic unit is obtained by multiplying the thicknesses by the actual length from depth of burial. The radiometric dates are from Veevers *et al.* (1994); Bordy *et al.* (2004), Rubidge (2005), Isbell *et al.* (2008), and references therein.

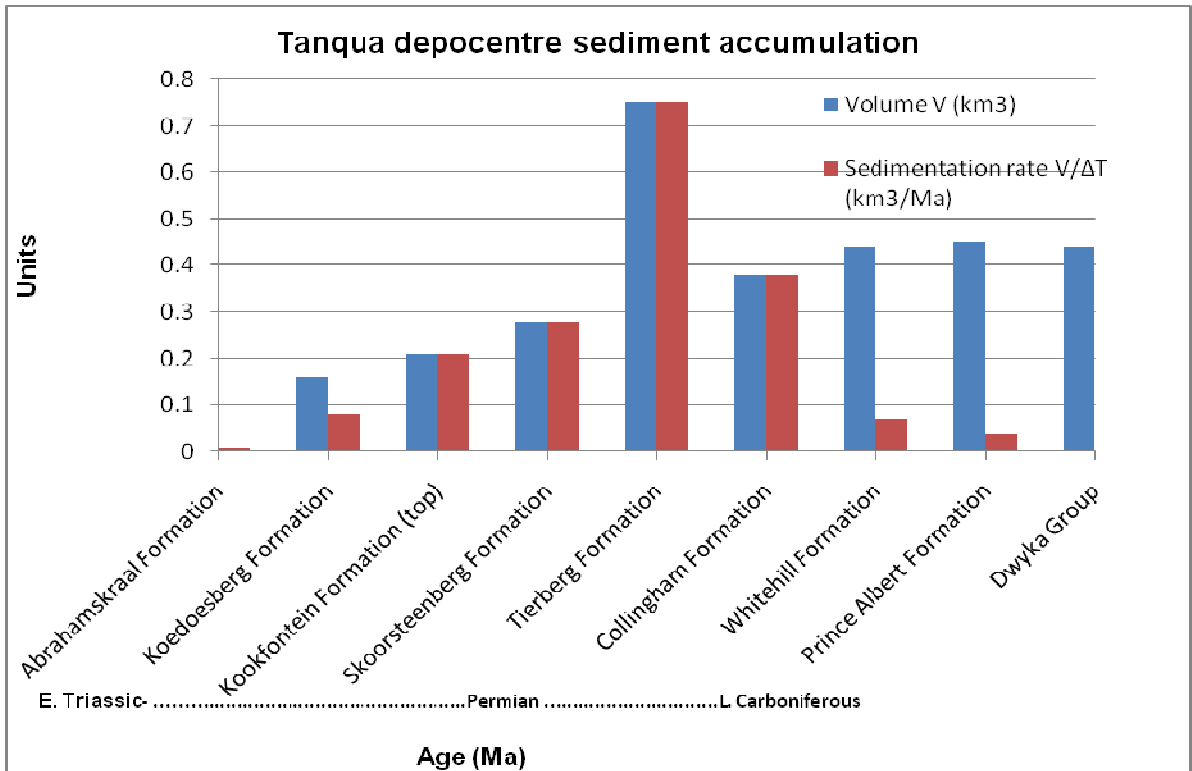


Figure 5.02: Graph of sediment volume and accumulation rate against time for Tanqua depocentre during the Permo-Carboniferous Period.

### 5.3 RELATIONSHIP OF SUBSIDENCE AND SEDIMENTATION TRENDS IN TANQUA DEPOCENTRE

The underfilled stage (Catuneanu *et al.*, 1998) of the Tanqua depocentre corresponds to deposition of carbonaceous shale of the Whitehill and Prince Albert Formation, and the orogenic unloading event in the CFB at  $278 \pm 2$  Ma (Hälbich, *et al.*, 1983). Likewise, Tankard *et al.* (2009) proposed subduction of the Karoo Basin at this period, possibly because the margin areas of the Tanqua depocentre were uplifted due to isostatic rebound and exposed to erosion resulting in dissection of the continental uplands by major river systems and the formation of an adjoining fairly flat-lying basinal plain. This is confirmed by the presence of inflections (red arrows) in the tectonic subsidence curve in the previous chapter (Fig. 4.10). Hence, this stage dominated by

fine-grained sedimentation (i.e. fine grained sandstone, shale, siltstones, mudstone and diamictites) in an open marine setting signifies the onset of a starved-basin stage. During this under-filled stage, siliciclastic sedimentation is confined to the proximal Karoo foredeep in the form of glacial influenced and deep marine deposits (i.e. turbidites reflecting low sediment supply) due to limited subaerial orogen relief caused by delayed orogenic pulses from the CFB, while there was high subsidence rate in the depocentre (Fig. 5.03 a & b).

On the other hand, the subsequent filled stage corresponds to the second compressional event at  $258 \pm 2$  Ma, involving deformation (uplift) at the CFB, which was enough to cut-off sedimentation paths and stop submarine fan deposits in the depocentre, possibly with the sand now trapped between the source area (i.e. Patagonian Massif (Van Lente, 2004)) and the CFB. This led to a shallowing of the earlier underfilled interior seaway and establishment of a shallow marine environment. Therefore, the Tanqua depocentre experienced predominantly hemipelagic and muddy turbidite deposition amidst deltaic successions i.e. mud and sand of the upper Ecca Group.

Lastly, the overfilled stage corresponds to a transition stage from the initial underfilled to the overfilled stage when sediment supply outpaced the creation of accommodation space by subsidence. This is clearly seen in the coarsening-upward (progradational) trend in the deltaic successions and palaeoflow patterns observed during fieldwork in the Tanqua. Overall, these findings show a close correlation between subsidence mechanism and rates of sediment accumulation, as sedimentation rates correspond to subsidence trends and tectonic subsidence during formation and filling of the Tanqua depocentre.

Conclusively, to determine the relationship between eustatic sea-level and tectonics (autogenic or allogenic factors respectively) within the Tanqua depocentre, and also the timing either one was active over the other, a comparison of each curves are therefore compared (see Fig. 5.04). This comparison displays that during deposition in the Tanqua depocentre both factors were mostly inversely proportional to each other i.e. while one factor was active or high, the other was

inactive or low. For instance tectonic activity was high while relative sea-level low during the deposition of the Upper Ecca Group i.e. the deltaic succession of the Kookfontein, Koedoesberg and also the turbidite fans of the Skoorsteenberg Formation. Hence, in this study, it is speculated that deposition was directly caused by tectonic movements. This strongly suggests that neotectonic activity influenced the location of deposition sites after the influence of sea level rise decreased.



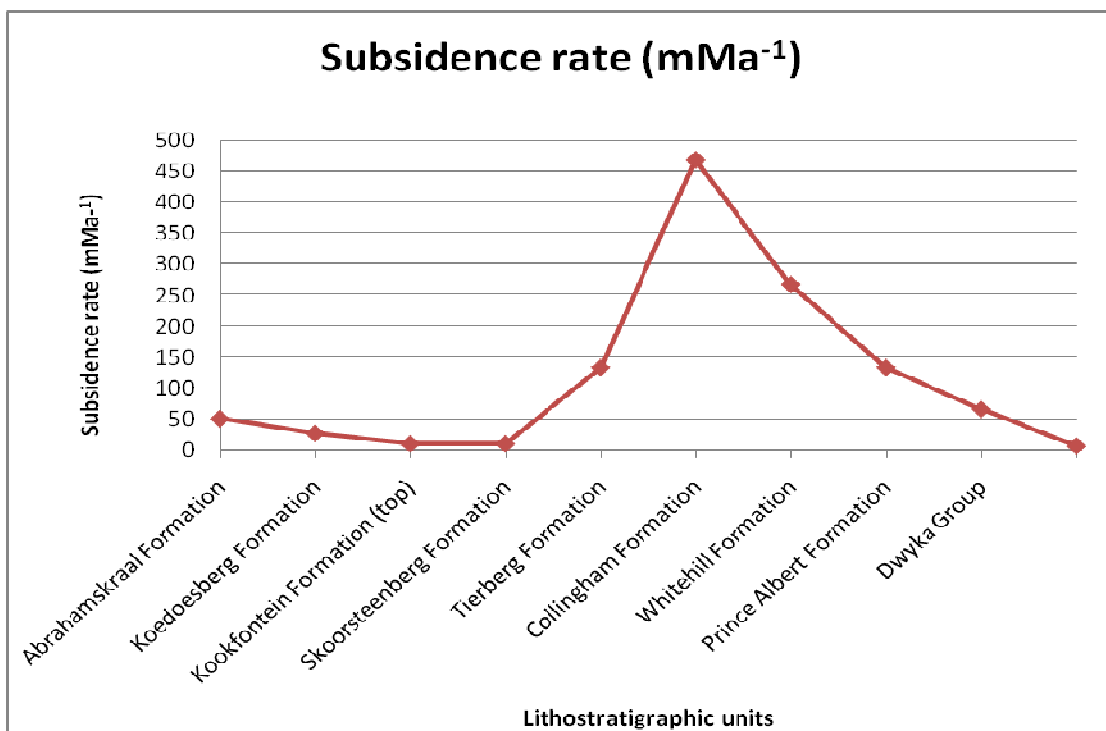
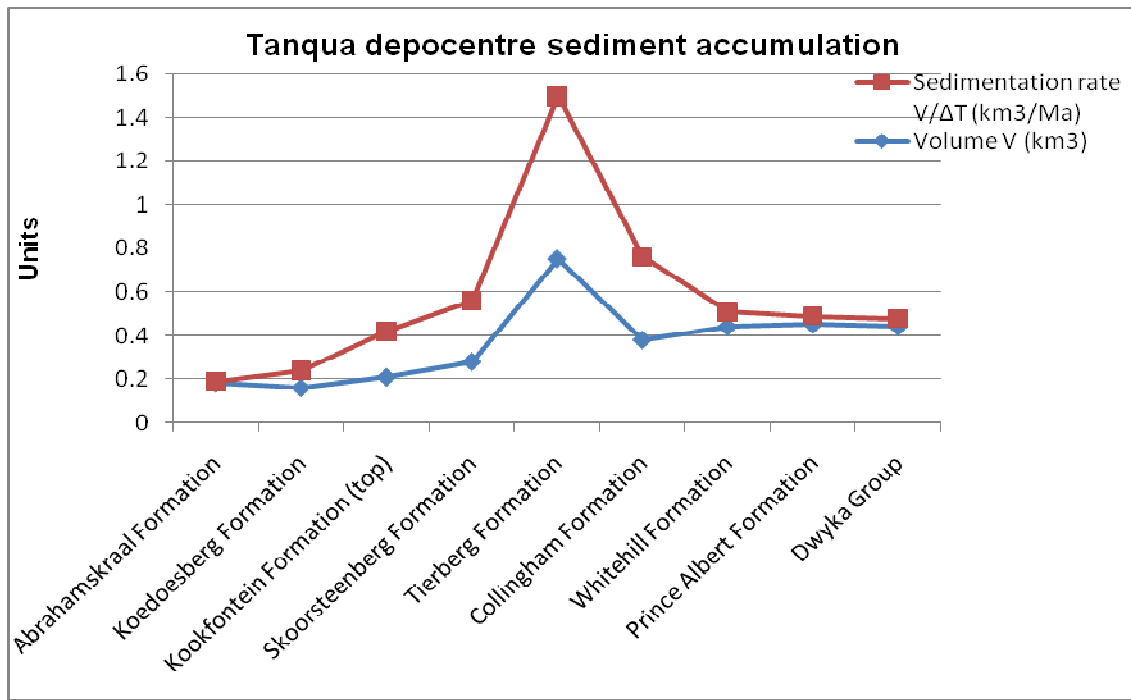


Figure 5.03: Comparison of the subsidence and sedimentation rate (a) Graph of the sedimentation rate and volume accumulation in Tanqua depocentre (b) Graph of the subsidence rate of the Tanqua depocentre.

The relationship between the sedimentation rate in the Tanqua depocentre, the orogenic loading pulses and unloading quiescence of the adjacent CFB and eustatic sea-level is also investigated and presented in figure 5.04. Hälbich *et al.* (1983) identified eight tectonic pulses by the CFB at  $292 \pm 5$  Ma,  $278 \pm 2$  Ma,  $258 \pm 2$  Ma,  $247 \pm 3$  Ma,  $230 \pm 3$  Ma,  $215 \pm 3$  Ma and 208 Ma whereby the second evidence of a compressional paroxysm at  $\sim 278 \pm 2$  Ma suggests the onset of a transition from extensional to compressional conditions within the back-arc basin. Furthermore, a major compressional paroxysm in the CFB at  $\sim 258$  Ma which suggests that ongoing compression along the inner arc eventually produced a retro-arc fold-thrust belt. The effects of these episodes of intense crustal shortening include thrusting and folding of Cape Supergroup and lowermost Karoo Supergroup rocks. The deformation is most intense in the east-west trending southern branch of the Cape Fold Belt (which is adjacent to Laingsburg depocentre), whereas the north-south trending western branch of the fold belt (which is adjacent to Tanqua depocentre) is less severely deformed (Shone and Booth, 2005).

Inferences drawn from figure 5.04 of the relationship between sedimentation rates, tectonic deformation and eustatic sea-level curve are presented below:

- The eustatic sea-level curve is seen to fall during deposition of the lower Beaufort Group (Abrahamskraal and Koedoesberg Formation) concomitant with CFB deformation thrusting at  $247 \pm 3$  Ma.
- A rise in sea-level elevation occurred during deposition of the Prince Albert Formation, and was concomitant with CFB deformational thrusting at  $278 \pm 2$  Ma. Therefore, the major transgression in the depocentre was controlled by sheer sediment volume and sedimentation rate exceeding subsidence rate. This is illustrated by a continuous increase in sedimentation rate in the depocentre during the late Permian (Fig. 5.02).

- Post-glacial mudrock deposition was characterised by relatively high sea-levels i.e. an extremely high sea-level elevation (Fig. 5.04) during deposition of the Lower Ecca Group successions (i.e. Tierberg, Collingham, Whitehill and Prince Albert Formations). The Collingham Formation dominantly composed of siltstone has a low mass accumulation rate and corresponds to a significant long-term rise in eustatic sea-level. The Whitehill and Prince Albert Formations dominantly composed of shale also have a very low accumulation rate and correspond to a high eustatic sea-level on the curve of Haq *et al.* (1987).
- A very high sea-level occurred in the Late Carboniferous during the final collapse of the marine ice sheet (i.e. associated with a major transgression) and deposition of the Dwyka Group.

Overall, it appears that during periods of low sediment influx sea-level is sufficiently high to trap sand at the edge of the depocentre and deposit shale and siltstone i.e. deposition of lower Ecca Group successions. Also, it appears that all the recorded deformational thrusting at the CFB occurred during low eustatic sea-levels, and deposition of sandstone successions in the Tanqua depocentre occurred at a high accumulation rate.

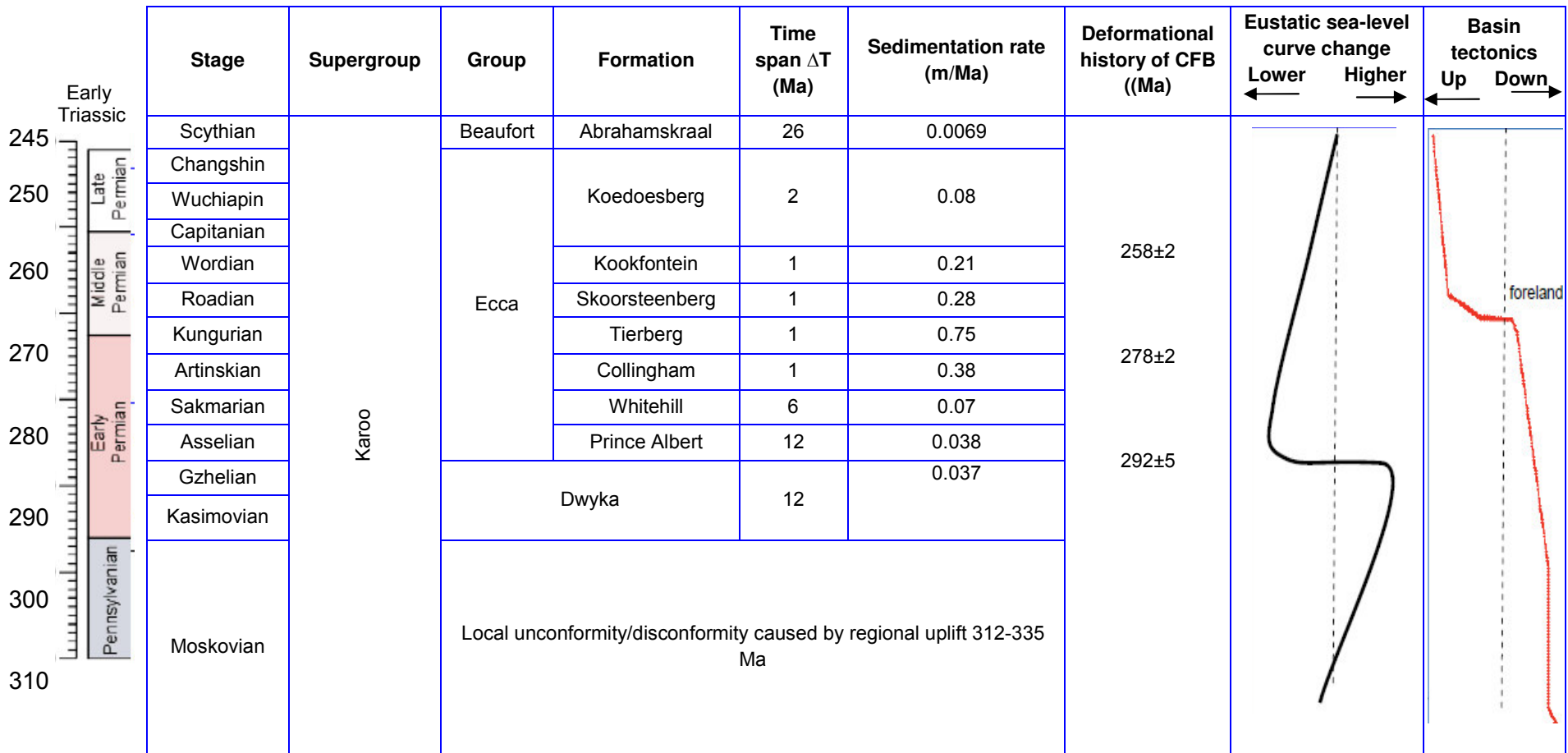


Figure 5.04: Generalized chronostratigraphic nomenclature and comparison between eustatic curve and the tectonic subsidence curve obtained from backstripping the lithostratigraphic units in Tanqua depocentre. The eustatic curves are taken from Haq *et al.*, 1987; tectonic paroxysms of the Cape Fold Belt from Hålbich *et al.* (1983) and Gresse *et al.* (1992). The time scale of Gradstein *et al.* (2004), time duration and mass accumulation rate (averaged across the study area) are estimates derived in this study.

#### **5.4 BASIN MIGRATION AND REGIONAL IMPLICATIONS**

Sediments become more compact and denser with depth of burial, thus, with respect to gravity and magnetic interpretation, sedimentary basins show up as gravity lows and low magnetic relief respectively, and these are of particular interest in hydrocarbon exploration. Also, traditionally, magnetic data have been used in early phases of exploration programs to map depth to magnetic basement and define the basin architecture. Sediments usually are considerably less magnetic than basement rocks, so deep sedimentary basins show as areas of generally low magnetic relief. 1:250, 000 scale tiff images of gravity and magnetic profiles (Fig. 5.04 and 5.05) covering the study area provided by the Council for Geosciences have been used to yield information on basin geometry and also the depth of subsidence of Tanqua depocentre. In these geophysical profiles, the Karoo foredeep is located NW-NE (inferred from the low gravity values), while the basement high is south. Interpretation of the magnetic and gravity profile was done by incorporating the contour values and running a couple of cross sections across it (Fig. 5.06 and 5.07).

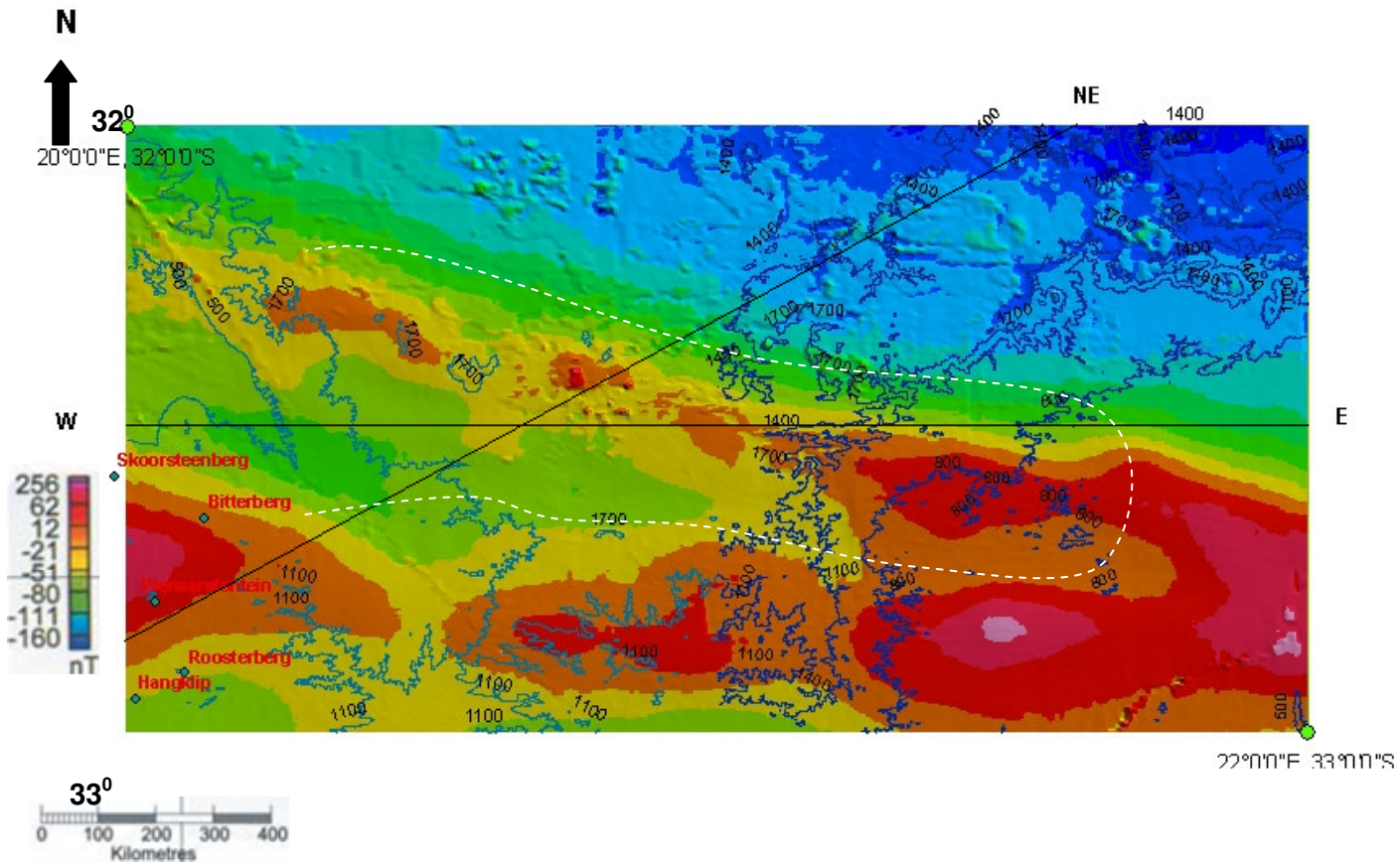


Figure 5.05: Magnetic profile covering the Tanqua depocentre (co-ordinates  $3220^{\circ}$  i.e.  $20^{\circ}.0' - 22^{\circ}.0'$  E and  $32^{\circ} - 33^{\circ}$  S); White dots = Beattie Magnetic Anomaly (BMA) axes (a distinct set of east-west trending magnetic anomalies confined to the basement beneath the Karoo Basin cover), and showing the cross-sections SW - NE and W - E (map is courtesy of the Council for Geoscience).

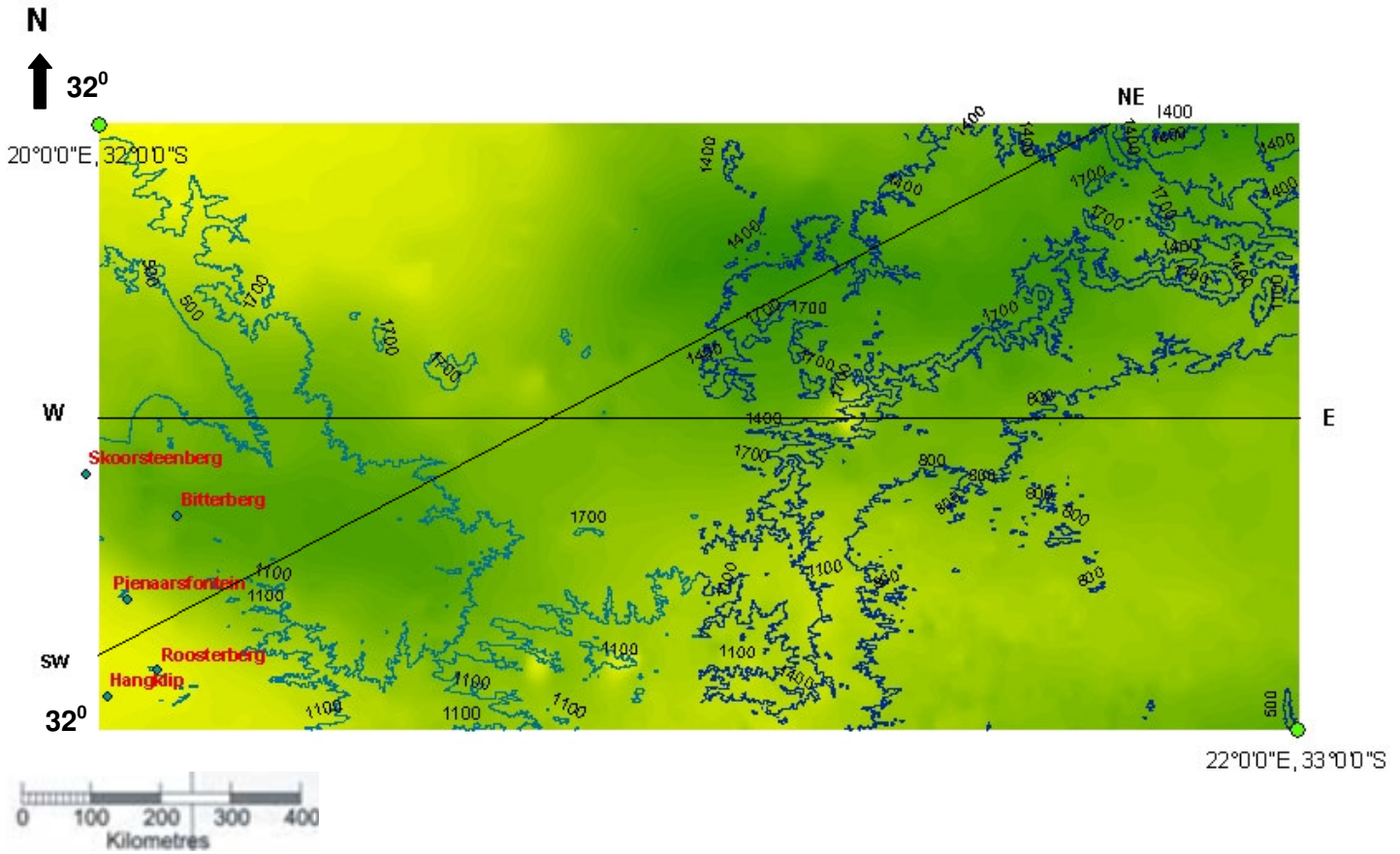


Figure 5.06: Gravity profile covering the Tanqua depocentre (co-ordinates 3220° i.e. 20°.0'–22°.0' E and 32°–33° S), also showing the cross-sections SW - NE and W - E (map is courtesy of the Council for Geoscience).

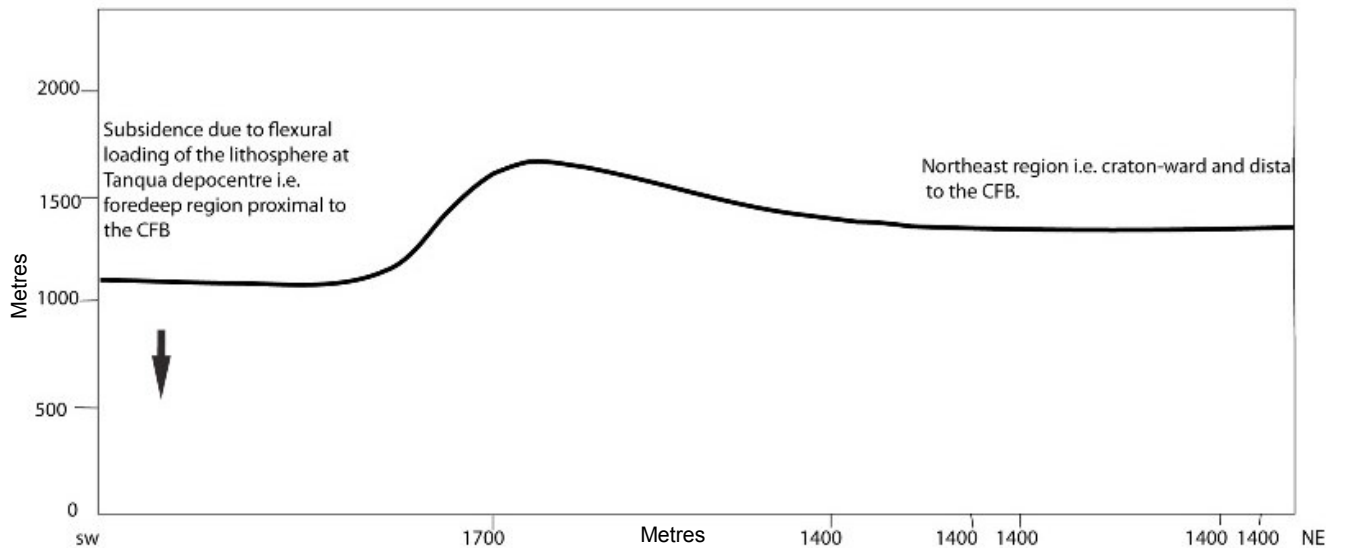


Figure 5.07: The SW - NE cross section using the contour lines along the magnetic and gravity profile of Tanqua depocentre. This shows the present-day topography of the land surface across the associated profile.



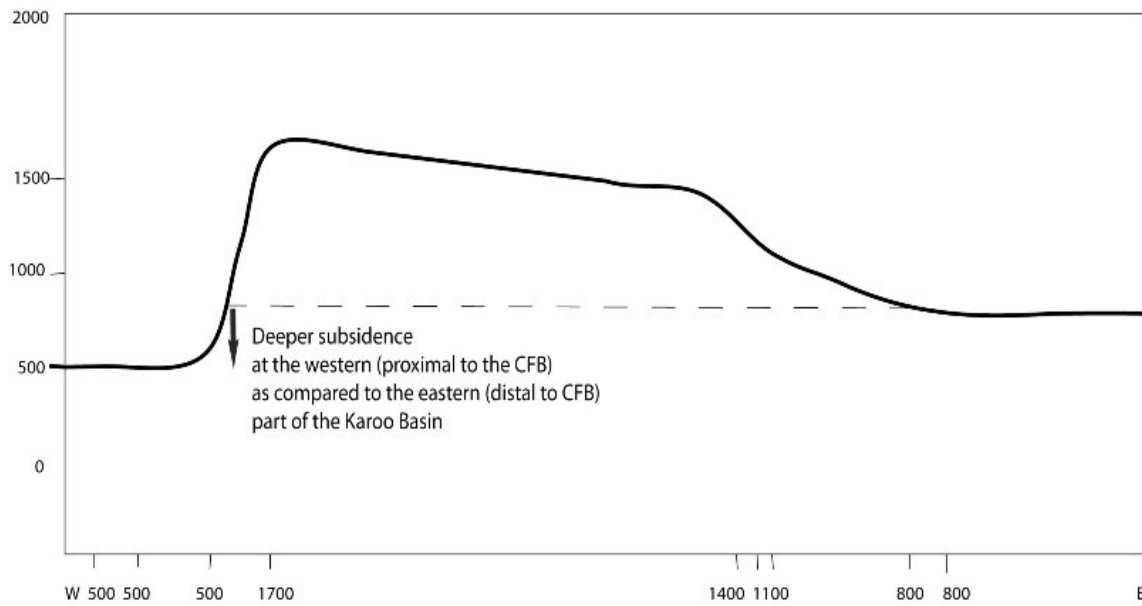


Figure 5.08: The W - E cross section using the contour lines across the magnetic and gravity profile of the Tanqua depocentre.

In general, the entire region is at high elevation (i.e., »1700 m) in the southwest and gently slopes downward to the northeast. The profile along the central and north-eastern side of the basin (fig. 5.07) shows the highest average topography. The topography progressively decreases for the western profiles, likely as a result of increased erosion of these regions. The basin is composed of a long wedge of sediments that trends east-west and thins to the north. The thickest and most extensive sediments occur in the central part of the basin (Fig. 5.08). This profile shows tectonic compression and the development of the Cape Fold Belt as a fold-thrust belt provided by supracrustal load to support these near-field lithospheric deflections.

Thrust sheet advancement from the CFB caused northward migration of the hinge-line separating the different facies types of the N and S. Along a dip-oriented profile, the Karoo sedimentary fill displays a wedge-shaped geometry, typical for foreland successions, with a maximum preserved thickness in excess of 7 km adjacent to the Cape Fold Belt (Rubidge, 1995). Likewise, the underlying lower crustal layer is described as wedge-shaped: ~24 km thick in the north and decreasing to ~12 km thick beneath the Cape Fold Belt by Lindeque *et al.*

(2007)'s near vertical reflection profile, that provides the first clear seismic image of a ~100 km long crustal section below the Karoo Basin, the frontal section of the Cape Fold Belt, and the basement region around the Beattie Magnetic Anomaly hosted by a well-defined 20 km thick mid-crustal layer occurring below a seismically imaged unconformity. Lindeque *et al.* (2007) interpreted the internal seismic fabric of this layer as a tectonic fabric dipping to the north in contrast to previous tectonic models. The seismic image reveals no significant stratigraphic thickening of the Karoo basin towards the CFB tectonic front as postulated on geological grounds (e.g. Cole, 1992; Catuneanu *et al.*, 1998). The significant flexural component across the basin (e.g. Cloetingh *et al.*, 1992; Milani and De Wit, 2007) therefore needs further analyses.

The stratigraphy of the Karoo Supergroup is markedly different between the southern (proximal) and northern (distal) regions of the basin (Fig. 5.08). These differences reflect contrasting tectonic histories across the flexural hinge line of the foreland system (Catuneanu *et al.*, 1998). Catuneanu *et al.* (1998) modelled the changes in accommodation in the Karoo Basin as being controlled by the flexural response of the lithosphere to orogenic cycles of loading and unloading. They further showed that the out-of-phase history of base level changes between the foredeep and the forebulge flexural provinces generated contrasting stratigraphies with a timing that matches the dated compressional events in the Cape Fold Belt (Hälbich, 1983, 1992; Hälbich *et al.*, 1983; Gresse *et al.*, 1992).

The W - E cross-section (Fig. 5.08) also shows the flexural response of the lithosphere in the west to east direction. The dynamic topography displays a subsidence similar to a wave-like deflection of the lithosphere caused by mantle flow rather than due to orogenic thrusting or loading. Across this W -E direction is the Beattie Magnetic Anomaly (BMA) axis (a distinct set of east-west trending magnetic anomalies confined to the basement beneath the Karoo Basin cover). There is an interpreted mid-crust ophiolite wedge (e.g., a fossil subduction zone) in the region of the BMA associated with *south*-dipping thrust faults, thus the possible reason for ridge-like profile of the interpretation.

The Karoo foredeep region is a zone of rapid subsidence and subsequent removal of the thrust load by erosion and other processes results in flexural rebound of the thrust belt and formation of an adjacent foreland basin. Proximal deposits along with thrust-derived sediment are re-deposited in the distal foreland basin. This two-phase model of foreland sedimentation predicts that coarsening-upward sequences in the proximal and distal parts of the Karoo Basin have reciprocal significance, whereby the proximal sequence represents thrust-belt advancement and the distal sequence represents thrust-belt cessation (Catuneanu et al., 1998). Reciprocal stratigraphies consist of correlative proximal transgressive and distal regressive facies, and vice versa, and the interface separating them termed the hinge line. Retro-foreland basins, including the Karoo Basin, are subject to static and dynamic (mantle corner flow - Tankard, et al., 2009) loads, which cause subsidence with respective wavelengths, and the sedimentary response to these combined tectonic loads is a likely cause of reciprocal stratigraphies.

## CHAPTER SIX: DISCUSSIONS AND CONCLUSIONS

### 6.1 SEQUENCE STRATIGRAPHY

In foredeep basins, alternating periods of tectonic uplift and subsidence mostly control cyclicity and sequence development (Mutti *et al.*, 2003). Eustatic controls on late Palaeozoic sequences are recognized on stable cratonic platforms, but in adjacent orogenic basins eustatic controls are not easily separated from tectonic controls (Ross and Ross, 1988). Thick successions of the basin floor shales and siltstone intervals (i.e. Whitehill, Prince Albert, Collingham and Tierberg Formations) indicate that the Tanqua depocentre was once an underfilled foredeep, where accommodation space was little constrained by eustasy.

The shale units record starved basin conditions that developed after foredeep subsidence but before significant influx of sediment (i.e. Upper Ecca Group Formations) was eroded from the thrust belt (Figure 4.10). The condensed section (a sequence or strata much thinner than developed elsewhere, and caused by diminished sediment supply) in the chronostratigraphic reconstruction of the Tanqua and Laingsburg depocentre proposed by Flint *et al.* (2004) serves as a marine hiatus and could be interpreted as indicating a rapid sea-level rise, with sediment starvation in the basin floor because of temporary entrapment of the detritus in the overlying shallow water delta complexes.

The generally progradational and coarsening-upward depositional style of the deltaic successions (Kookfontein and Koedoesberg Formation) is a response to shoaling (reduction of accommodation space) and uplift on the north margin of the basin (Fig. 5.08). It is suggested that controls on the routing and storage of sediment from source to the basin floor was spatially and temporally complex, and not simply related to regional base level changes (Wickens, 1994; Wickens and Bouma, 2000), or tectonic quiescence and channel avulsion (Scott *et al.*, 2000).

However, this study shows that low sea-level and high sedimentation rate occurred during the deposition of these deltaic successions adjacent to the deformed belt, as a result of more

localized loading events i.e. thrusting at the CFB. The allogenic factors influencing deposition of these deltaic successions are changes in base-level and tectonic activity from the CFB, whereby their effect caused a high sedimentation rates in Tanqua depocentre, the water discharge to sediment load ratio, and land surface gradients Both regional and local progradation rates are influenced by tectonic movements, subsidence due to compaction, and changes in base-level, discharge, and sediment load. The newly formed channels from the deltas tend to shift toward areas of maximum subsidence. Although we cannot prove that deposition was directly caused by tectonic movements, this strongly suggests that neotectonic activity influenced the location of deposition sites after the influence of sea level rise decreased (Fig. 5.04).

## **6.2 TECTONIC SUBSIDENCE**

The method of subsidence analysis involving decompaction and backstripping has rarely been used for Lower Palaeozoic sequences or foredeep regions of a retro-foreland basin. However, it is suggested here that it is feasible to analyse such basins for subsidence if : (1) all the errors involved are considered, including the issues of stratigraphic resolution and sampling, and (2) the subsidence data are used in conjunction with other lines of evidence in order to determine basin controlling mechanisms. The ability of this technique to discriminate different Karoo foredeep basin-controlling mechanisms emphasizes the validity and importance of its application to ancient sequences.

Delayed filling is common in foreland basins and may result from the rate of subsidence outpacing the rates of sediment erosion, transport, and deposition (Flemings and Jordan, 1990). In Tanqua depocentre, much of the lag time results from infilling asymmetrically from the south as the foredeep migrated northward in response to plate convergence. The initial fill of the SW Karoo was dominated by glacial influenced sedimentation followed by basin expansion caused by tectonic subsidence. At the first subsidence phase, each thrust fault is induced by a vertical load, i.e. for each thrust, the depression (subsidence) and the bulge migrates in the opposite direction of the fold belt (cratonward/northward). The calculation of the tectonic subsidence by

“backstripping” indicates that tectonic subsidence was quite important during the initial stages, but it progressively decreases significantly.

A feature mentioned in Allen *et al.* (1986) is that at the stage of rapid subsidence, curves are straight or convex upward. For the Tanqua depocentre, this can be seen in Fig. 4.10, and it seems obvious that the relatively short phase of rapid subsidence cannot be due to lithosphere cooling, but should be caused by other geodynamic process. All subsidence curves show a cessation in tectonic event in the Tanqua depocentre during deposition of the Karoo Supergroup sediments, as revealed by the slowing down of subsidence. In this study, the zone of maximum thickness of sediments correlates with the area of maximum subsidence, therefore from graphs 5.03a and 4.11 representing sediment accumulation rate in the subsiding Tanqua depocentre, the following inferences are drawn:

- The highest sediment accumulation rates occurred during times of greatest subsidence. The reason for this is possibly because the amount of preserved sediment was dependent directly on the amount of basement subsidence.
- Moderate accumulation rate corresponds to the deposition of the Dwyka Group diamictites, and the Lower Ecca Group shale and mudstones. It correlates with the extension stage depicting the visual expression of foreland basin-generating mechanisms on the subsidence curve shape, which includes short/intermittent inflexions in the subsidence curves during the interval of 302 – 290 Ma and 272 – 270 Ma respectively.
- Moderate to low accumulation rate occurred predominantly in a short and intermittent subsidence phase from 269 – 266 Ma (foreland basin development - red arrow inflexions in stage V – see Fig. 4.10). It corresponds to the deposition of the Abrahamskraal Formation sandstones, Koedoesberg Formation and the Upper Ecca Group successions consisting of sandstone, shales and sandstone with interbedded shale.

However, in this study, the subsidence curves of the Tanqua depocentre of the Karoo foredeep revealed the migration of the depocentre, as the phenomenon of migration seems to be closely related to kinematics of the adjacent fold thrust belt, and an apparent migration of the depocentre in the Karoo foredeep depends upon movements along thrusts.

### 6.3 CONCLUSIONS

In the process of foredeep formation a first phase of slow to moderate subsidence ends by relative extension (hiatus), and then followed by a series of episodes of rapid subsidence. Based on these observations on the subsidence curves, it is possible to infer that the first stage of relative inflection (~ 290 Ma) is therefore recognised as the first stage of Tanqua depocentre formation.

An inverse relation between orogenic thrusting in the Cape Fold Belt (CFB), deposition of sandstone, and fall in eustatic sea-level is identified for late Palaeozoic sedimentation, particularly with deposition of the Upper Ecca and Upper Beaufort Group (deltaic and fluvial successions respectively). The late Carboniferous to early Permian sea-level fluctuations in the Tanqua depocentre show correspondence with global eustatic cycles reflecting low tectonic interference with sea-level patterns. However, late Permian sea-levels were predominantly tectonically controlled as a result of orogenic thrusting from the CFB associated with foreland basin evolution.

The measure of relative sea-level change in a basin is the interaction of regional tectonics, eustasy and the rate of sediment supply (Haq, 1991). Siliciclastic cover in the Tanqua depocentre expanded from minimal values in the early Triassic (Early to late Anisian) to a maximum in the middle Permian (Wordian -Roadian) (Fig. 5.02), accompanying a global falling trend in eustatic sea-level and favoured by a compressional phase involving a regional shortening due to orogenic thrusting and relative inflections (causing the bulge effect – see Fig.



4.14). Despite the lack of good age constraints on the late Palaeozoic Karoo strata certain correlations between their relative sea-level curve of the Karoo Basin proposed by Visser (1993) and global eustatic events are evident. The estimate of sediment volume obtained in this study for the early Carboniferous Period to a maximum in the Triassic is therefore consistent with published eustatic sea-level and stress regime data (Haq *et al.* 1987; and Ziegler, 1988). Hence, suggesting that increasing sediment volumes in the early Carboniferous in the Tanqua depocentre are reflected in the drawdown in the eustatic sea-level recorded.

From the Westphalian (Moscovian – Early Carboniferous) into the Sakmarian (Early Permian), the Dwyka ice cover gradually decreased as a result of fragmentation due to basin formation and marine flooding of glaciated areas of Gondwana (Fig. 5.02). Regional subsidence allowed the preservation of a thick and widespread glacially influenced marine record. Subsequent reduction of the ice cover during approximately Westphalian time reflects subsidence and marine incursions into Tanqua depocentre. This transgression greatly increased the glacially influenced marine areas and resulted in the preservation of a very large volume of glacial and marine strata.

In conjunction with sedimentological and tectonic data, the subsidence patterns for the Karoo Supergroup indicate deposition in a flexurally-loaded foreland basin which migrated north-eastwards with time. However, early Permian sedimentation may represent the onset of foreland basin deposition. The new data are consistent with a diachronous cessation of marine incursion and closure of the Tanqua depocentre, and related to a compressional stress regime in Gondwana interior during the late Palaeozoic. Early Permian oblique collision produced transpression in the SW Karoo. Subsequent rotation of motions of the mega-blocks and also regional geodynamic settings produced more orthogonal collision. Thus, continental flexure was felt initially in SW Karoo region in late Permian times, followed by migration of the resultant foreland basin to the northeast.

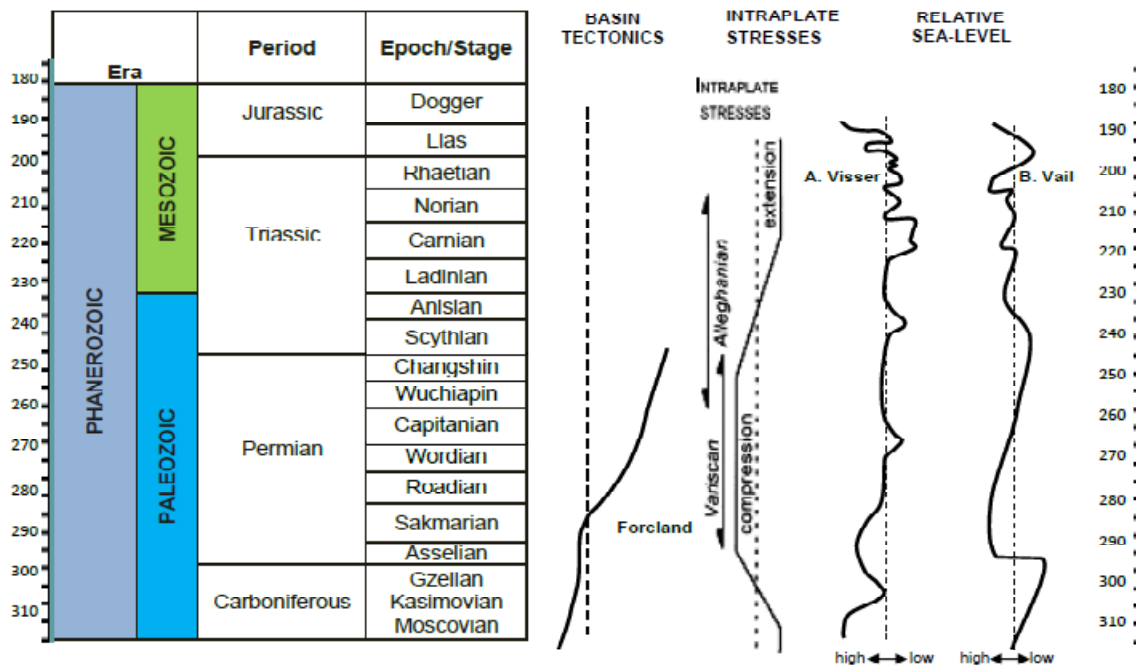


Figure 6.01: Summary data involved in the estimate of the Tanqua depocentre basin-fill. Significance of columns are: basin tectonics— uplift-subsidence history for Tanqua depocentre; intraplate stresses—stress regime in Gondwana interior with approximate durations of Variscan and Alleghanian orogenies (Ziegler, 1988); relative sea-level fluctuations during the late Carboniferous and Permian: A. Karoo Basin (after Visser, 1993); B. inferred global fluctuations (after Vail, 1977). The time scale is after Harland *et al.* (1982).

## 6.4 RECOMMENDATIONS

Sandstone distribution patterns also provide information useful for reconstructing tectonic history of sedimentary basins. The changes in locations of sand deposition, transport directions, and source areas reveal a more detailed history of episodic thrusting and intrabasinal uplift than do gross thickness changes alone. Sand is a sensitive indicator because (1) an extrabasinal source is commonly needed to supply large volumes of sand to the basin floor (Galloway, 1989) and (2) sand transport and deposition are more focused and confined relative to mud. Hence, suggestion for contour mapping of grain size and succession thickness would reveal 3D

architecture, palaeogeography, routing and tectonic events all at the same time in Tanqua depocentre.

Likewise, from this improved understanding of the evolution of the basin-fill of the Tanqua depocentre, it may be possible to undertake a three dimensional reverse modelling and arrive at a deeper understanding of the controls on sequence architecture. Conclusively, there is a need to establish whether and when Karoo was partially and completely closed, as this would set the boundary conditions for the influence of eustatic variations in the basin.

With subsidence followed by uplift and denudation, the thermal history of the Karoo Basin exhibits a phase of conductive heating and a phase of cooling. However, the reconstruction of the thermal and stress history of the rocks is complex due to tectonic implications i.e. deeply seated sedimentary rocks not affected by subsequent folding or thrusting. To verify the estimation of the maximum temperature and dates during the burial history of the SW Karoo, which is outside the scope of this work, independent methods could be applied. These include:

- investigation of fission tracks in apatite grains to determine the uplift date;
- study of fluid inclusions and determination of the vitrinite reflectance of the organic matter (probably the carbonaceous shale of Whitehill Formation) to estimate the maximum depth of burial

The results obtained from these independent methods would most likely show significant changes in the evolution of the thermal gradients, and subsequent cooling due to uplift and exhumation. The extensive apatite fission-track survey of the Tanqua depocentre successions of the Karoo foredeep could show a general decrease of the maximum palaeotemperature undergone by the sediments towards the Karoo foreland areas, and also indicate that the previously assessed total thickness of 7 Km overburden stripped off from the SW Karoo (Van Lente, 2004) is far too large to justify the determined temperature values with regards to eroded successions of the Tanqua depocentre.

## REFERENCES

- Allen, P.A., Homewood, P. and Williams, G.D. (1986). Foreland basins: an introduction. In Allen, P.A. and Homewood, P. (Eds): "Foreland Basins". Special Publications International Association of Sedimentologists, **8**, 3 -12.
- Allen, P.A. and Allen, J.R. (1990). Basin Analysis: Principles and Applications, Blackwell Scientific Publications, Oxford, 449.
- Angevine, C.L., Turcotte, D.L. (1983). Porosity reduction by pressure solution: a theoretical model for quartz arenites. *Geol. Soc. Am. Bull.* **94**, 1129 – 1134.
- Baldwin, B. and Butler, C.O. (1985) Compaction curves. *American Association of Petroleum Geology Bulletin*, **69**, 622 – 626.
- Bamford, M.K. (2000). Fossil wood of Karoo age deposits in South Africa and Namibia as an aid in biostratigraphical correlation. *Journal of African Earth Sciences*, **31**, 119 – 132.
- Bangert, B., Stollhofen, H., Lorenz, V. and Armstrong, R. (1999). The geochronology and significance of ash-fall tuffs in the glaciogenic Carboniferous – Permian Dwyka Group of Namibia and South Africa. *Journal of African Earth Sciences*, **29**, 33 – 49.
- Bathurst, R.G.C. (1971). Carbonate Sediments and their Diagenesis. Elsevier, Amsterdam.
- Beaumont, C. (1981). Foreland basins. *Geophys. J. R. Astron. Soc.* **65**, 291 – 329.
- Boggs, S. Jnr. (2006). Principles of sedimentology and stratigraphy, fourth Edition, Pearson Prentice Hall, **662**, 409pp.
- Bond, G.C. and Kominz, M.A. (1984). Construction of tectonic subsidence curves for the early Palaeozoic miogeocline, southern Canadian Rocky Mountains: Implications

- for subsidence mechanisms, age of breakup, and crustal thinning. *Geological Society of America Bulletin*, **95** (2), 155 - 173.
- Booth, P.W.K. and Shone, R.W. (1992). Structure of the Table Mountain Group in Port Elizabeth area. *South African Journal of Geology*, 95, 29 – 33.
- Booth, P.W.K., Brunsdon, G. and Shone, R.W. (2004). A duplex model for the Eastern Cape?
- Booth, P.W.K. (2009). A review of the structural geology of the Cape Fold Belt and challenges towards Future research. 11<sup>th</sup> SAGA Biennial Technical meeting and exhibition, Swaziland, 16-18 September, 2009. 481 - 485.
- Bordy, E.M., Hancox, P.J. and Rubidge, B.S. (2004). Basin development during deposition of the Elliot Formation (Late Triassic – Early Jurassic), Karoo Supergroup, South Africa. *South African Journal of Geology*, **107**, 397 - 412.
- Bouma, A.H. and Wickens, H.Dev. (1991). Permian passive margin submarine fan complex, Karoo basin, South Africa: possible model to Gulf of Mexico. *Transactions of the Gulf Coast Association of Geological Societies*, **41**, 30 - 42.
- Bouma, A.H. (1997). Comparison of fine-grained, mud-rich and coarse-grained, sand-rich submarine fans for exploration-development purposes. *Gulf Coast Association of Geological Societies Transactions* **47**, 59 – 64.
- Bouma, A.H. (2000). Fine-grained, mud-rich turbidite systems: model and comparison with coarse-grained, sand-rich systems. In: *Fine grained turbidite systems*, (Ed. by Bouma, A. H. and C. G. Stone), *AAPG Memoir 72/SEPM Special Publication*, **68**, 9 – 20.
- Broquet, C.A.M. (1992). The sedimentary record of the Cape Supergroup: A review. In: *Inversion Tectonics of the Cape Fold Belt, Karoo and Cretaceous Basins of*

- Southern Africa* (Ed. by M.J. De Wit and I.G.D. Ransome), Rotterdam, A.A. Balkema, 159 – 183.
- Caspers, H. (1957). Black Sea and Sea of Azov. In treatise of marine ecology and paleoecology, Edited by J. Hedgepeth, Boulder: Geological Society of Amsterdam, 801 – 90.
- Catuneanu, O., Hancox, P.J. and Rubidge, B.S. (1998) Reciprocal flexural behaviour and contrasting stratigraphies: a new basin development model for the Karoo retroarc foreland system, South Africa. *Basin Research*, **10**, 417 – 439.
- Catuneanu, O., Hancox, P.J., Caincross, B. and Rubidge, B.S. (2002). Foredeep submarine fans and forebulge deltas: orogenic off-loading in the underfilled Karoo Basin. *Journal of African Earth Sciences* **35**, 489 – 502.
- Catuneanu, O. (2004). Retroarc foreland systems—evolution through time. *Journal of African Earth Sciences*, **38 (3)**, 225 – 242.
- Chilingar, G.V. (1956). Use of Ca/Mg ratio in porosity studies. *American Association of Petroleum Geologists Bulletin*, **40**, 2489 – 2493.
- Cloetingh, S., Kooi, H. and Groenewoud, W. (1989). Intraplate stress and sedimentary basin evolution. *Am. Geophys. Union. Geophys. Monogr.* **48**, 1 – 16.
- Cloetingh, S., Lankreijer, A., De Wit, M.J. and Martinez, I. (1992). Subsidence history analysis and forward modelling of the Cape and Karoo super groups. In: *Inversion Tectonics of the Cape Fold Belt, Karoo and Cretaceous Basins of Southern Africa* (Ed. by M.J. De Wit and I.G.D. Ransome), Rotterdam, A.A. Balkema, 239 – 248.
- Cole, D.I. (1992). Evolution and development of the Karoo Basin. In: *Inversion Tectonics of the Cape Fold Belt, Karoo and Cretaceous Basins of Southern Africa* (Ed. by M.J. De Wit and I.G.D. Ransome), Rotterdam, A.A. Balkema, 87 – 99.

- Cole, D.I. and McLachlan, I.R. (1991). Oil Potential of the Permian Whitehill Shale Formation in the Main Karoo Basin, South Africa. In: Ulbrich, H. and Rocha Campos, A.C., (Eds.). *Proceedings and Papers of the Seventh Gondwana Symposium, Sao Paulo. Instituto de Geosciences, Universidade de Sao Paulo*: 379 - 390.
- Cole, D.I. and Wipplinger, P.E. (2001). Sedimentology and molybdenum potential of the Beaufort Group in the main Karoo basin, South Africa. *Memoir, Council for Geoscience, South Africa*, **80**, 225pp.
- Cole, D.I. and Smith, R.M.H., (2008). "Fluvial architecture of the Late Permian Beaufort Group deposits, S.W. Karoo Basin: Point bars, crevasse splays, palaeosols, vertebrate fossils and uranium". Field Excursion Guidebook, *American Association of Petroleum Geologists International Conference, Cape Town*, **FT02**, 1 - 110.
- Compton, J.S. (2004). *The Rocks and Mountains of Cape Town*. Cape Town: Double Story, 2004.
- Dapples, E.C. (1959). The behaviour of silica in diagenesis. In: *Silica in Sediments – S.E.P.M., Spec. Publ.*, **7**, 36 - 54.
- Dapples, E.C. (1962). Stages of Diagenesis in the development of sandstones. *Bull. Geol. Soc. Am.*, **73**, 913 – 934.
- De Beer, C.H. (1989). Structure of the Cape Fold Belt in the Ceres Syntaxis, *M.Sc. dissertation*, Stellenbosch University, Stellenbosch, Republic of South Africa, 135pp.
- De Beer, C.H. (1990). Simultaneous folding in the western and southern branches of the Cape Fold Belt. *South African Journal of Geology* **93**, 583 – 591.



- De Beer, C.H. (1992). Structural evolution of the Cape Fold Belt syntaxis and its influence on syntectonic sedimentation in the SW Karoo Basin. In: *Inversion Tectonics of the Cape Fold Belt, Karoo and Cretaceous Basins of Southern Africa* (Ed. by M.J. De Wit and I.G.D. Ransome), Rotterdam, A.A. Balkema, 197 – 206.
- DeCelles, P.G. and Currie, B.S. (1996). Long-term sediment accumulation in the Middle Jurassic-early Eocene Cordilleran retroarc foreland-basin system. *The Geological Society of America*, **24**, 591 – 594.
- DeCelles, P.G. and Giles, K.A. (1996). Foreland basin systems. *Basin Research* **8**, 105 – 123.
- De Swardt, A.M.J. and Rowsell, D.M. (1974). Note on the relationship between diagenesis and deformation in the Cape fold belt. *Transactions of the Geological Society of South Africa*, **77**, 239 – 245.
- De Wit, M.J., Jeffery, M., Nicolaysen, L.O.N. and Bergh, H. (1988). Explanatory notes on the Geologic Map of Gondwana. *American Association Petroleum Geology, Tulsa*.
- De Wit, M.J. and Ransome, I.G.D. (1992). Regional inversion tectonics along the southern margin of Gondwana. In: *Inversion Tectonics of the Cape Fold Belt, Karoo and Cretaceous Basins of Southern Africa* (Ed. by M.J. De Wit and I.G.D. Ransome), 15 – 21.
- Dingle, R.V., Siesser, W.G. and Newton, A.R. (1983). *Mesozoic and Tertiary Geology of Southern Africa*, Balkema, Rotterdam (1983).
- Doucouré, C.M., De Wit, M.J. and Mushayandebvu, M.F. (1996). Effective elastic thickness of the continental lithosphere in South Africa. *J. Geophys. Res.*, **101 (B5)**, 11,291 – 11,303.

- Duncan, R.A., Hooper, P.R., Rehacek, J., Marsh, J.S. and Duncan, A.R. (1997). The timing and duration of the Karoo igneous event, southern Gondwana. *Journal of Geophysical Research* **102**, 127 – 138.
- Einsele, G. (2000). Sedimentary basins: evolutions, facies and sediment budget. 2nd edition, **792**, 387 – 533.
- Faure, K. and Cole, D.I. (1999). Geochemical evidence for lacustrine microbial blooms in the vast Permian main Karoo, Paraná, Falkland Islands and Huab basins of southwestern Gondwana. *Palaeogeography, Palaeoclimatology, Palaeoecology*, **152**, 189 – 213.
- Fildani, A., Drinkwater, N.J., Weislogel, A., McHargue, T., Hodgson, D.M. and Flint, S. (2007). Age Controls on the Tanqua and Laingsburg Deep-Water Systems: New Insights on the Evolution and Sedimentary fill of the Karoo Basin, South Africa. *Journal of Sedimentary Research*, **77** (11), 901 – 908.
- Flemings, P.B. and Jordan, T.E. (1989). A synthetic stratigraphic model of foreland basin development, *Jour. Geophys. Res.*, **94**, 3851 – 3866.
- Flemings, P.B., and Jordan, T.E. (1990). Stratigraphic modelling of foreland basins: interpreting thrust deformation and lithospheric rheology: *Geology*, **18**, 430 - 435.
- Flint, S.S., Hodgson, D.M., King, R.C., Potts, G.J., Van Lente, B. and Wild, R.J. (2004). The Karoo Basin Slope Project: Phase 1. Industry consortium report, (unpublished) University of Liverpool.
- Fridge, J. and Bouma, A.H. (2003). Comparisons between compacted and decompactured turbidite systems, Tanqua Karoo, South Africa. *GCAGS/GCSSEPM, 53<sup>rd</sup> Annual convention*, 252 – 261.

- Frostick, L.E. and Steel, R.J. (1993). Tectonic controls and signatures in sedimentary successions: *special publication of the International Association of Sedimentologists*, Published by Blackwell Scientific Publications, **20**, 139 – 142.
- Gaetani, M. and Garzanti, E. (1991). Multicyclic history of the northern India continental margin (north-western Himalaya), *Am. Assoc. Petrol. Geol. Bull.* **75**, 1427 – 1446.
- Gradstein, F.M., Ogg, J.G., Smith, A.G., Bleeker, W. and Lourens, L.J. (2004). A new geologic time scale, with special reference to Precambrian and Neogene. *Episodes*, **27**: 83 - 100.
- Grecula, M. (2000). Stratigraphy and architecture of tectonically controlled turbidite systems, Laingsburg Formation, Karoo Basin, South Africa. PhD Thesis, University of Liverpool, 184pp.
- Grecula, M., Flint, S.S., Wickens, H.DeV. and Johnson, S.D. (2003a). Upward-thickening patterns and lateral continuity of Permian sand-rich turbidite channel fills, Laingsburg Karoo, South Africa. *Sedimentology*, **50**, 31 – 83.
- Grecula, M., Flint, S.S., Potts, G., Wickens, H.DeV and Johnson, S. (2003b). Partial ponding of turbidite systems in a basin with subtle growth-fold topography: Laingsburg-Karoo, South Africa. *Journal of Sedimentary Research*, **73**, 603 – 620.
- Gresse, P.G., Theron, J.N., Fitch, F.J. and Miller, J.A. (1992). Tectonic inversion and radiometric resetting of the basement in the Cape Fold Belt. In: *Inversion Tectonics of the Cape Fold Belt, Karoo and Cretaceous Basins of Southern Africa* (Ed. by M.J. De Wit and I.G.D. Ransome), 217 – 228.
- Hälbich, I.W. (1983). A tectogenesis of the Cape Fold Belt (CFB). In: *Geodynamics of the Cape Fold Belt*. (Ed. by Söhnge A. P. G. and Hälbich I. W.), *Special Publications of the Geological Society of South Africa*, **12**, 165 – 175.

- Hälbich, I.W., Fitch, F.J. and Miller, J.A. (1983). Dating the Cape orogeny, In: *Geodynamics of the Cape Fold Belt* (Ed. by Söhnge A.P.G. and Hälbich I.W.), *Special Publications of the Geological Society of South Africa*, **12**, 149 – 164.
- Hälbich, I.W. (1992). The Cape Fold Belt Orogeny: State of the art 1970s – 1980s. In: *Inversion Tectonics of the Cape Fold Belt, Karoo and Cretaceous Basins of Southern Africa* (Ed. by M.J. De Wit and I.G.D. Ransome), 141 – 158.
- Haq, B., Hardenbol, J., and Vail, P. (1987). Chronology of fluctuating sea levels since the Triassic. *Science* 6 March: **235 (4793)**, 1156 – 1167.
- Haq, B.U. (1991). Sequence stratigraphy, sea-level change, and significance for the deep sea. In: D.I.M. Macdonald (Ed.), *Sedimentation, Tectonics and Eustasy: Sea-level Changes at active Margins. Spec. Publ. int. Assoc. Sedimentol.*, **12**, 3 - 39.
- Harland, W.B., Cox, A.V., Llewellyn, P.G., Pickton, C.A.G., Smith, A.G. and Walters, R. (1982). *A geologic time scale*: Cambridge, Cambridge University Press, 131pp.
- Hodgson, D.M., Flint, S.S., Hodgetts, D., Drinkwater, N.J., Johannessen, E.P. and Luthi, S.M. (2006). Stratigraphic evolution of fine-grained submarine fan systems, Tanqua depocentre, Karoo basin, South Africa. *Journal of Sedimentary Research*, **76**, 20 – 40.
- Ingersoll, R.V. and Busby, C.J. (1995). Tectonics of sedimentary basins. In: *Tectonics of sedimentary basins* (Ed. by C.J. Busby and R.V. Ingersoll), *Blackwell Scientific Publications, USA*, 1 – 51.
- Isbell, J.L., Cole, D.I. and Catuneanu, O. (2008). Carboniferous - Permian glaciation in the main Karoo Basin, South Africa: Stratigraphy, depositional controls, and glacial dynamics. In: Fielding, C.R., Frank, T.D., and Isbell, J.L. (Eds.). *Resolving the Late Palaeozoic Ice age in Time and Space. Geological Society of America Special Paper*, **441**, 71 - 82.

- Johnson, M.R. (1976). Stratigraphy and sedimentology of the Cape and Karoo Sequences in the Eastern Cape Province. PhD thesis, Rhodes University, Grahams town, unpublished.
- Johnson, M.R. (1991). Sandstone petrography, provenance and plate tectonic setting in Gondwana context of the south-eastern Cape-Karoo Basin. *South African Journal of Geology* **94** (2/3), 137 – 154.
- Johnson, M.R., Van Vuuren, C.J., Hegenberger, W.F., Key, R. and Shoko, U. (1996). Stratigraphy of the Karoo Supergroup in southern Africa: an overview, *J. Afr. Earth Sci.* **23** (1), 3 –15.
- Johnson, M.R., Van Vuuren, C.J., Visser, J.N.J., Cole, D.I., Wickens, H.DeV. Christie, A.D.M. and Roberts, D.L. (1997). The Foreland Karoo Basin, South Africa. In: *Sedimentary basins of the world* (Ed. by K.J. Hsü and R.C. Selley), *African Basins Elsevier*, 269 – 317.
- Johnson, S.D. Flint, S.S. Hinds, D. and Wickens, H.DeV. (2001). Anatomy of basin floor to slope turbidite systems, Tanqua Karoo, South Africa: sedimentology, sequence stratigraphy and implications for subsurface prediction, *Sedimentology* **48**, 987 – 1023.
- Johnson, M.R., Van Vuuren, C.J., Visser, J.N.J., Cole, D.I., Wickens, H.DeV., Christie, A.D.M., Roberts, D.L. and Brandl, G. (2006). Sedimentary rocks of the Karoo Supergroup. In: M. R. Johnson, C. R. Anhaeusser and R. J. Thomas, (Eds.), *The Geology of South Africa, Geological Society of South Africa and Council for Geoscience*, 461 – 499.
- Jordan, T.E. (1981). Thrust loads and foreland basin evolution, Cretaceous, western United States. *Amer. Assoc. Petrol. Geol. Bull.*, **65**, 2506 – 2520.

- Jordan, T.E. (1995). Retroarc foreland basins. In *Tectonics of sedimentary basins*, (ed.) C. Busby and R.V. Ingersoll, Cambridge, MA: Blackwell Scientific, 330 - 62.
- Karner, G.D., and Watts, A.B. (1983). Gravity anomalies and flexure of lithosphere at mountain ranges, *Jour. Geophys. Res.*, **88**, 10 449 – 10 477.
- Kauffman, E.G. (1977). Geological and biological overview: western interior Cretaceous basin. *Mm Geol.* **14**, 75 - 99.
- Keyser, A.W. and Smith, R.M.H. (1979). Vertebrate biozonation of the Beaufort Group with special reference to the Western Karoo Basin, *Ann. Geol. Survey S. Afr.* **12**, 1 – 36.
- King, R.C., Van Lente, B., Potts, G., Hodgson, D.M., Andersson, P.O.D., Worden, R.H., Flint, S.S. and Wickens, H.DeV. (2004). Extra foreland source to turbidite sink in the early Karoo Basin, South Africa. AAPG Annual meeting 2004: Embrace the Future, Celebrate the Past Technical Program. (Poster).
- King, R.C. (2005). Structural Evolution of the Cape Fold Belt; Implications for Sediment Routing to the SW Karoo Basin. Unpublished Ph.D. thesis, University of Liverpool, United Kingdom.
- Kingsley, C.S. (1977). Stratigraphy and Sedimentology of the Ecca Group in the Eastern Cape Province, South Africa. Unpublished Ph.D. thesis, University of Port Elizabeth, South Africa, 296pp.
- Kingston, D.R., Dishroon, C.P. and Williams, P.A. (1983). Global basin classification. *American Association of Petroleum Geologists Bulletin*, **67**, 2194 - 2198.
- Kitching, J.W. (1977). The distribution of the Karroo vertebrate fauna. Memoir Bernard Price Institute Palaeontological Research, University Witwatersrand, **1**, 1 – 131.

- Kneller, B.C. (1991). A foreland basin on the southern margin of Iapetus. *Journal of the Geological Society, London*, **148**, 207 – 210.
- Larsen, G. and Chilingar, G.V. (1983). Diagenesis in sediments and sedimentary rocks, 2: New York, Elsevier Scientific Publishing Company, Developments in Sedimentology 25B, 572p.
- Lawrence, S.R., Johnson, M., Tubb, S.R. and Marshallsea, S.J. (1999). Tectono-stratigraphic evolution of the North Falkland region. In: *The Oil and Gas Habitats of the South Atlantic* (Ed. by N.R. Cameron, R.H. Bate and V.S. Clure), *Geological Society, London, Special Publication* **153**, 409 – 424.
- Lindeque, A.S., Ryberg, T., Stankiewicz, J., Weber, M.H. and De Wit, M.J. (2007). Deep Crustal Seismic Reflection Experiment across the Southern Karoo Basin, South Africa. *South African Journal of Geology*, **110**, 419 – 438.
- Lister, G.S. and Davis, G.A. (1989). The origin of metamorphic core complexes and detachment faults formed during Tertiary continental extension in the northern Colorado River region, U.S.A. *J. Struct. Geol.*, **11**, 65 – 94.
- Lock, B.E. (1978). The Cape Fold Belt of South Africa; tectonic control of sedimentation. *Proceedings of the Geologists' Association*, **89 (4)**, 263 - 281.
- Lock, B. E. (1980). Flat-plate subduction and the Cape Fold Belt of South Africa. *Geology*, **8**, 35 – 39.
- López-Gamundi and Rossello, E.A. (1998). Basin fill evolution and palaeotectonic patterns along the Samfrau geosyncline: the Sauce Grande basin – Ventana Fold Belt (Argentina) and Karoo basin - Cape Fold Belt (South Africa) revisited. *Geologische Rundschau*, **86**, 819 – 934.



- Luthi, S.M., Hodgson, D.M., Geel, C.R., Flint, S.S., Goedbloed, J.W., Drinkwater, N.J. and Johannessen, E.P. (2006). Contribution of research borehole data to modelling fine-grained turbidite reservoir analogues, Permian Tanqua–Karoo basin-floor fans (South Africa). *Petrol. Geosci.*, **12**, 1 – 16.
- Lyon-Caen, H. and Molnar, P. (1985). Gravity anomalies, flexure of the Indian plate, and the structure, support and evolution of the Himalaya and Ganga Basin, *Tectonics*, **4**, 513 – 538.
- Mabesoone, J.M., and Neumann, V.H. (2005). Cyclic Development of sedimentary Basins. In: *Developments in sedimentology* (Ed. by A.J. Van Loon), *Elsevier Journal*, **57**, 80, 445.
- Maccelari, J.C.D., Corner, B. and Niccoli, S.L. (1991). Major magnetic anomalies in western Dronning Maud Land: their possible origin and correlates within a Gondwana framework. *S. Afr. Geophys. Ass. 2nd Tech. Meet Abstr.*: 118 – 121.
- Magara, K. (1978). Compaction and fluid migration: practical petroleum geology. *Elsevier, New York*, 319pp.
- Magara, K. (1980). Comparison of porosity-depth relationships of shale and sandstone. *Journal of Petroleum Geology*, **3 (2)**, 175 – 185.
- Marsh, J.S., Hooper, P.R., Rehacek, J., Duncan, R.A. and Duncan, A.R. (1997). Stratigraphy and age of Karoo basalts of Lesotho and implications for correlations within the Karoo Igneous Province. In: *Large Igneous Provinces* (Ed. by J.J. Mahoney and M. Coffin), *American Geophysical Union Geophysical Monograph*, **100**, 247 – 272.
- McKenzie, D. (1978). Some remarks on the development of sedimentary basins. *Earth planet science letters, Earth planet. Sci. Lett.* **40**, 25 - 32.

- McRae, M. (1992). Geology of the south-western part of the Uchee belt in Lee County, Alabama. (MSc. Thesis), Auburn University, 108pp.
- Miall, A.D. (1990). Principles of Sedimentary Basin Analysis, Second Edition Springer-Verlag, New York Inc., 668pp.
- Miall, A.D. (1997). The Geology of Stratigraphic Sequences. Springer, Berlin, 433pp.
- Milani, E.J. and M.J. De Wit. (2008). Correlations between classic Parana and Cape-Karoo basins of South America and southern Africa and their basin infills flanking the Gondwanides: Du Toit revisited. In West Gondwana: Pre-Cenozoic correlations across the South Atlantic region. In: R.J. Pankhurst, R.A.J. Trouw, B.B. De Brito Neves and M.J. De Wit, (Eds.), *Geological Society, London, Special Publication*, **294**, 319 – 342
- Mutti, E., Tinterri, R., Benevelli, G., Di Biase, D. and Cavanna, G. (2003). Deltaic, mixed and turbidite sedimentation of ancient foreland basins. *Marine and Petroleum Geology*, **20 (6-8)**, 733 - 755.
- Newton, A.R., Shone, R.W. and Booth, P.W.K. (2006). The Cape Fold Belt. In: Johnson, M.R., Anhaeusser, C.R. and Thomas E.R., (Eds.). *The Geology of South Africa. The Geological Society of South Africa. Johannesburg/Council for Geoscience, Pretoria*, 521 - 530.
- Oelofsen, B.W. and Araujo, D.C. (1987). *Mesosaurus tenuidens* and *Stereosternum tumidum* from the Permian Gondwana of both southern Africa and South America. *South African Journal Science*, **83**, 370 - 372.
- Pankhurst, R.J., Rapela, C.W., Fanning, C.M. and Márquez, M. (2006). Gondwanide continental collision and the origin of Patagonia. *Earth-Science Reviews*, **76**, 235 – 257.

- Pate, C.R. (1986). Cretaceous compaction and tectonic subsidence of the Albert Basin. MSc Thesis, University of Alberta, Canada.
- Patel, M. (in preparation) Palaeoenvironmental Reconstruction of the Kookfontein Formation, Tanqua Depocentre, Southwest Karoo, South Africa. Unpublished MSc Thesis, University of Stellenbosch, South Africa.
- Pitman, W.C. and Andrews, J.A. (1985). Subsidence and thermal history of small pull-apart basins. In: Biddle, K.T. and Christie-Blick, N. (Eds) *Strike-Slip Deformation, Basin Formation and Sedimentation*, Special Publications of the Society of Economic Palaeontologists and Mineralogists, **37**, 45 - 49.
- Ricci Lucchi, F. (1986). The Oligocene to recent foreland basins of the northern Apennines. *Spec. Publ. Int. Assoc. Sedimentol.* **8**, 105 – 139.
- Rieke, H.H. III and Chilingarian, G.V. (1974). Compaction of Argillaceous sediments, In: *Developments in sedimentology* **16**. Elsevier scientific publishing company, 123 – 133.
- Ross, C.A., and Ross, J.R.P. (1988). Late Palaeozoic transgressive-regressive deposition: *Society of Economic Palaeontologists and Mineralogists Special Publication*, **42**, 227 – 247.
- Rowell, D.M and De Swardt, A.M.J. (1976). Diagenesis in Cape and Karoo sediments, South Africa, and its bearing on their hydrocarbon potential. *Transactions of the Geological Society of South Africa*, **79**, 81 – 145.
- Rubidge, B.S. (1995). Biostratigraphy of the *Eodicynodon* Assemblage Zone. In: Rubidge, B.S. (Ed.). *Biostratigraphy of the Beaufort Group (Karoo Supergroup)*. South African Committee for Stratigraphy, Biostratigraphic Series 1. *Council for Geoscience, Pretoria*: 3 - 7.

- Rubidge, B.S., Modesto, S.P., Sidor, C. and Welman, J. (1999). *Eunotosaurus africanus* from the Ecca–Beaufort contact in Northern Cape Province, South Africa – implications for Karoo Basin development, *South African Journal of Science*, **95**, 553 – 555.
- Rubidge, B.S. (2005). Re-uniting lost continents – Fossil reptiles from the ancient Karoo and their wanderlust. *South African Journal of Geology*, **108**, 135 - 172.
- Rust, I.C. (1975). Tectonic and sedimentary framework of Gondwana Basins in southern Africa. *Third Gondwana Symposium*, **5**, 554 – 564.
- Rutter, E. (1983). Pressure solution in nature, theory and experiment. *Journal of the Geological society of London*, **140**, 725 – 740.
- Ryan, P.J. (1967). Stratigraphic and Palaeocurrent Analysis of the Ecca Series and Lowermost Beaufort Beds in the Karroo Basin of South Africa. Unpublished Ph.D. thesis, University of the Witwatersrand, South Africa, 210pp.
- Ryan, P.J. and Whitfield, C.G. (1979). Basinal analysis of the Lowermost Beaufort Beds and associated coal, uranium and heavy mineral beach sand occurrences. *Geocongress 1977: Geol. Soc. of S. Afr. Spec. Publ.* **6**, 91 – 101.
- SACS, South African Committee for Stratigraphy, (1980). Stratigraphy of South Africa, Part 1 (Compiler, L.E. Kent). *Handbook Geol. Surv. S. Afr.*, Pretoria, **8**, 690pp.
- Sadler, P.M. (1981). Sediment accumulation rates and the completeness of stratigraphic sections. *Journal of Geology*, **89 (5)**, 569 – 584.
- Santos, R.V., Souza, P.A., Souza De Alvarenga, C.J., Dantas, E.L., Pimental, M.M., De Oliveira, C.G. and De Araújo, L.M. (2006). Shrimp U-Pb zircon dating and palynology of bentonitic layers from the Permian Irati Formation, Paraná Basin, Brazil. *Gondwana Research*, **9**, 456 - 463.

- Sawyer, D.S., Toksöz, M.N., Sclater, J.G. and Swift, B.A. (1982). Thermal evolution of the Baltimore Canyon trough and Georges Bank basin. In: J.S. Watkins and D.L. Drake, Editors, *Studies in Continental Margin Geology. Am. Assoc. Pet. Geol. Mem.* **34**, 743 – 764.
- Schmoker, J.W. and Halley, R.B., (1982). Carbonate porosity versus depth: a predictable relation for South Florida: *AAPG Bull.*, **66**, 2561 - 2570.
- Sclater, J.G. and Christie, P.A.B. (1980). Continental stretching: an explanation of the post-mid-Cretaceous subsidence of the Central North Sea basin, *Journal of Geophysical Research*, **85**, 3711 – 3739.
- Scott, E.D. (1997). *Tectonics and Sedimentation: The Evolution, Tectonic Influences and Correlation of the Tanqua and Laingsburg Subbasins, Southwest Karoo Basin, South Africa.* Unpublished Ph.D. thesis, Louisiana State University, USA.
- Scott, E.D. Bouma, A.H. and Wickens, H.D. (2000). Influence of tectonics on submarine fan deposition; Tanqua and Laingsburg subbasins, South Africa. In: Fine-grained turbidite systems (Ed. by A.H. Bouma and C.G. Stone), *AAPG Memoir 72/SEPM Special Publication*, **68**, 47 – 56.
- Scott, E.D. and Bouma, A.H. (2003). Influence of shelf and slope processes on deep-water sedimentation. In: Roberts, H.H., Rosen, N.C., Fillion, R.H. and Anderson, J.B. (Eds.). *Shelf margin deltas and linked down slope petroleum systems.* Gulf Coast Section Society of Economic Palaeontologists and Mineralogists, Foundation 23<sup>rd</sup> Annual Bob F. Perkins Research Conference, 577 - 596.
- Shone, R.W. and Booth, P.W.K. (2005). The Cape Basin, South Africa: A review. *Journal of African Earth Sciences*, **43**, 196 – 210.

- Sinclair, H.D. Coakley, B.J., Allen, P.A. and Watts, A.B. (1991). Simulation of foreland basin stratigraphy using a diffusion model of mountain belt uplift and erosion: an example from the Central Alps, Switzerland. *Tectonics*, **10**, 599 – 620.
- Sinclair, H.D., and Allen, P.A. (1992). Vertical versus horizontal motions in the Alpine orogenic wedge: stratigraphic response in the foreland basin, *Basin Res.* **4**, 215 – 232.
- Sixsmith, P.J. (2000). Stratigraphic development of a Permian turbidite system on a deforming basin floor: Laingsburg Formation, Karoo Basin, South Africa. Ph.D. Thesis, University of Liverpool, 229pp.
- Sleep, N.H. (1971). Thermal effects of the formation of Atlantic continental margins by continental break up, *Geophys. J.R. Astron. Soc.*, **24**, 325pp.
- Smith, R.H.M. (1990). A review of stratigraphy and sedimentary environments of the Karoo Basin of South Africa. *J. Afr. Earth Sci.*, **10**, 117 – 137.
- Smith, R.M.H., Ericksson, P.G. and Botha, W.J. (1993). A review of the stratigraphy and sedimentary environments of the Karoo-aged basins of Southern Africa. *Journal of African Earth Sciences*, **16 (132)**, 143 – 169.
- Söhnge, A.P.G. and Hälbich, I.W.E. (1983). Geodynamics of the Cape Fold Belt. *Geological Society of South Africa Special Publication* **12**, 1 – 184.
- Sonibare, W.A. (2009). Lithofacies analysis and modelling of the Kookfontein deltaic succession, Tanqua depocentre, SW Karoo Basin, South Africa. Unpublished BSc Honours Thesis, University of Stellenbosch, South Africa, 55pp.
- Stankiewicz, J., Ryberg, T., Schulze, A., Lindeque, A., Weber, M.H. and De Wit, M.J. (2007). Initial results from wide-angle seismic refraction lines in the southern Cape. *South African Journal of Geology*, **110**, 407 – 418.

- Steckler, M.S. and Watts, A.B. (1978). Subsidence of the Atlantic-type continental margin off New York. *Earth planet, Sci. Lett.*, **41**, 1pp.
- Stockmal, G., Beaumont, C. and Boutillier, R. (1986). Geodynamic models of convergent margin tectonics: Transition from rifted margin to overthrust belt and consequences for foreland-basin development, *Amer. Assoc. Petrol. Geol.*, **70**, 181 – 190.
- Tada, R. and Siever, R. (1989). Pressure solution during diagenesis. *Annu. Rev. Earth Planet. Sci.* **17**, 89 – 118.
- Tankard, A.J., Jackson, M.P.A., Eriksson, K.A., Hobday, D.K. and Minter, W.E.L. (1982). Crustal evolution of Southern Africa – 3.8 billion years of Earth history. *Springer-Verlag, New York*, 523pp.
- Tankard, A., Welsink, H., Aukes, P., Newton, R., Stettlere, E. (2009). Tectonic evolution of the Cape and Karoo basins of South Africa. *Journal of Marine and Petroleum Geology*, **26 (8)**, 1379 – 1412.
- Theron, J.C. (1973). Sedimentological evidence for the extension of the African continent southwards during the Late Permian-Early Triassic times. *Proc. Pap., 3<sup>rd</sup> Gondwana Symp., Canberra, Australia*, 61 – 71.
- Theron, J.N. Gresse, P.G. Siegfried, H.P. and Rogers, J. (1992). Explanation sheet 3318 - The Geology of the Cape Town Area. Geological Survey, Department of Mineral and Energy Affairs, Government Printer, Pretoria.
- Thomas, J.B., Marshall, J., Mann, A.L., Summons, R.E. and Maxwell, J.R. (1993). Dinosteranes (4, 23, 24-trimethylsteranes) and other biological markers in dinoflagellate-rich marine-sediments of Rhaetian age: *Organic Geochemistry*, **20**, 91 - 104.

- Turner, B.R. (1980). Braid plain deposition of the Upper Triassic Molteno Formation in the main Karoo (Gondwana) Basin, South Africa, *Sedimentology* **30**, 77 – 89.
- Turner, B.R. (1983). Braid-plain deposition of the Upper Triassic Molteno Formation in the main Karoo (Gondwana) Basin, South Africa. *Sedimentology*, **30**, 77 – 89.
- Turner, B.R. (1999). Tectonostratigraphical development of the Upper Karoo Foreland Basin: orogenic unloading versus thermally – induced Gondwana rifting. *Journal of African Earth Sciences*, **28**, 215 – 238.
- Underschultz, J.R. (1991). Tectonic loading, sedimentation, and sea-level changes in the foreland basin of north-west Alberta and north-east British Columbia, Canada. *Basin Research*, **3**, 165 – 174.
- Vail, P.R., Mitchum, R.M. and Thompson, S. (1977). Seismic stratigraphy and global changes of sea level. In: Seismic stratigraphy – Applications to hydrocarbon exploration (Ed. by C.E. Payton), *American Association of Petroleum Geologists Memoir*, **26**, 83 – 97.
- Vail, P.R., Hardenbol, J. and Todd, R.G. (1984). Jurassic unconformities, chronostratigraphy, and sea-level changes from seismic stratigraphy and biostratigraphy. In: Interregional unconformities and hydrocarbon accumulation (Ed. by J.S. Schlee), *AAPG Memoir*, **36**, 129 – 144.
- Van der Werff, W. and Johnson, S.D. (2003). High resolution stratigraphic analysis of a turbidite system, Tanqua Karoo Basin, South Africa, *Marine Petrol. Geol.* **20**, 45 – 69.
- Van Hinte, J.E. (1978). Geohistory analysis—application of micropaleontology in exploration geology. *Bulletin of the American Association of Petroleum Geologists* **62**, 201 – 222.



- Van Lente, B., Wickens, H.DeV., Flint, S.S. and Worden, R.H. (2003). Petrographic evolution of the early SW Karoo Basin, South Africa. *British Sedimentological Research Group Annual General Meeting, 2003, Leeds*. (Poster).
- Van Lente, B. (2004). Chemostratigraphic Trends and Provenance of the Permian Tanqua and Laingsburg Depocentre, Southwest Karoo Basin, South Africa. Unpublished Ph.D. thesis, University of Stellenbosch, South Africa.
- Van Lente, B., Flint, S.S. and Wickens, H.DeV. (2005). Extra-foreland provenance of sandstone from the south-western Karoo Basin, South Africa: implications for timing of retro-arc fold belt/foreland basin development in western Gondwana.
- Veevers, J.J., Powell, C., Collinson, J.W. and López-Gamundi, O.R. (1994). Synthesis. In *Permian-Triassic Pangaeen Basins and Fold belts along the Panthalassan Margin of Gondwanaland* (Ed. by J.J. Veevers and C. Powell), *Geological Society of America Memoir*, **184**, 223 – 279.
- Viljoen, J.H.A. (2005). Tierberg Formation; In: Catalogue of South African Lithostratigraphic units, (ed) M.R. Johnson. *SA Committee for stratigraphy*.
- Visser, J.N.J. and Lock, J.C. (1978). Water depth in the main Karoo Basin in South Africa during Permian sedimentation. *Trans. Geol. Soc. S. Afr.* **81**, 185 – 191.
- Visser, J.N.J., Lock, J.C. and Jordan, M.J. (1980). Permian deltaic sedimentation in the western half of the Karoo Basin, South Africa. *Trans. Geol. Soc. S. Afr.*, **83**, 415 – 424.
- Visser, J.N.J. (1987a). The influence of topography on the Permo-Carboniferous glaciation in the Karoo basin and adjoining areas, Southern Africa. In: *Gondwana Six* (Ed. by D.H. Elliot, J.W. Collison, G.D. McKenzie and S.M. Haban), *American Geophysical Union*, 123 – 129.

- Visser, J.N.J. (1987b). The pale geography of part of south-western Gondwana during the Permo-Carboniferous glaciation. *Palaeogeography, Palaeoclimatology, Palaeoecology*, **61**, 205 - 219.
- Visser, J.N.J. (1990). The age of the Late Palaeozoic glacigene deposits in Southern Africa. *South African Journal of Geology*, **93**, 366 – 375.
- Visser, J.N.J. (1991a). Geography and climatology of the Late Carboniferous to Jurassic Karoo Basin in south-western Gondwana. *Ann. S. Afr. Museum* **99**, 415 – 431.
- Visser, J.N.J. (1991b). The palaeoclimatic setting of the Late Palaeozoic marine ice sheet in the Karoo Basin of Southern Africa. In: Anderson, J.B., Ashley, G.M. (Eds.), *Glacial Marine Sedimentation: Palaeoclimatic Significance. Geological Society of America Special Paper*, 261, 181–189.
- Visser, J.N.J. (1991c). Self-destructive collapse of the Permo-Carboniferous marine ice sheet in the Karoo Basin: evidence from the southern Karoo: *South African Journal of Geology*, **94**, 255 – 262.
- Visser, J.N.J. (1992a). Basin tectonics in south-western Gondwana during the Carboniferous and Permian. In: *Inversion Tectonics of the Cape Fold Belt, Karoo and Cretaceous Basins of Southern Africa*, (Ed. by M.J. De Wit and I.G.D. Ransome), 109 – 115.
- Visser, J.N.J. (1992b). Deposition of the Early to Late Permian Whitehill Formation during a sea-level highstand in a juvenile foreland basin: *South African Journal of Geology*, **95**.
- Visser, J.N.J. (1993). Sea-level changes in a back-arc foreland transition-the Late Carboniferous – Permian Karoo Basin of South Africa. *Sediment. Geol.*, **83**, 115 – 131.

- Visser, J.N.J. (1997). Deglaciation sequences in the Permo-Carboniferous Karoo and Kalahari basins of southern Africa: a tool in the analysis of cyclic glacio-marine basin fills. *Sedimentology*, **44** (3), 507 – 521.
- Visser, J.N.J., Praekelt, H.E. (1996). Subduction, mega-shear systems and Late Palaeozoic basin development in the African segment of Gondwana. *Geol. Rundsch.* **85**, 632 – 646.
- Visser, N.J. and Praekelt, H.E. (1998). Late Palaeozoic crustal block rotations within the Gondwana sector of Pangaea. *Tectonophysics*, **287**, 201 – 212.
- Waltham, D., Taberner, C., and Docherty, C. (2000). Error estimation in decompacted subsidence curves. *Bulletin of the American Association of Petroleum Geologists* **84** (8), 1087 – 1094.
- Watts, A.B. (1978). An analysis of isostasy in the world's oceans: 1. Hawaiian-Emperor Seamount Chain, *Jour. Geophys. Res.*, **83**, 5989 - 6004.
- Watts, A.B., Karner, D. and Stecklemer, S. (1982). Lithospheric flexure and the evolution of sedimentary basins. *Phil. Trans. R. Sol. A.*, **305**, 249 – 281.
- Watts, A.B. (1992). The effective thickness of the lithosphere and the evolution of foreland basins, *Basin Research*, **4**, 169 – 178.
- Watts, A.B. (2001). Isostasy and flexure of the lithosphere. Cambridge University press, 1 – 26.
- Wickens, H.DeV. (1994). Basin Floor Fan Building Turbidites of the South-western Karoo Basin, Permian Ecca Group, South Africa. Unpublished Ph.D. thesis, University of Port Elizabeth, South Africa, 233pp.
- Wickens, H.DeV., and Bouma, A.H. (2000). The Tanqua Fan Complex, Karoo Basin, South Africa – Outcrop analogue for fine-grained, deepwater deposits. In: *Fine-grained*

*turbidite systems* (Ed. by A.H. Bouma and C.G. Stone), *AAPG Memoir 72/SEPM Special Publication*, **68**, 153 – 164.

Wild, R.J. (2005). Sedimentology and Sequence Stratigraphy of a Permian Lower Slope to Shelf Succession, Tanqua Depocentre, SW Karoo Basin, South Africa. Unpublished Ph.D. thesis, University of Liverpool, United Kingdom.

Winter, H.De la R. (1984). Tectonostratigraphy as applied to analysis of South African Phanerozoic basins. *Transactions of the Geological Society of South Africa*, **87**, 181 – 193.

Yang, X.S. (2001). A unified approach to mechanical compaction, pressure solution, mineral reactions and the temperature distribution in hydrocarbon basins. *Tectonophysics*, **330**, 141 – 151.

Ziegler, P. (1988). Evolution of the Arctic–North Atlantic and the Western Tethys. *American Association of Petroleum Geologists Memoir*, **43**, 198pp.

Ziegler, P. (1992). Europe Cenozoic rift zones. *Tectonophysics*, **208**, 91 – 111.

<https://zulu.ssc.nasa.gov/mrsid/>

## APPENDIX A

### BOREHOLE AND SEDIMENTOLOGICAL LOGS WITH SAMPLE LOCATIONS

(For location of borehole see Fig. 4.04)

#### Abbreviations used:

Lt. gy: light grey

Vf: very fine

M. gy: medium grey

F: fine

D. gy: dark grey

Lam: lamination

Br: brown

Hor lam: horizontal lamination






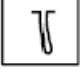


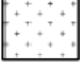





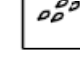



Alt: alternation

X lam: cross lamination

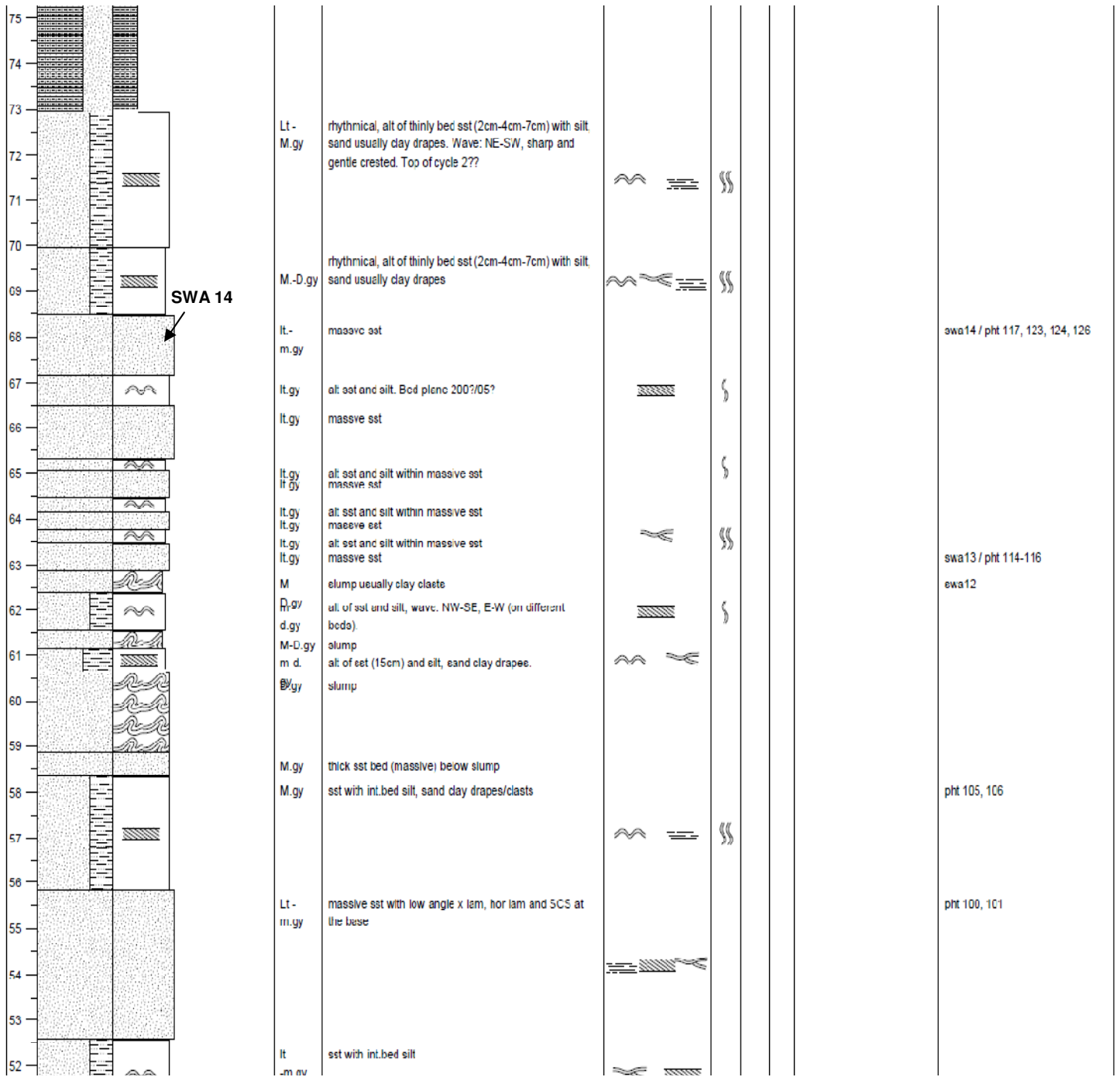
Int: intercalated

Sst: sandstone

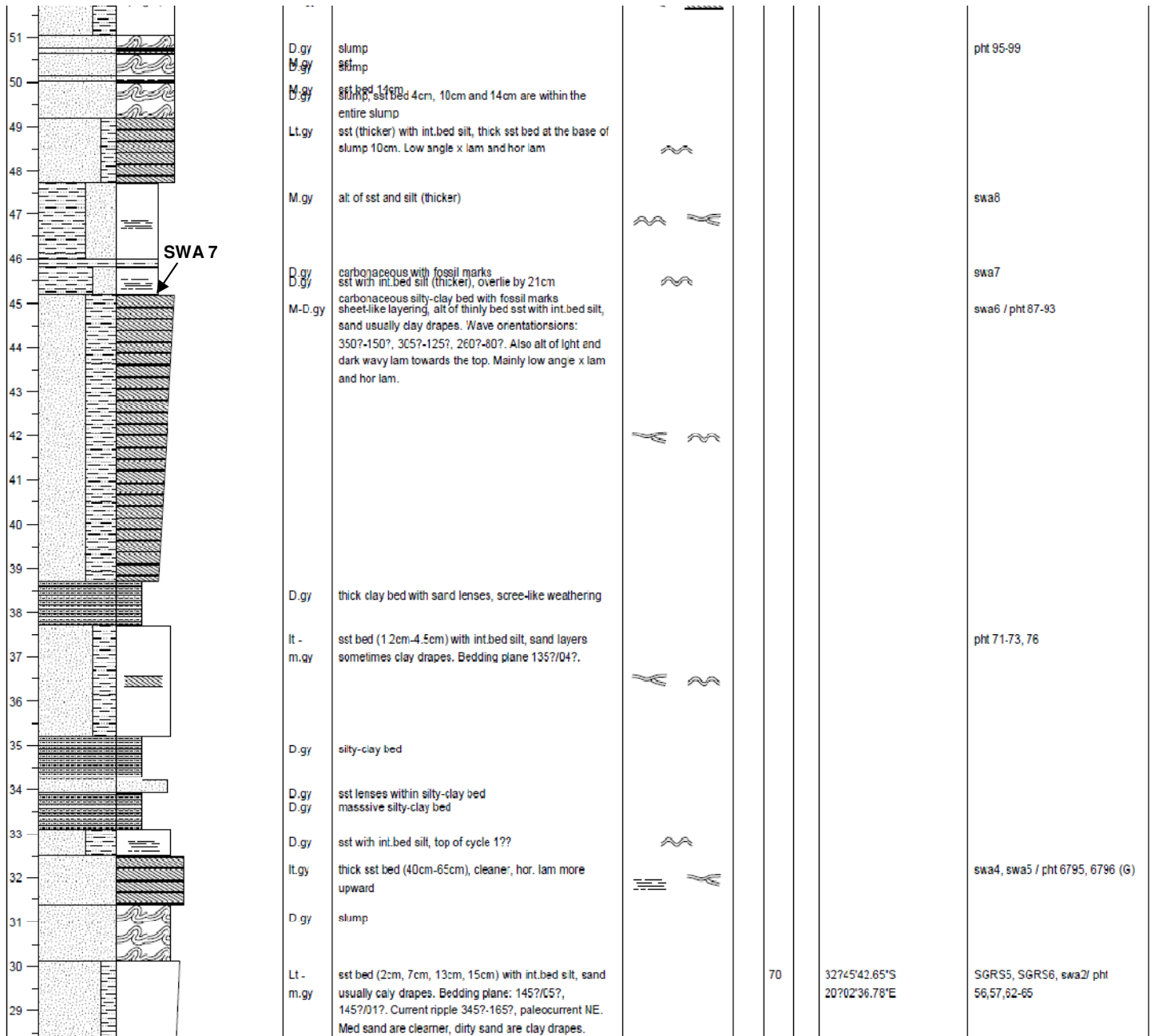
Pht: photograph

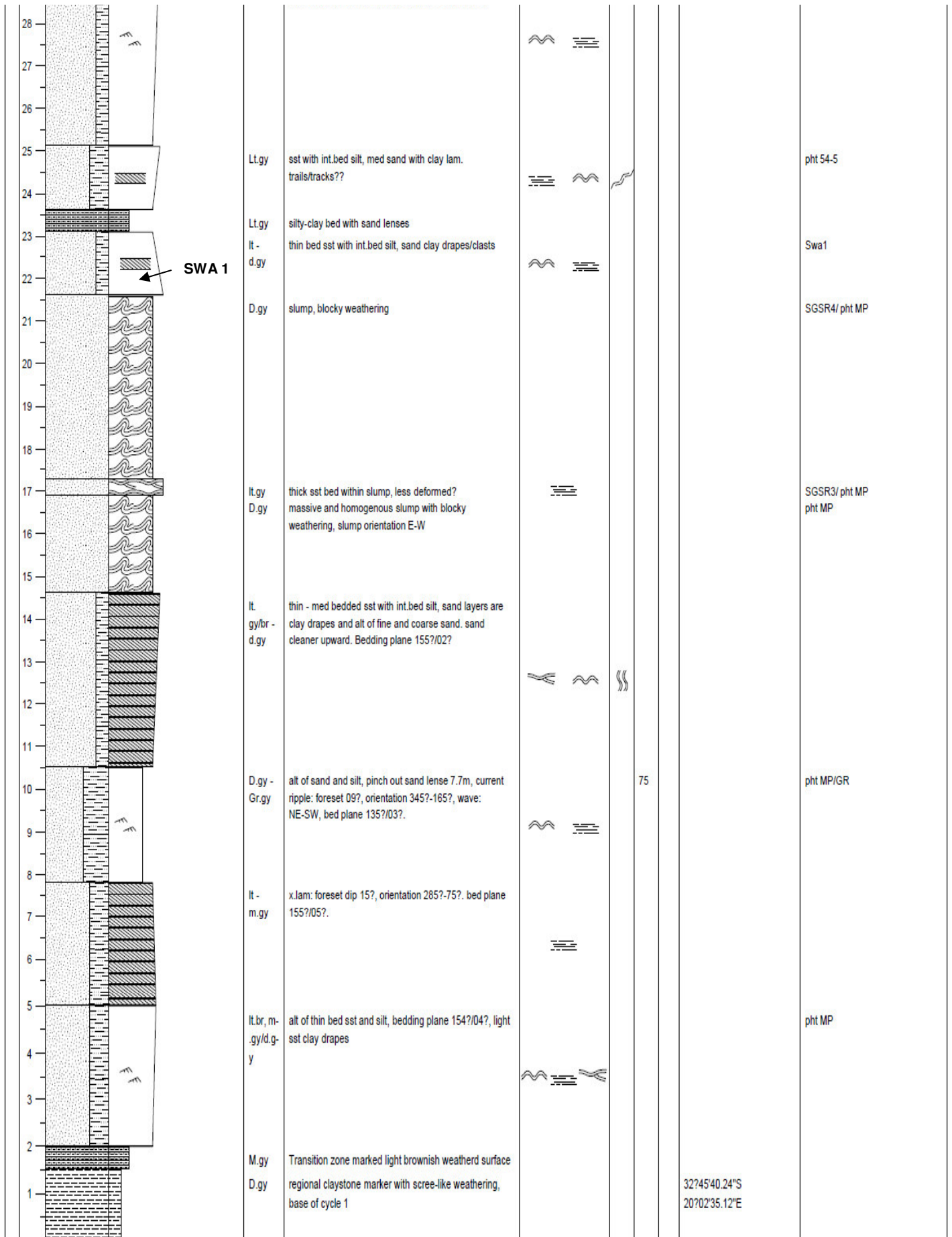
Lithologies	Symbols	Base Boundaries
	Mudstone	 Wave ripple cross-lamination
	Sandstone	 Planar cross bedding
	Claystone	 Vertical burrows
	Siltstone	 Horizontal planar lamination
	Halite	 Trough cross bedding
		 Current ripple cross-lamination
		 Hummocky cross stratification
		 Moderate bioturbation
		 Swaley cross stratification
		 Tracks
		 Minor bioturbation
		 Convolute lamination
		 Gradational

Piensaarsfontein se Berg Vertical Section 1		LITHOLOGY			COLOUR	NOTES	STRUCTURES / FOSSILS	BIOTURBATION	PALAEOCURRENT	FACIES	GPS	SAMPLE/PHOTO
FORMATION	SCALE (m)	MUD	SAND	GRAVEL								
		-clay -silt -vf -m -c	-gran -pebb -cob -boul									
	93				Li -	sst with int.bed silt sand cleaner but sometimes clay drapes. Top of Cycle 3 or very close to top?? Above the slump is observed.						
	92				M.gy							
	91											
	90				M.gy	alt of sst and silt, clay drapes						
	89				Li							
	88				M.gy	alt of vf sst with int.bed silt, clay drapes, repetition of hor lam and x lam, clay drapes sst are usually darker, cleaner sand as we go up but clay drapes.						
	87				D.gy	alt of vf sst with int.bed silt						
	86				D.gy	silty-claystone bed						
	85				M -							
	84				D.gy	alt of sst with int.bed silt, sand are clay drapes, less wave influenced, some sand lenses lighter and coarser						
	83											
	82											
	81				D.gy	alt of vf sst with int.bed silt, very few lam, hor lam lam and low angle x lam.						
	80											
	79											
	78											
	77											
	76				M - D gy	silty-clay with very thin int.bed sst silty layers are structureless with scree-like weathering						

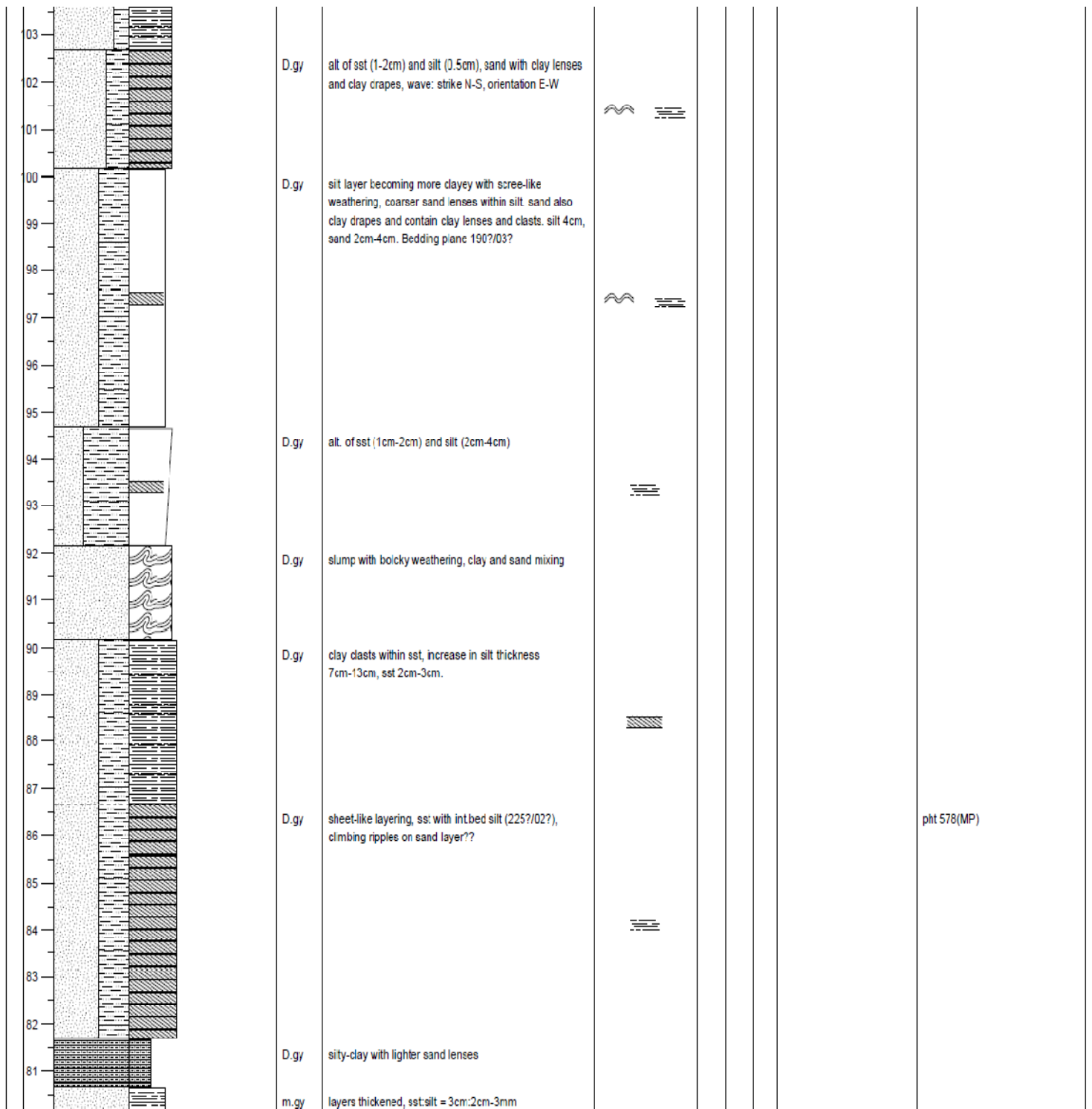


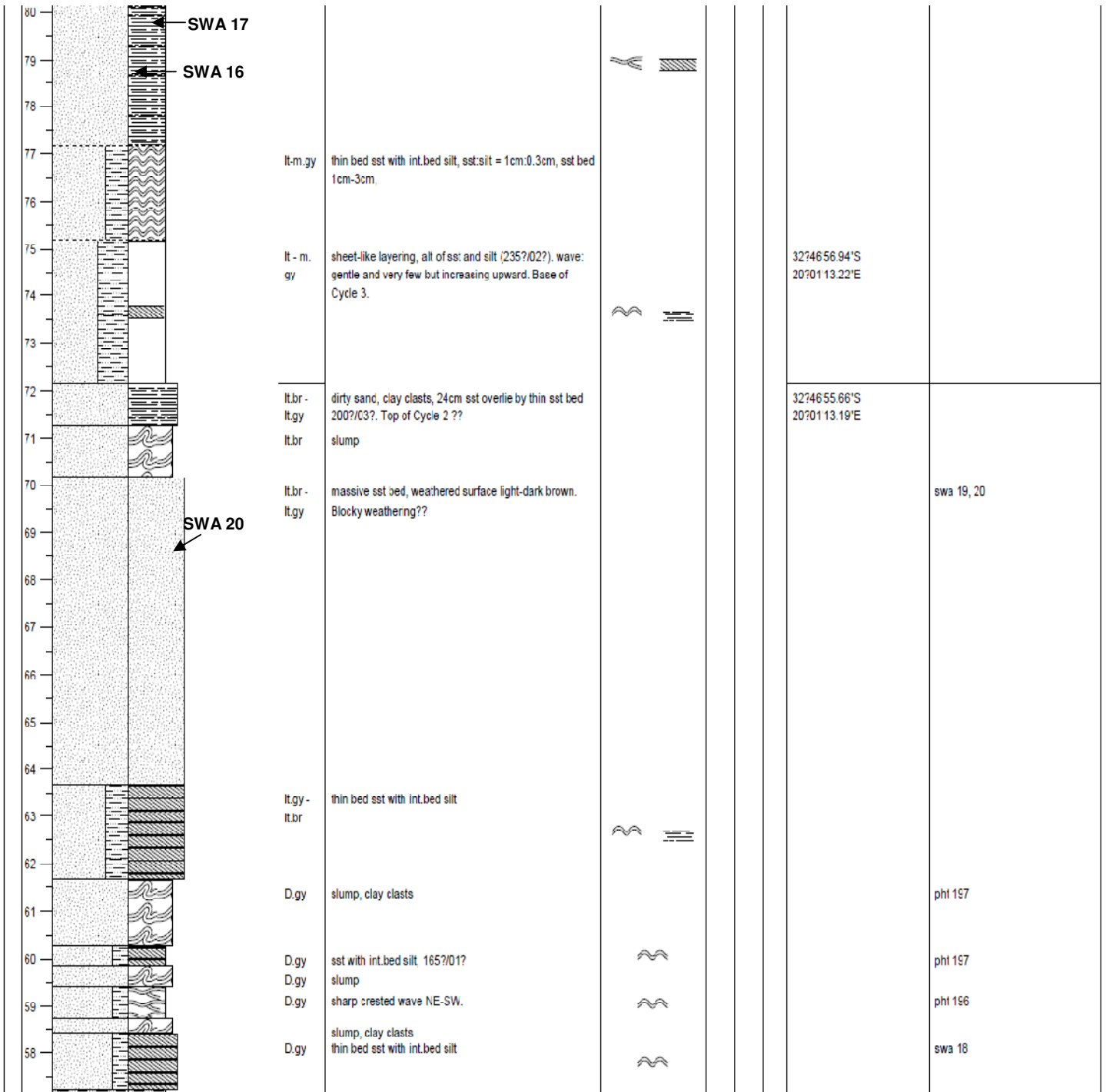


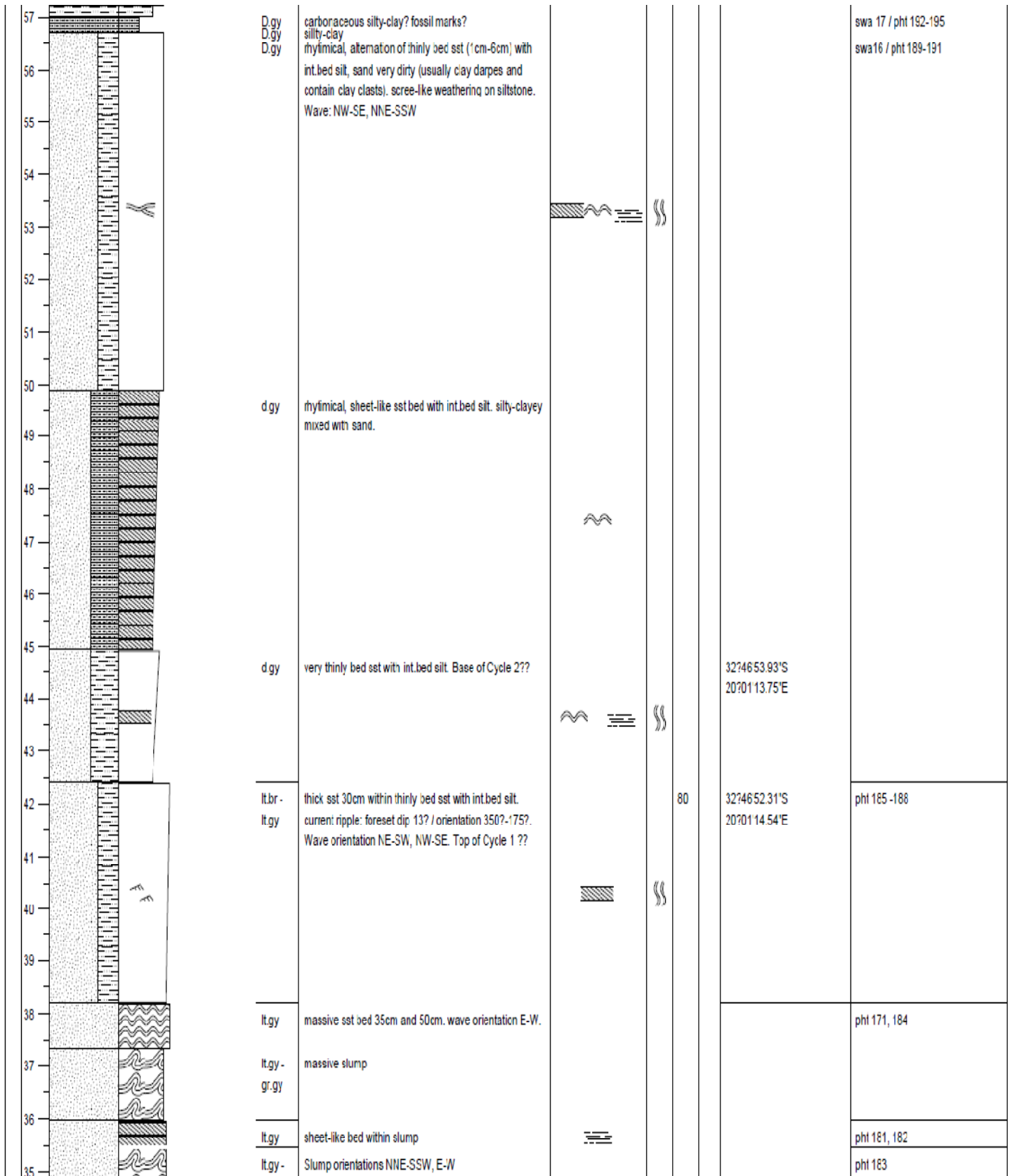




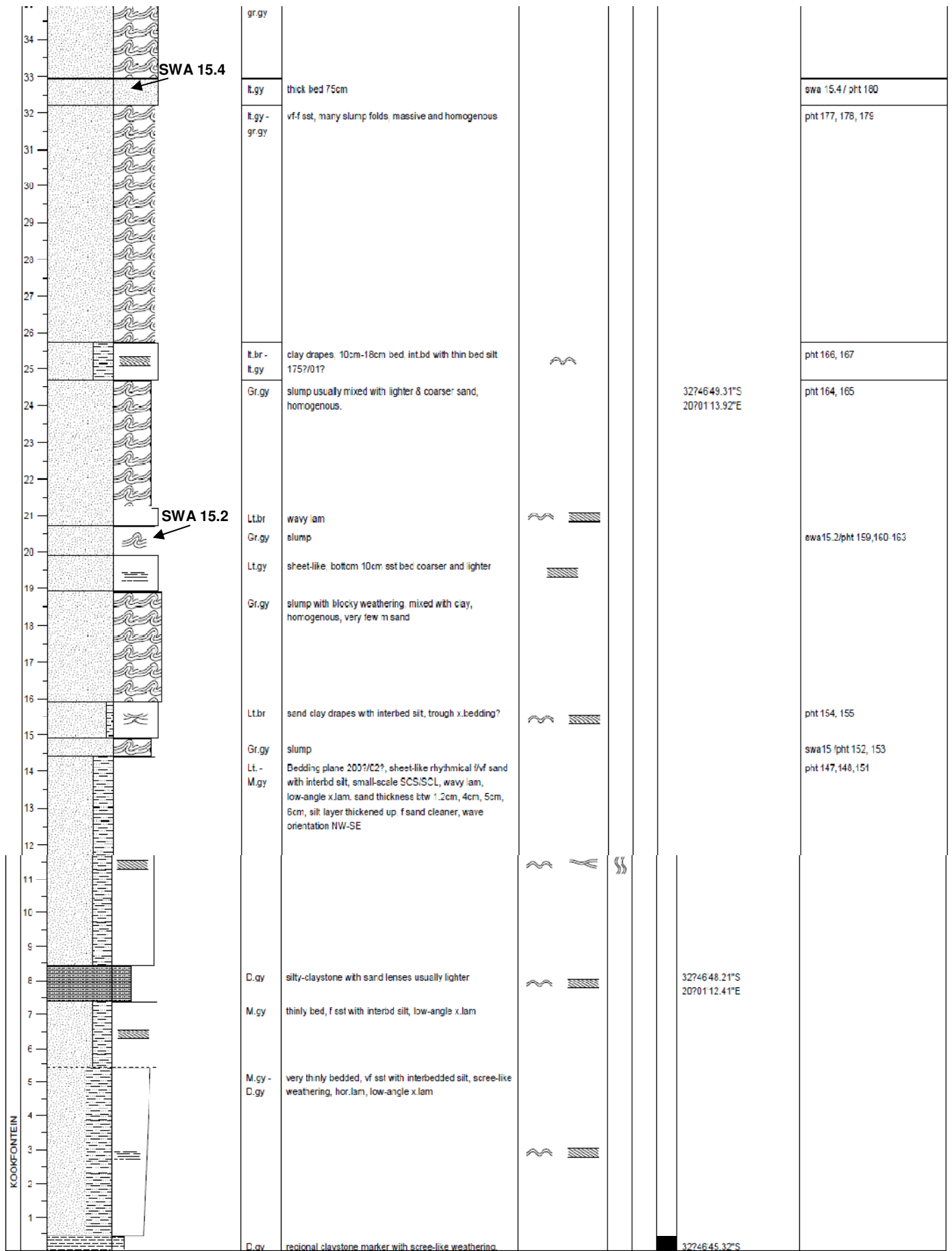
Pienaarstonein se Berg Vertical Section 2											
FORMATION	SCALE (m)	LITHOLOGY	MUD SAND GRAVEL	COLOUR	NOTES	STRUCTURES / FOSSILS	BIOTURBATION	PALAEOCURRENT	FACIES	GPS	SAMPLEPHOTO
			clay silt vf m vc gran pebb cobb boul						1		
	20			D.gy	slump (massive, homogenous and very extensive), base of cycle 4?? mixing of sand and clay						
	19										
	18										
	17										
	16										
	15										
	14			Lt. - M.gy	increasing sst (1.5cm-6cm) and silt layers, wave: strike NE-SW, orientation NW-SE. Top of Cycle 3??					32°46'59.24"S 20°01'13.40"E	swa 22
	13										
	12										
	11										
	10			M.gy	trough x bed (low angle), bedding plane 245°/01?,						
	09										
	08										
	07										
	06			lt/olive gy - lt. br	sst with int bed silt. alt: of light/coarser and dark/fine laminae within sst layers,					32°46'58.68"S 20°01'13.20"E	swa 21
	05										
	04										











## APPENDIX B

## PETROGRAPHIC AND SEM ANALYSIS DESCRIPTION

Samples	Grain size	Composition	Texture	Diagenetic feature from SEM analysis
SWA 6 silty sand	very fine	Quartz, Feldspar, Clay drapes, Calcite	moderately sorted with high matrix content	<p>I. Sub-angular – sub-rounded shaped Quartz grains, mostly fractured (denoting deformation of grains due to overburden pressure)</p> <p>II. Diminished porosity and permeability caused by</p> <ul style="list-style-type: none"> <li>• Quartz overgrowth and cement</li> <li>• presence of fractured quartz grains</li> <li>• presence of lithic fragments</li> <li>• mica grains squeezed between grains</li> </ul>
SWA 7 carbonaceous silty sand	very fine	Feldspar, quartz, Muscovite, Anhydrite	visible intergranular contact in a dark greenish- brown matrix	<ul style="list-style-type: none"> <li>• Presence of Chlorite grains</li> </ul>
SWA 13 sandstone	Fine	Quartz, Feldspar,	sutured grain contacts, moderately sorted with a mosaic polygonal texture	<ul style="list-style-type: none"> <li>• Alteration of feldspar (albite) grains to illite</li> <li>• presence of quartz cement</li> <li>• presence of Chlorite grains</li> </ul>
SWA 14 sandstone	fine to medium		Moderately to well sorted grains. Very high grain- boundary contact leaving no visible pores.	<ul style="list-style-type: none"> <li>• presence of Altered feldspar grains</li> <li>• presence of lithic fragments</li> <li>• presence of quartz cement and overgrowth</li> </ul>
SWA 15.2	very fine		Poorly sorted silt, clay clasts that appear as nodules with black rims and opaque minerals.	<ul style="list-style-type: none"> <li>• Deformation of the quartz grains</li> <li>• Presence of calcite cement</li> </ul>
SWA 20	medium	Quartz, feldspar	well sorted, sub-rounded with little matrix and no visible porosity i.e. presence of intergranular contact	<ul style="list-style-type: none"> <li>• presence of quartz overgrowths and cement</li> <li>• presence of Lithic fragments</li> <li>• Alteration of feldspar to illite</li> </ul>

Table B1: Detailed description from petrographic and SEM study of the sandstone and silty sand lithologies collected from the Tanqua depocentre.



**SAMPLE MICROGRAPHS**

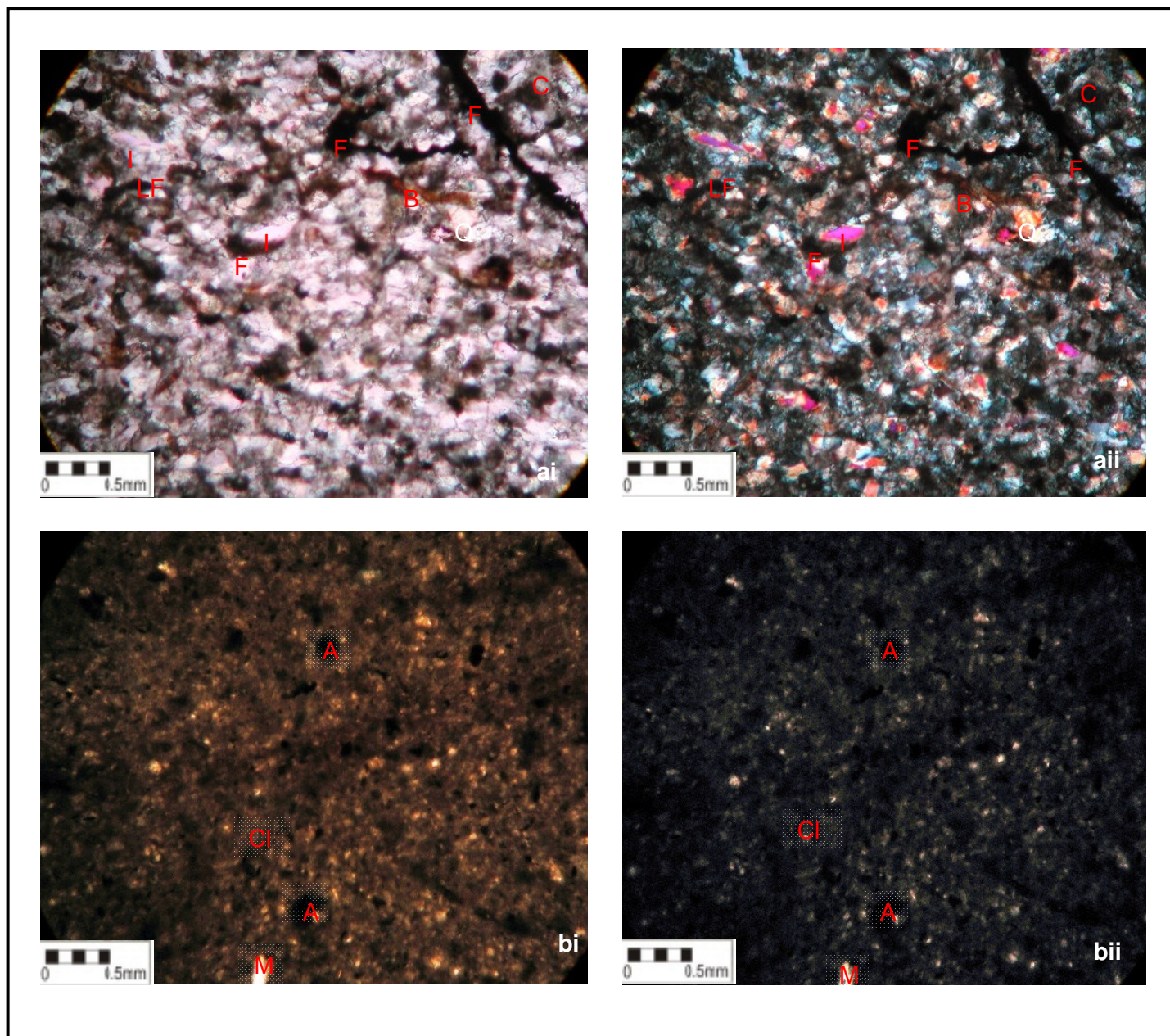


Plate 1a: Sample Microphotographs of thin sections (a) SWA6 from a carbonaceous silty clay bed at a depth of 44m and (b) SWA7 from a carbonaceous silty sand bed A collected from PFVS 1 location in Tanqua depocentre. Note: (i) view under plane polarized light (ii) view under crossed nicols. C – Clay; F - Feldspar; I - Illite; LF- Lithic fragment; Q - Quartz; Cl - Chlorite; M - Muscovite; A - Anhydrite; B - Biotite.



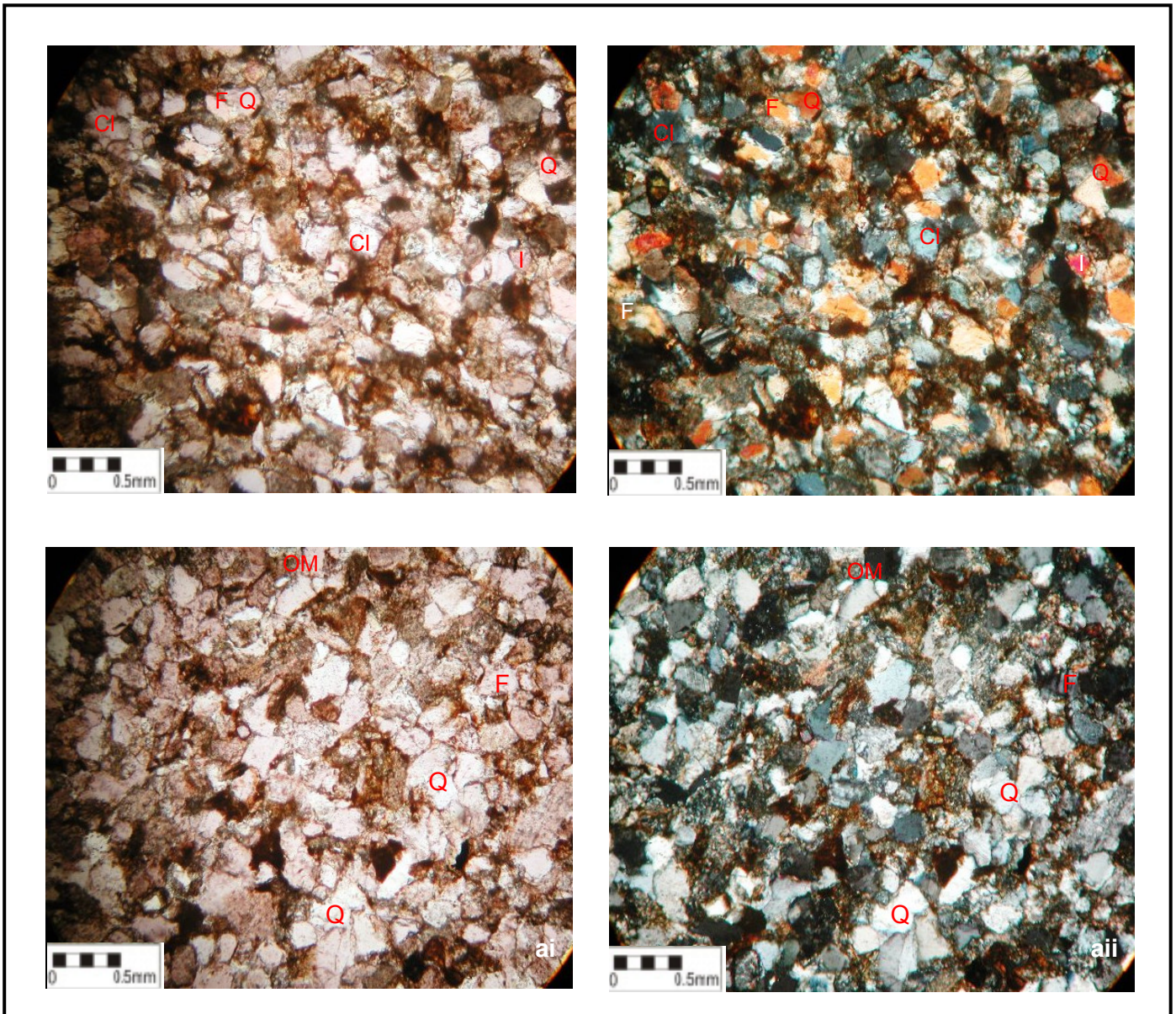


Plate 2a: Sample Microphotographs of thin sections (a) SWA13 from a massive sandstone bed at 63 m depth and (b) SWA14 from a massive sandstone bed at 68m depth collected from PFVS 1 location in Tanqua depocentre. Note: (i) view under plane polarized light (ii) view under crossed nicols. C – Clay; F - Feldspar; I - Illite; LF- Lithic fragment; Q - Quartz; Cl - Chlorite; M - Muscovite; A - Anhydrite; B - Biotite; OM - Opaque minerals.



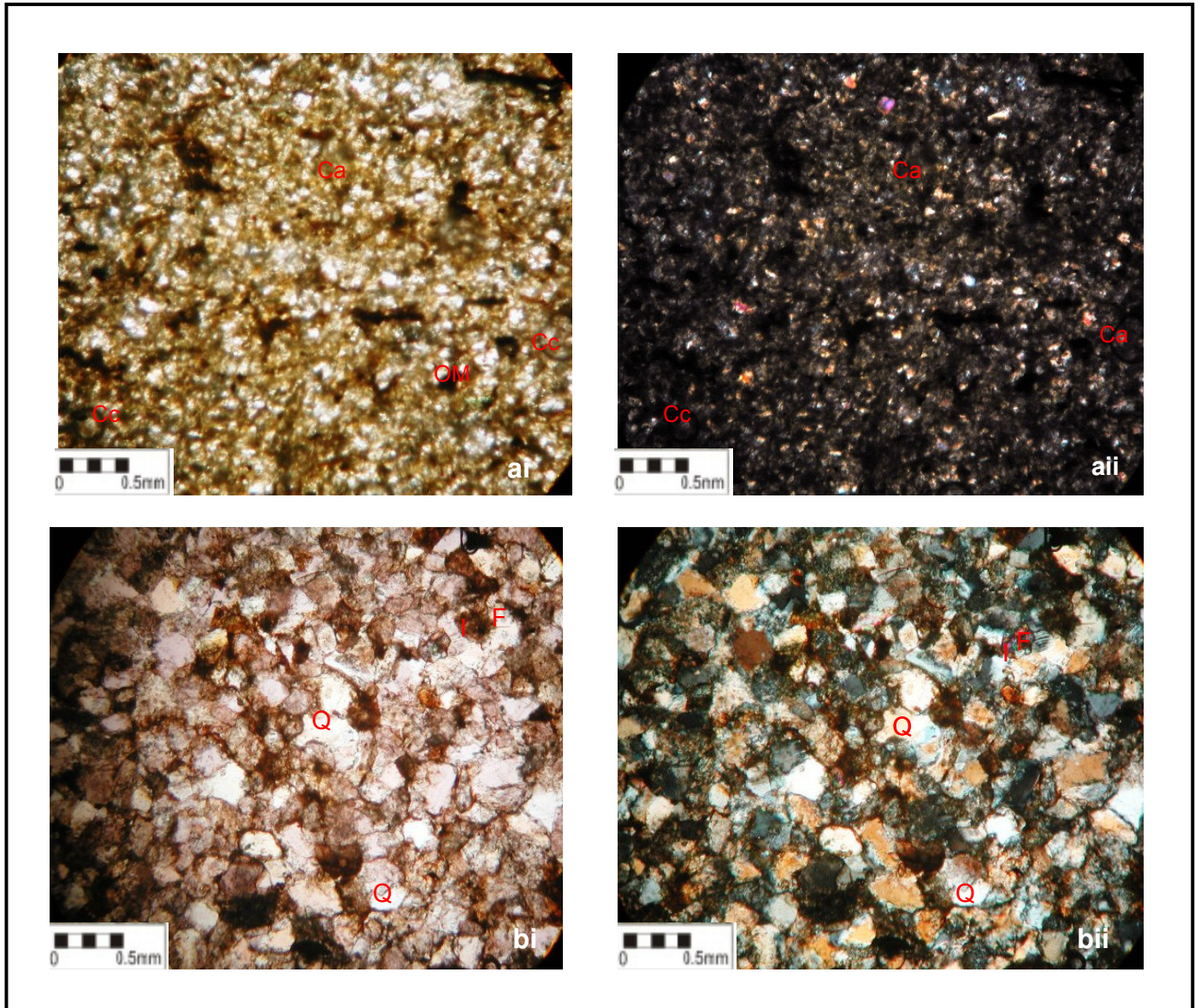


Plate 3: Sample Microphotographs of thin sections (a) SWA15-2 from slump bed with wavy lamination at 20 m depth and (b) SWA20 from massive sandstones bed at 70 m depth collected from PFVS 1 and PFVS 2 locations in Tanqua depocentre. Note: (i) view under plane polarized light (ii) view under crossed nicols. Cc – Clay clast; F - Feldspar; I - Illite; LF - Lithic fragment; Q - Quartz; Ca - Calcite cement with greenish colour; OM - Opaque minerals.

## APPENDIX C

### OSXBACKSTRIPPING EQUATIONS

#### C1. Decompaction equation

Exponential decrease of porosity with depth:

$$\phi = \phi_0 e^{-cy}$$

Where  $c$  is the porosity coefficient,  $\phi_0$  is surface porosity;  $\phi$  is porosity at depth  $y$

General decompaction Equation

$$Y'2 - Y'1 = y2 - y1 - \left\{ e^{(-cy'1)} - e^{(-cy'2)} \right\} + \left( \frac{\phi_0}{C} \right) * \left\{ \left[ e^{(-cy'1)} - e^{(-cy'2)} \right] \right\}$$

Where  $y'1$  &  $y'2$  are the base and top of a stratigraphic unit before compaction,

$y1$  &  $y2$  are the present base and top of the unit after compaction

#### Note

The type of setting, marine or continental affects the correction for sedimentary and water loads.

In a marine basin (type 0), any depression is filled with air which has a density near zero.

Therefore, the density of the fluid that supports the load is ( $\rho_m$ ).

While in continental basin (Type 1), any depression is filled with air.

#### C2. Sediment Loading Equation

Continental Basin (type 1)

$$Y = S \frac{(\rho_m - \rho_s)}{(\rho_m - \rho_w)}$$

Marine basin (type 0)

$$Y = S \frac{(\rho_m - \rho_s)}{(\rho_m - \rho_w)}$$

Where Y is the depth to the basement corrected for sediment load

S is the total thickness of the column corrected for compaction

$\rho_m$ ,  $\rho_s$  and  $\rho_w$  are mantle, mean sediment column densities and water respectively (Allen and Allen, 1990; Watts, 2001).

### C3. Water loading Equation

Marine basin type (0)

$$Y_t = Y \frac{\Delta SL}{(\rho_m - \rho_w)} + WD$$

Where  $Y_t$  is the depth with

$\Delta SL$  is the change in sea-level and WD is the water depth

### C4. Data input

Bases should be deeper than tops, and the depth, age, sea-level and water depths at the base of a given unit are equal to the depth, age, sea-level and water-depth at the top of the unit immediately below (see table below).

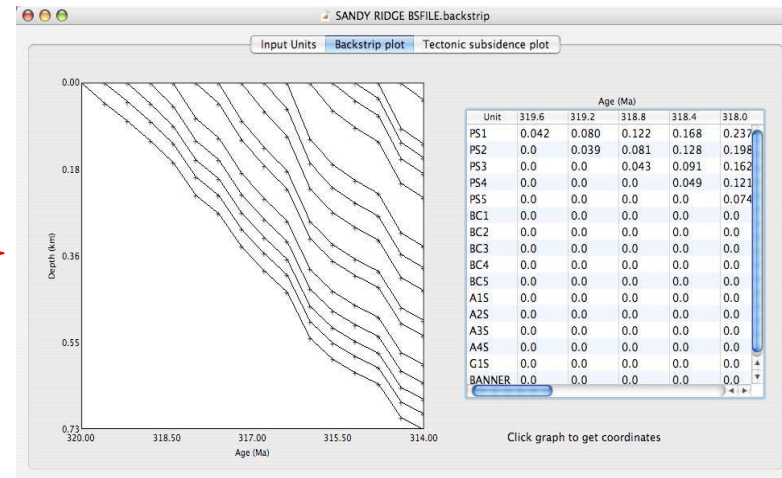
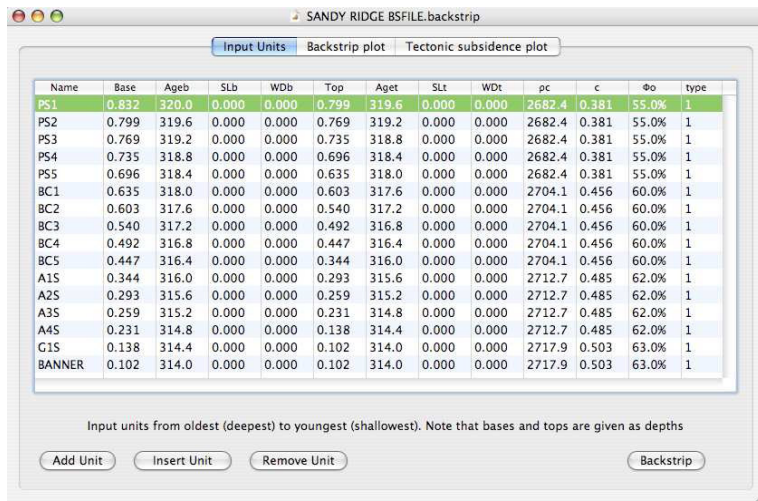
- Unit base (base) and top (top) as depths (km) from the ground surface.
- The age of unit base (Age b) and the unit top (Age t) in Ma
- Sea-level at the time of deposition of the unit base (SLb) and top (SLt) in km

- The sea-level is reported relative to present sea-level; positive numbers indicate above present sea-level, while negative numbers below sea-level for type 1 basin.
- Water depth at the time of deposition of the unit base (WDb) and top (WDt) in Km, WD should be positive numbers
- Porosity coefficient (C) in  $\text{Km}^{-1}$  is between 0-1.
- Grain density ( $\rho_c$ ) in  $\text{Kg/m}^3$ . The dry density is a positive number.
- Surface porosity ( $\phi^s$ ) as percentage %, between 0 – 100.

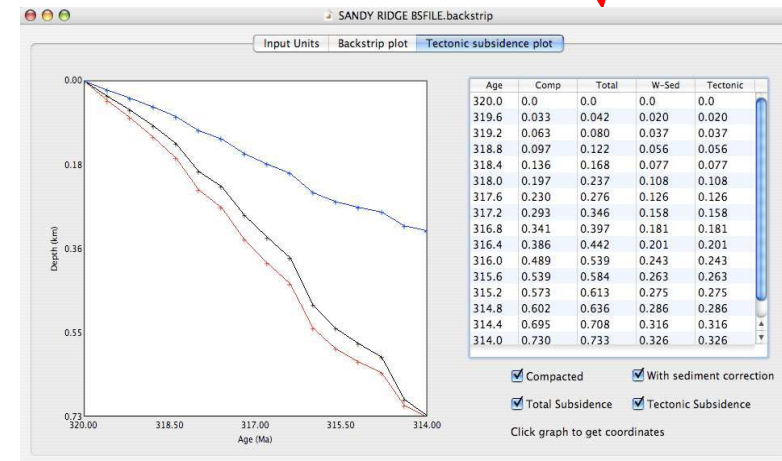
Name	Base	Ageb	SLb	WDb	Top	Aget	SLt	WDt	P <sub>c</sub>	C	Φ <sub>0</sub>	Type
Cape Supergroup	9.765	483	0	0	2.765	335	0	0	2680	0.39	56	1
Hiatus	2.765	335	0	0	2.465	312	0	0	0	0	0	1
Dwyka Group	2.765	312	0	0	2.465	290	0	0	2600	0.51	56	1
Prince Albert Formation	2.465	290	0	0	2.3	278	0	0	2720	0.51	56	1
Whitehill Formation	2.3	278	0	0	2.22	272	0	0	2720	0.51	63	1
Collingham Formation	2.22	272	0	0	2.15	271	0	0	2700	0.45	56	1
Tierberg Formation	2.15	271	0	0	1.40	270	0	0	2720	0.51	63	1
Skoorsteenber g Formation	1.40	270	0	0	1.00	269	0	0	2680	0.39	56	1
Kookfontein Formation	1.00	269	0	0	0.75	268	0	0	2700	0.45	56	1
Koedoesberg Formation	0.75	268	0	0	0.55	266	0	0	2700	0.45	56	1
Abrahamskraal Formation	0.55	266	0	0	0.05	240	0	0	2680	0.39	56	1

Data input table for the Backstripping and plotting of the subsidence curve on OSXBackstrip programme.





### Outputs – Total and Tectonic subsidence



OSX  
Backstrip  
v2.7



The OSXBackstrip Program description and work flow (<http://homepage.mac.com/nfcd/work/programs.html>). The software formulas are based on Allen and Watts, 1990; Watts, 2001.



## **APPENDIX D**

### **SEM PROCEDURE**

Imaging of the samples and analysis of the compaction characteristics in terms of extent of quartz overgrowth and fracturing, and feldspar deformation was accomplished using a Leo® 1430 VP Scanning Electron Microscope at the CAF centre in Stellenbosch University. Cathode Luminescence (CL) images require 15 micrometre thickness (peacock blue colour) of carbon coating, a flat and polished surface (rock sample thin sections).

Beam conditions during the CL imaging were EHT of 20 KV and approximately 1.5 nA, with a working distance ranging from 16 mm – 18 mm, and a specimen beam current of -3.97 nA. The counting time was 50 seconds live-time.